AN INVESTIGATION INTO THE PERFORMANCE CHARACTERISTICS OF A HYDROSTATIC OIL BEARING SYSTEM

A Thesis submitted to

The Victoria University of Manchester

for the Degree of

Doctor of Philosophy

by

Ashok K. Kher

B.Sc.Engg (Hons.), M.Tech., M.Sc.

Faculty of Technology

July, 1968.

ProQuest LLC.
789 East Eisenhower Parkway
P.O. Box 1346
Ann Arbor, MI 48106 – 1346

ACKNOWLEDGEMENTS

The author wishes to express his sincere thanks to Professor F. Koenigsberger for the facilities provided for carrying out research on this project, and to Mr. A. Cowley for his helpful guidance and encouragement throughout the course of this work.

Thanks are also due to Mr. J. Bullock and Mr. J. Farrell for their invaluable assistance in the assembly of the test rig, to Mr. F. Kniveton, to all members of the technical staff in the Royce Laboratory and Miss A.L. Foster, Mr. A. Appleby, Mr. J. Howe and Mr. G. Guiney for their help in preparing the thesis.

Finally, thanks are due to the Burmah Shell/C.S.I.R., New Delhi, India, for sponsoring the author for post graduate studies in the U.K.

After taking his B.Sc. Engg. (Hons.) degree with First Class First, from the Panjab Engineering College, Chandigarh, India, in July 1963, the author joined the Indian Institute of Technology, Bombay and obtained his M.Tech degree in August, 1965, specializing in Machine Design.

On being awarded the Burmah Shell/C.S.I.R. Scholarship for higher studies in U.K., the author came to the University of Manchester, Institute of Science and Technology, and took his M.Sc. degree in December 1966. A part of this work was presented at the 8th International Machine Tool Design and Research Conference held in September 1967.

The present thesis is an account of the further work carried out since October 1966, on a Capillary Compensated Hydrostatic Bearing System.

The present investigation has been carried out to determine the performance characteristics of a Capillary Compensated Hydrostatic Bearing System, consisting of two journal and one double film thrust bearing. A theoretical analysis of the journal bearing, including the squeeze film equation, is presented and a procedure for the design of the bearing pad geometry for both the steady and dynamic loads is outlined.

Digital Computer Programs have been employed to determine the steady load deflection curve, the resonant frequency, damping ratio, modal shapes etc. of the spindle in the bearing system, and these have been discussed with the experimental results on the test rig.

The importance of the temperature effects on the performance of hydrostatic bearings has been studied, and the heat dissipation in the journal bearing was obtained from the circumferential and radial temperature measurements.

CONTENTS

		Page
CHAPTER I	INTRODUCTION	1
	1.1. Dynamic Analysis of Hydrostatic Bearings.	2
	1.2. Temperature Effects in Journal Bearings.	5
CHAPTER II	ANALYSIS AND DESIGN OF HYDROSTATIC JOURNAL BEARINGS WITH CAPILLARY COMPENSATION	11
	2.1a. Load Carrying Capacity	12
	2.1b. Stiffness	13
	2.1c. Oil Flow	13
	2.1d. Total Power Requirement	14
	2.1e. Resistance to Tilting	14
	Analysis	15
	2.1f. Selection of Pad Geometry for a Journal Bearing	18
	2.1g. Steady Load Analysis of a Hydrostatic Bearing System	20
	2.2. Dynamic Load Considerations	22
	2.2a. Squeeze Film Equation for a Hydrostatic Journal Bearing	23
	2.2b. Dynamic Load Analysis of a Hydrostatic Bearing System	29
	2.3. Hydrostatic Thrust Bearing	31
	2.3a. Oil Flow	31
	2.3b. Load Capacity and Stiffness	31
	2.3c. Total Power Requirement	32
CHAPTER III	EXPERIMENTATION AND RESULTS	33
	3.1. Temperature Distribution and Heat Balance	33
	3.1a. Journal Bearing	33

	3.1b.	Thrust Bearing	34
	3.1c.	The Hydraulic Circuit	34
	3.1d.	Capillary Restrictors	34
	3.1e.	Temperature Measurement	34
	3.1f.	Torque Measurement	36
	3.2.	Steady Load Deflection	38
	3.3.	Dynamic Response	39
	3.3a.	Frequency Response Curves	40
	3.3b.	Damping Ratio	41
	3.3c.	Modal Shapes	42
CHAPTER IV	DISCUSSION		43
	4.1.	Temperature Distribution and Heat Balance	43
	4.2.	Steady Load Deflection	45
	4.3.	Dynamic Response	47
CHAPTER V	CONCLUSION		53
BIBLIOGRAPHY			55
APPENDICES			i

LIST OF APPENDICES

		Page
I	LIST OF NOTATIONS	i
II	SQUEEZE FILM EQUATION FOR A RECTANGULAR PAD	iv
III	HEAT DISSIPATION IN HYDROSTATIC JOURNAL BEARINGS	ix
IV	CALCULATION OF DAMPING RATIO FROM FREQUENCY RESPONSE CHARACTERISTICS	xi
V	COMPUTER PROGRAM TO DETERMINE THE EFFECT OF DESIGN FACTOR ON THE LOAD FACTOR AND THE FLOW FACTOR OF A HYDROSTATIC JOURNAL BEARING	xiii
VI	COMPUTER PROGRAM TO DETERMINE THE EFFECT OF OIL FILM THICKNESS ON THE OIL FLOW, STIFFNESS AND TOTAL POWER REQUIREMENT OF A HYDROSTATIC JOURNAL BEARING	xv
VII	COMPUTER PROGRAM TO DETERMINE THE ROTATIONAL FLEXIBILITY OF THE HYDROSTATIC JOURNAL BEARING	xviii
VIII	COMPUTER PROGRAM TO DETERMINE THE DAMPING CONSTANT OF THE JOURNAL BEARING	xx
IX	COMPUTER PROGRAM TO DETERMINE THE STEADY LOAD DEFLECTION OF THE SPINDLE IN A HYDROSTATIC BEARING SYSTEM	xxii
X	COMPUTER PROGRAM TO DETERMINE THE DYNAMIC RESPONSE OF THE HYDROSTATIC BEARING SYSTEM	xxix
XI	COMPUTER PROGRAM TO STUDY THE EFFECT OF RADIAL LAND WIDTH ON THE OIL FLOW AND POWER REQUIREMENT OF A HYDROSTATIC THRUST BEARING	XLiii

CHAPTER I

INTRODUCTION

A hydrostatic bearing supports a load on a fluid film, maintained under pressure by an external source of power, whereas this power has to be generated within the bearing by the relative movement of the mating components, in a hydrodynamic bearing. Hence, the main attraction of hydrostatic bearings is their ability to carry loads even at zero relative velocities. Since there is never any metal to metal contact, the power loss due only to the shearing of the oil film, is generally small, approaching almost negligible values for low speeds. This also eliminates wear of the components and ideally they need never be changed. Besides being capable of carrying large loads, very high stiffness can be obtained with the range of compensating elements and techniques available to the designer today. They are suitable for automatic control operations and lend themselves easily to pressure feed back systems for design of bearings with almost infinite stiffness.

For these and a few other reasons, the hydrostatic bearings are now being incorporated in a range of equipment and a considerable volume of literature has accummulated describing their various applications.

Since these bearings have a separating oil film between mating machine elements even at zero speed, they are useful for supporting and easy starting of heavy loads, like turbogenerators, telescopes, etc., thus eliminating the high starting torque inherent in any hydrodynamic bearing. Machine tool manufacturers are employing these bearings to support large machine tool beds capable of moving easily and rapidly without any stick-slip motion. Air bearings are being developed for high speed spindles of grinding machines for very accurate machining

processes, the low viscosity of the air keeping the power requirement and heating to a minimum, while the load is supported by the external pressure.

While a considerable amount of research has been done in the field of hydrostatic bearings, it has largely been confined to the development of the theoretical analysis and design procedures from static stiffness considerations. Recently, some work has been done on tapered land journal bearings for self alignment by MANNAM, FOWLER and CARPENTER[1]* and by KEARNEY[2] on Master and Slave bearings. HIRS[3] has worked on bearings with inherent friction compensation and investigations were carried out by SHINKLE and HORNUNG[4] on the friction characteristics of journal bearings including the effects of turbulence.

However, not much work has been reported on the dynamic analysis of hydrostatic bearings, nor the effect of temperature on their performance characteristics. With increased emphasis on surface finish in metal cutting processes and application of these bearings for high speed spindles both these factors have assumed great importance and further investigation is necessary for a complete understanding of these phenomena.

1.1. Dynamic Analysis of Hydrostatic Bearings

ROYLE, HOWARTH and CASELEY-HAYFORD[5] presented a theoretical analysis for static and dynamic performance of single circular and rectangular pads (with one dimensional flow), and discussed the application of pilot pad sensing technique with an external compensating valve to provide almost infinite stiffness for a journal bearing. The oil flow being two dimensional in a journal bearing, the damping coefficient is likely to be much smaller and in the absence of experimental investigation it is difficult to say how far this analysis is applicable to it. Since the automatic control valve is likely to prove even more useful for dynamic

* Numbers refer to Bibliography.

loading, it would have been of interest to know more about the dynamic behaviour of the bearing.

In his M.Sc. thesis submitted at M.I.T., U.S.A., SCHER[6] investigated the dynamic performance of a hydrostatic journal bearing with feed back control, and step input to the bearing system. The test rig consisted of a bearing with only two pads, grooved inside the journal and the discussion was confined to a stationary journal (no rotation) and load applied only along the centre line of the top and bottom pads. However, discrepancies were noticed between the experiments and the theoretical analysis and it seems that the squeeze film equation is considerably altered due to the oil flow in both the axial and circumferential directions, and even with large circumferential lands, the latter cannot be neglected.

BROWN[7] simplified the analysis of a thrust bearing by converting its parameters into an enclosed piston and cylinder arrangement with oil flow through an external restrictor, thus considering the combined effects of hydrostatic oil flow and oil compressibility, neglecting the squeeze film effect. Since the squeeze film effect is considered to be more important in hydrostatic bearings, than the oil compressibility, it is doubtful how far the claims of good experimental results are justified or may be generalized for predicting behaviour of other bearing systems. Moreover, the convertion of the system into a piston cylinder arrangement is in effect a closed bearing and not a total loss system as the hydrostatic thrust bearing.

The frequency response characteristics show that the dynamic stiffness of the system is greater than the static stiffness at all times, with a considerable degree of damping, making the hydrostatic thrust bearings very suitable for machine tool applications.

The dynamic analysis and the squeeze film equation for a flat rectangular pad with one dimensional and two dimensional flow was presented by MORI and YABE[8], and it was then modified for a 4-pad journal bearing

with axial pressure relief grooves. The equations for the two dimensional flow were solved independently in the two directions of flow, but without any experimental verification the validity of the assumptions could not be established.

A detailed analysis of a circular pad thrust bearing for dynamic loads was presented by LICHT[9], and the equations for the local stiffness and damping constants for the evaluation of the dynamic response were derived. The results for the equation of motion were obtained with an analog computer. A few important points raised in the discussion of the paper are worth mentioning here. RICHARDSON suggested the consideration of the liquid compressibility effects in the analysis, since it had been found by LUMING at M.I.T., that compressibility of the oil could not be neglected. SNECK presented a modified continuity equation as it was doubtful if the steady state flow equation presented in the paper, could be used to describe a non-steady phenomenon. He also derived equations for determining the permissible vibrational frequency for which the inertial effects could be neglected.

HUNT and TORBE[10] also analysed a circular pad thrust bearing for static and dynamic sinuisoidal loads. Equations for static load capacity and stiffness were derived and were later extended to include the effects of the dynamic load. Though rotation of the pad was not considered, yet considerable agreement was obtained with experiments performed in the static condition. Further work was proposed to determine the inaccuracy involved in assuming the hydrostatic bearing as a linear system, i.e,constant stiffness, and since the stiffness of the thrust bearing varies with film thickness, it would be of interest to see the results of the further analysis.

In his paper presented at the 7th International Machine Tool Design and Research Conference, DE GAST[11] referred to the experimental work done on a journal bearing with dynamic load, though no theoretical analysis

was included. A graph showing the change in phase angle between load and deflection and the change in deflection amplitude for different supply pressures (at the same load and frequency) was presented. The damping was found to increase with the frequency and due to excellent damping characteristics and high natural frequency of the restrictor membrane, no instability problems were encountered in the system.

1.2. Temperature Effects in Journal Bearings

With the increased application of hydrostatic bearings, a discussion on its relative merits and demerits over the traditional hydrodynamic bearing, for all aspects of performance, is inevitable. The development of design procedures for hydrodynamic bearings had generally been based on their load carrying capacity and stiffness characteristics. However, with the application of bearings for very high speeds, the temperature and heat dissipation aspects became increasingly important, as very often the bearings designed to provide adequate load capacity failed due to excessive temperature rise. It is felt that the development of the hydrostatic bearings is also likely to follow a similar cycle. Therefore, though the temperature effect is important by itself in the study of hydrostatic bearings, yet any such work will necessarily be considered in the light of results obtained for hydrodynamic bearings.

Research on heat dissipation and temperature distribution in bearings has been going on since the early 1930's and in his paper KINGSBURY[12] showed that the internal heating of the oil film was an important factor in limiting its load capacity, which was approximately proportional to the shear stress that could be maintained. Three fundamental equations relating oil viscosity, shear stress and temperature were derived and experimental verification was obtained by determining the reduction in shear stress due to temperature rise.

The heat generated in a bearing is clearly dissipated along three paths, i.e. heat conducted to the bearing housing and to the journal, and heat carried away by the oil. However, it is interesting to see the different results obtained by various authors depending upon the assumptions made in their respective analyses. KARELITZ[13] defined the types of bearings according to the oil supply, upon which depended the main mode of heat transfer. He showed the essential difference between bearings with copious supply of oil, such as oil ring lubricated bearings where the oil was brought into contact with the shell all around the circumference, heat was transferred to the bush at all points and a large variation in temperature along the bush did not occur - and bearings with drop feed where bearing clearance was substantially empty and not only was the heat generation more concentrated but the transmission of heat to the shell was also localized to the pool of oil between the journal and the bearing. It follows that in the first type of bearings, the oil would carry away a substantial portion of the heat generated, while in the second type the heat must be transferred mainly by conduction through the bearing housing.

HERSEY[14] outlined in detail the problems of temperature rise in the bearings and the research necessary for better understanding of their performance characteristics. It was stated that while the previous design considerations had been the load capacity and stiffness, in future the limiting factor would be the temperature rise in the bearing. An analytical method for the solution of temperature rise was discussed in terms of heat generated and heat dissipated with the intermediary of an independently determined relation between the lubricant viscosity and its temperature. MUSKAT contended however, that this procedure required the heat transfer coefficients for a bearing design which are not readily available and if indeed there were a satisfactory method for determining the lubricant film temperature independently, the procedure put forward

may perhaps be better used for the calculation of effective heat transfer constants. A method was suggested and was later employed by MUSKAT and MORGAN[15] to obtain the friction coefficient by torque measurement and thus the oil viscosity, and from the oil viscosity - temperature charts, the average film temperature.

An analysis for lightly loaded bearings at high speeds with negligible spindle eccentricity was presented by BOYD and ROBERTSON[16]. While MUSKAT and MORGAN assumed negligible heat flow to the oil, BOYD and ROBERTSON neglected the heat lost to the bearing housing. For hydrodynamic bearings, where the oil flow is not extremely high, this assumption with bush temperatures of 180°F could not be valid and hence the two analyses are likely to oversimplify the theoretical calculations.

CLAYTON and WILKIE[17] experimentally determined the circumferential and the radial temperature distribution in the journal bearing and from the radial temperature gradient extrapolated the actual temperature of the bearing bush. However, this method of extrapolation could lead to erroneous results, especially when the bush and the main housing are of different materials (as is often the case) and inclusion of a thin fluid film between them cannot be overruled.

An experimental investigation on temperature effects in journal bearings was also carried out by COLE[18], by setting thermocouples in the circumferential and radial directions. The temperature maxima were observed to be displaced in the direction of motion from the load line, and were probably at the minimum film thickness. An approximate figure for heat loss by conduction was obtained as 20 to 25% of the total power loss and the oil flow accounted for 40% heat dissipated at low speeds and 60% at high speeds. The experiments showed the occurrence of large variations of temperature, hence viscosity, circumferentially in high speed journal bearings. The bush crown temperature gave a fair approximation of the maximum temperature but the oil outlet temperature, which

is often taken as the measure of operational safety, was well below the maximum and hence was an unreliable criterion. The heat balance showed that the assumption of complete dissipation of heat by the oil could be misleading.

PINKUS and STERNLICHT[19] presented an analysis for the circumferential temperature distribution in the mid-section of a journal bearing. Since the maximum temperature in the bearing occurs in the oil film with maximum rate of shear and its experimental determination is difficult, this analysis is useful, however, the neglect of heat transfer to the bearing body by conduction and the assumption of all the power dissipated to the oil film, divorced as it is from actual conditions of performance, make the analysis of limited use.

The equations for the adiabatic temperature distribution for both the short and the infinite bearing were presented by PURVIS, MEYER and BENTON[20]. This theory also neglected the heat conduction to the bearing housing and the maximum temperatures are therefore likely to be higher than found in practice. Moreover, only oil flow due to viscosity was considered and since flow in the axial and circumferential directions due to pressure gradient and velocity was neglected, it is likely to introduce serious errors while performing with high spindle speeds and eccentricities.

ORLOFF[21] presented the analysis for the coefficient of friction for journal bearings from Reynold's equations, which correlated well with the results of the experimental investigation. A heat balance of the bearing was prepared and though it neglected the heat loss to the bearing body, yet it demonstrated the considerable effect of temperature rise on the load capacity of the bearing. It was suggested that better performance and greater load capacity of the bearing could be achieved by lowering the inlet oil temperature.

As has been mentioned earlier, not much work has been reported on the effects of temperature rise in hydrostatic bearings. DE GAST[11] obtained the temperature rise of the oil coming out of the bearing during performance. Since the oil outlet temperature has generally proved to be much lower than the temperature in the bearing, no real indication of the actual temperatures is thus available from these results.

CUENCA and RAYNER[22] presented a numerical solution for a circular pad hydrostatic thrust bearing with central fluid supply assuming negligible rotational speed and isothermal boundaries, and it was shown that the load capacity was 32% less than calculated by the isothermal theory. However, the analysis in its present form is inadequate and of limited practical use. Since the temperature is a function of the heat transfer to the oil and the bearing housing, the latter cannot be neglected for any realistic determination of the reduction in load capacity. Moreover, larger heat is generated due to the relative movement of the parts and shearing of the oil film during actual performance, while only the temperature due to the pressure gradient has been considered in this analysis.

An investigation into the performance characteristics of a capillary compensated hydrostatic bearing system for steady radial loads was carried out and submitted in an earlier thesis by the author[23], wherein results of the preliminary study of the temperature effects and temperature distribution in the bearing were also included. The present work may be considered as an extension of the previous work and therefore, has to be seen in that context. Effort has been made to preserve the continuity of the whole work by reference to salient features of the previous work and inclusion of the main results.

The purpose of the present work therefore, was to study the bearing system in greater detail with special reference to its dynamic characteristics, i.e. natural frequency, damping ratio etc., and to outline a

procedure for design of journal bearings from not only the steady load considerations, i.e. load capacity, stiffness, power requirement, rotational flexibility etc., but also the dynamic load. While the stress has been on the theoretical analysis and performance of the journal bearings, the whole system has been studied as envisaged for application to machine tools.

Computer programmes have been prepared to determine the static and dynamic response of the system and experiments were performed to see how far these could be applied to actual bearing systems.

The importance of studying the temperature effects in bearings needs no further elaboration and since the damping factor is so susceptible to oil viscosity changes due to temperature rise in the bearing, it becomes even more urgent for dynamic loads. Hence, it was proposed to study the effect of temperature rise on the performance of the journal bearing and to prepare a heat balance of the bearing from temperature measurements on the oil and in the bearing housing.

CHAPTER II

ANALYSIS AND DESIGN OF HYDROSTATIC JOURNAL BEARINGS WITH CAPILLARY COMPENSATION

ANALYSIS AND DESIGN OF HYDROSTATIC JOURNAL BEARINGS WITH CAPILLARY COMPENSATION

Hydrostatic journal bearings may consist of 3, 4 or more pressure pads, each supplied with oil of the same pressure and each independently compensated by restrictors of the same characteristics. Journal bearings with pressure relief grooves between pads as well as bearings with main pads to carry load and pilot pads for load sensing and pressure feed back control have also been employed.

The design of compensated hydrostatic journal bearings for application to machine tool spindles requires consideration of both the steady and the dynamic conditions of loading since they are subjected to steady preloads and dynamic cutting loads in metal cutting processes. The main factors of consideration for steady loads are;

(a) Load carrying capacity

(b) Stiffness

(c) Oil flow

(d) Total power requirement

(e) Resistance to tilting

In its broad form, therefore, the design of the hydrostatic bearing can be considered as the selection of a pad configuration (Fig. 1), its geometry and radial clearance, to carry the load, provide the stiffness and ensure that the power requirement and the oil flow are not excessive.

The analysis of a capillary compensated journal bearing for steady loads was partly covered in an earlier thesis and published by the author and COWLEY[24], where the expressions for load carrying capacity, stiffness, oil flow and power requirement were derived. To enable the present investigation to be seen in its true perspective, the results of the previous analysis will be included here, while the resistance to

tilting and subsequent work will be fully discussed.

A list of notations used in the analysis is given in Appendix I.

2.1a. Load Carrying Capacity

The load capacity of the journal bearing, for load acting into the pad as shown in Fig. 1, is given by the equation;

$$W = K_1 \, l_f \, p_s \qquad \ldots (1)$$

When the load acts in any arbitrary direction, the load capacity is given by;

$$W = K_1 \, p_s \sum_{n=1}^{n=4} p_n \text{ (vector sum)} \qquad \ldots (2)$$

where $K_1 = DL \, (1 - el) \sin \alpha_2 \qquad \ldots (3)$

$$l_f = (p_3 - p_1) \qquad \ldots (4)$$

and p_n = ratio of the nth pad pressure to the supply pressure.

The pad pressures can be determined by equating the oil flow through the bearing pad and the capillary restrictor[23]. Thus, when the load acts into the pad (Fig. 1) the ratios of the respective pad pressures to supply pressure are given by the equations;

$$p_3 = \frac{Z + 4mp_2 f_3''}{Z + f_3' + 4mf_3''} \qquad \ldots (5)$$

$$p_1 = \frac{Z + 4mp_2 f_1''}{Z + f_1' + 4mf_1''} \qquad \ldots (6)$$

$$\text{and } p_2 = p_4 = \frac{Z + 2m \, (p_1 f_1'' + p_3 f_3'')}{Z + f_2' + 2m \, (f_1'' + f_3'')} \qquad \ldots (7)$$

$$\text{where } Z = \frac{3\pi}{16} \left(\frac{d^4 \, L \, el}{h_o^3 \, Dl}\right) \qquad \ldots (8)$$

$$m = \left(\frac{L}{D}\right)^2 \frac{el(1 - 2\,el)}{\alpha_2(1 - e\alpha)} \qquad \ldots (9)$$

$$f_n' = \pi + 6e\left[(\cos\alpha + \sin\alpha)\sin\frac{n\pi}{2} + (\cos\alpha - \sin\alpha)\cos\frac{n\pi}{2}\right] + 3e^2\left[\frac{\pi}{2} - \cos n\pi \sin 2\alpha\right] + \frac{2}{3}e^3\left[(\sin\frac{n\pi}{2}\cos\alpha - \cos\frac{n\pi}{2}\sin\alpha)(\frac{5}{2} + \frac{1}{2}\cos n\pi\cos 2\alpha) + (\cos\frac{n\pi}{2}\cos\alpha - \sin\frac{n\pi}{2}\sin\alpha)(\frac{5}{2} - \frac{1}{2}\cos n\pi\cos 2\alpha)\right] \quad \ldots (10)$$

and $$f_n'' = \left[1 + e\cos\left(\frac{n\pi}{2} - \alpha\right)\right]^3 \quad \ldots (11)$$

Similarly, when the load acts into the circumferential land, the ratios of the pad pressures to the supply pressure are;

$$p_3 = p_2 = \frac{Z(Z + f_4' + 4mf_3'')}{(Z + f_4' + 2mf_3'')(Z + f_3' + 2mf_3'') - (2mf_3'')^2} \quad \ldots (12)$$

and $$p_4 = p_1 = \frac{Z(Z + f_3' + 4mf_3'')}{(Z + f_4' + 2mf_3'')(Z + f_3' + 2mf_3'') - (2mf_3'')^2} \quad \ldots (13)$$

2.1b. Stiffness

An exact expression for the stiffness of the journal bearings is rather complicated to derive and has not been included here, however the slope of the load eccentricity ratio curve gives a fair approximation of its value. Therefore, the stiffness can be obtained from the equation;

$$S \approx \frac{1}{h_o}\frac{dW}{de} \quad \ldots (14)$$

2.1c. Oil Flow

a) When the spindle is concentric in the bearing, the oil flow is given by the equation;

$$Q_o = \frac{p_s K_f h_o^3}{6\mu}\left(\frac{Z}{\pi + Z}\right) \quad \ldots (15)$$

where $$K_f = \frac{\pi D}{Lel} \quad \ldots (16)$$

b) When the spindle deflects in the bearing due to external load, the equation for oil flow is;

$$Q = \frac{p_s K_f h_o^3}{\pi . 24 \mu} \sum_{n=1}^{n=4} (p_n f_n') \qquad \ldots (17)$$

2.1d. Total Power Requirement

The total power requirement of a journal bearing is the sum of the power required to pump the oil and the power lost in shearing of the oil film due to spindle rotation, and is given by the equation;

$$P_o = \frac{K_f h_o^3}{39600 \mu} \left(\frac{Z}{\pi + Z}\right) p_s^2 + \frac{\mu N^2 K_p}{766000 h_o} \qquad \ldots (18)$$

where $K_p = D^3 L \left[1 - e\alpha(1 - 2\,el)\right]$ ... (19)

By differentiating equation (18), and equating to zero, the optimum oil film thickness can be calculated for which the total power requirement is a minimum. Hence;

$$h_{opt} = 0.362 \sqrt{\frac{\mu N}{p_s}} \left[\frac{K_p}{K_f} \left(\frac{\pi + Z}{Z}\right)\right]^{\frac{1}{4}} \qquad \ldots (20)$$

2.1e. Resistance to Tilting

There is nothing in the mechanism of operation of a hydrostatic journal bearing to readily suggest that it has any substantial resistance to spindle inclination in the bearing. However, a complete understanding of this phenomenon is necessary, not only for the correct prediction of the spindle deflection due to steady loads, but also for accurate evaluation of the natural frequency and damping ratio of a bearing system, as will be shown later. When the spindle assumes an inclined position in the bearing as shown in Fig. 2, it causes a convex pressure distribution over the axial land in section (a) and a concave pattern in section (b), instead of a linear drop assumed for horizontal position of the spindle. The difference between the forces acting over the lands, represented by the difference between the areas under the curves,

causes a balancing couple on the spindle. The moment produced by one radian inclination of the spindle will be called the rotational stiffness of the bearing, and its inverse will be referred to as the rotational flexibility.

To avoid any confusion between the bearing stiffness to steady normal loads discussed earlier, and the rotational stiffness, the former will henceforth be called the normal stiffness and its inverse as the normal flexibility.

Analysis

Consider the oil flow through section (a) (Fig. 2), then the equation of the equilibrium of forces acting over a small element of the oil of unit width is;

$$\left[\left(p + \frac{\partial p}{\partial x}\,dx\right) - p\right] dy = \left[\left(\tau + \frac{\partial \tau}{\partial y}\,dy\right) - \tau\right] dx \qquad \ldots (21)$$

from which on simplification,

$$\frac{\partial p}{\partial x} = \frac{\partial \tau}{\partial y} \qquad \ldots (22)$$

As shown in Appendix II, the equation of the oil flow is;

$$q_x = -\frac{h_x^3}{12\mu}\,\frac{dp}{dx} \qquad \ldots (23)$$

If the spindle inclination in the bearing is α, then the oil film thickness anywhere in section (a) can be expressed as;

$$h_x = (h_o + \alpha x) \qquad \ldots (24)$$

Now, the rate of flow is a constant; therefore,

$$\frac{dq_x}{dx} = \frac{d}{dx}\,\frac{(h_o + \alpha x)^3}{12\mu}\,\frac{dp}{dx} = 0$$

or $$(h_o + \alpha x)\,\frac{d^2p}{dx^2} + 3\alpha\,\frac{dp}{dx} = 0 \qquad \ldots (25)$$

The solution of the differential equation (25) is;

$$p_{xa} = \frac{C_1}{2\alpha} + \frac{\alpha^2 C_2}{(h_o+\alpha x)2} \quad \ldots (26)$$

Applying the boundary conditions,

$$p_{xa} = p, \quad x = -l_1$$

and $$p_{xa} = 0, \quad x = -l_2 \quad \ldots (27)$$

The equation for the pressure over the axial land in section (a) is;

$$p_{xa} = \frac{p(h_o - \alpha l_1)^2}{(h_o - \alpha l_2)^2-(h_o - \alpha l_1)^2} \left[\frac{(h_o - \alpha l_2)^2}{(h_o + \alpha x)^2} - 1 \right] \quad \ldots (28)$$

Similarly, the equation for the pressure in section (b) is;

$$p_{xb} = \frac{p(h_o + \alpha l_1)^2}{(h_o + \alpha l_2)^2-(h_o + \alpha l_1)^2} \left[\frac{(h_o + \alpha l_2)^2}{(h_o + \alpha x)^2} - 1 \right] \quad \ldots (29)$$

The forces acting over the axial lands in sections (a) and (b) can now be found by integrating the pressure equations; thus;

$$F_a = \frac{D}{2} \int_{-l_1}^{-l_2} \int_{-\alpha_2}^{\alpha_2} p_{xa} \cos \beta \, d\beta \, (-dx)$$

$$= D \sin \alpha_2 \int_{-l_1}^{-l_2} p_{xa} \, dx \quad \ldots (30)$$

Which on integration and simplification gives;

$$F_a = \frac{Dp \sin \alpha_2 (h_o - \alpha l_1)^2}{\alpha\left[(h_o - \alpha l_2)^2-(h_o - \alpha l_1)^2\right]} \left[(h_o - \alpha l_2) - \frac{(h_o - \alpha l_2)^2}{(h_o - \alpha l_1)} - \alpha(l_2 - l_1) \right] \quad \ldots (31)$$

And similarly, the equation for the force acting over the axial land in section (b) is;

$$F_b = \frac{Dp \sin \alpha_2 (h_o + \alpha l_1)^2}{\alpha\left[(h_o + \alpha l_2)^2 - (h_o + \alpha l_1)^2\right]} \left[\frac{(h_o + \alpha l_2)^2}{(h_o + \alpha l_1)} - (h_o + \alpha l_2) - \alpha(l_2 - l_1)\right] \quad \ldots (32)$$

Since the pressure profiles over the axial lands form approximately a triangular shape (Fig. 2), the resultant of the forces can be assumed to act at distances $\frac{2}{3}$ l from the side edges respectively. Hence, considering the forces acting on the top and the bottom sides of the spindle in a journal bearing, the total moment acting on the spindle is;

$$M = \frac{2}{3}(F_a - F_b)(l_2 + 2l_1) \quad \ldots (33)$$

Therefore, the expression for the rotational flexibility is;

$$RFl = \frac{3\alpha}{2(F_a - F_b)(l_2 + 2l_1)} \quad \ldots (34)$$

Representing the ratio of the axial land to the total length of the bearing as el, as in the previous analysis, the above equations can be modified; thus;

$$F_a = \frac{Dp \sin \alpha_2 \left[h_o - .5L\alpha(1 - 2el)\right]^2}{\alpha\left[(h_o - .5L\alpha)^2 - \left\{h_o - .5L\alpha(1 - 2el)\right\}^2\right]} \left[(h_o - .5L\alpha) - \frac{(h_o - .5L\alpha)^2}{\left\{h_o - .5L\alpha(1 - 2el)\right\}} - \alpha Lel\right] \quad \ldots (31a)$$

$$F_b = \frac{Dp \sin \alpha_2 \left[h_o + .5L\alpha(1 - 2el)\right]^2}{\alpha\left[(h_o + .5L\alpha)^2 - \left\{h_o + .5L\alpha(1 - 2el)\right\}^2\right]} \times \left[\frac{(h_o + .5L\alpha)^2}{\left\{h_o + .5L\alpha(1 - 2el)\right\}} - (h_o + .5L\alpha) - \alpha Lel\right] \quad \ldots (32a)$$

$$M = (F_a - F_b)L(1 - 1.33el) \quad \ldots (33a)$$

and $$RFl = \frac{\alpha}{(F_a - F_b)L(1 - 1.33el)} \quad \ldots (34a)$$

A typical pressure distribution over the axial lands due to spindle inclination is shown in Fig. 2, while the variation in the rotational flexibility for various axial land ratios is shown in Fig. 3. It is

evident that a reduction in rotational flexibility is obtained by increasing the axial land ratio as well as the spindle inclination.

2.1f. Selection of Pad Geometry for a Journal Bearing

The procedure for selection of the radial clearance for a particular journal bearing configuration, for minimum power requirement and the calculation of the capillary restrictor dimensions for maximum load carrying capacity has been outlined in an earlier thesis. It was shown that the load capacity of a compensated bearing was a function of the design factor, Z (ratio of the respective resistances of the bearing and the compensating element, to oil flow), as shown in Fig. 4, and therefore depending upon the eccentricity ratio at which the bearing was intended for operation under full load, the design factor could be selected to give maximum load capacity of the bearing. It was also shown how the radial clearance could be selected for minimum power requirement.

The effect of the oil film thickness on the rotational flexibility, normal stiffness, power requirement and oil flow in the bearing is shown in Fig. 5. It is clear that if the minimum power requirement were considered the main criterion for the selection of the radial clearance, then it would result in a bearing with lower normal stiffness, higher rotational flexibility and oil flow.

In the application of journal bearings for machine tool spindles, the stiffness is always more important than the power requirement, which may only be a small proportion of the total power requirement of the machine. From equation (14), it can be inferred that the stiffness of the bearing can be increased by reducing the oil film thickness. Hence, it seems quite fair to select the radial clearance from considerations of stiffness and manufacture, and then to select the pad geometry to satisfy the other factors i.e. power requirement, oil flow, rotational

flexibility etc., according to their relative importance in the system.

The effect of the pad geometry factor, m, on the load factor, load carrying capacity and the power requirement is shown in Figs. 6 and 7, for the bearing with the following specifications;

Length of the bearing, $L = 2.50$ in

Diameter of the spindle, $D = 2.00$ in

Radial clearance, $h_o = 2 \times 10^{-3}$ in

Design factor, $Z = \pi$

Oil supply pressure, $p_s = 400$ psi

Spindle speed, $N = 2000$ rpm

In general, it is found that increasing the pad geometry factor, reduces the load capacity of the bearing. This is because increasing the axial land ratio, el, reduces the effective area under the pressure curve (Fig. 1), while higher circumferential land ratio induces greater oil flow across the pads with consequent drop in pressures of the pads supporting the load.

As stated before, the total power requirement is composed of the power required to pump the oil and that lost in shearing of the oil film. While reducing the axial land ratio reduces the shearing loss, it is partly offset by increase in oil flow and oil pumping power. Hence, one axial land ratio will require minimum total power and this can be found by differentiating equation (18) and equating to zero. Therefore;

$$\frac{dP_o}{del} = -\frac{\pi D h_o^3}{Lel^2(39600\mu)} \left(\frac{Z}{Z+\pi}\right) p_s^2 + \frac{\mu D^3 NL}{766000 h_o} \cdot 2 e\alpha \quad \ldots (35)$$

$$\text{or} \quad el = 5.51 \frac{h_o^2 p_s}{\mu DNL} \sqrt{\left(\frac{Z}{\pi+Z}\right) \cdot \frac{1}{e\alpha}} \quad \ldots (36)$$

It is found from the above equation, and also seen in Fig. 7, that axial land ratio, el $\approx .10$, for all the circumferential land ratios, requires minimum power, under the present conditions of performance.

The least power, anywhere, would obviously be required for the maximum possible circumferential land ratio. However, on closer examination of Fig. 7, it is found that a high circumferential land ratio considerably reduces the load capacity of the bearing. Hence, it may be necessary to sacrifice on the power requirement to obtain greater load capacity, depending on the requirements of the system.

From the derivation of the rotational flexibility, it is clear that increasing the axial land ratio increases the resistance of the bearing to spindle tilt. The variation of rotational flexibility, normal flexibility and power requirement with axial land ratio is shown in Fig. 8, and it is evident that while normal flexibility and power requirement increase slightly, the rotational flexibility decreases considerably for higher axial land ratios. Hence, it is now necessary to consider a bearing system and evaluate the total effect of the normal and rotational flexibility on the spindle deflection to select the axial land ratio for a hydrostatic journal bearing.

2.1g. Steady Load Analysis of a Hydrostatic Bearing System

A number of computer programmes have been developed at UMIST to determine the static and dynamic characteristics of machine tool structures. One such programme permits the calculation of the deformation shape of a general three dimensional structure composed of beam like elements, to steady loads.

The details of the mathematical background to these programmes has been given earlier by MIGLIARDI[25] and hence will not be covered over here. The essential feature of the technique used is to subdivide the structure into a number of lumped masses, connected together by massless elastic elements. The input data required consists of the bending, shear and torsional elastic characteristics of each of the constituent structural elements. The resulting output gives the

deflection of all the points of connection between the elements (station points) resulting from any set of loads applied to the station points.

The main spindle of the bearing system consisting of two hydrostatic journal bearings, and the equivalent discrete model required for the computer analysis is shown in Fig. 9. The system was divided into eight elements and the distributed mass was represented by seven discreet mass points. The division of the structure is based on the discontinuities in the elastic structural elements. Obviously, greater accuracy is obtained with as large a number of divisions as possible, but based on previous results obtained by FAWCETT and COWLEY[26], and MUNSON[27], this subdivision was considered adequate for the present case. The bearing characteristics are expressed by a single helical spring, and a torsional spring of stiffnesses equivalent to the normal and the rotational stiffness of the bearing respectively, as determined from the analysis described earlier. The computer programme for determining the static deflection shapes and compilation of the data is shown in Appendix IX.

The results have been obtained in terms of the spindle end deflection for a load at that point. The variation in the spindle end deflection with the bearing rotational flexibility for various normal flexibilities is shown in Fig. 10. The two extremes of bearing behaviour can either be almost zero rotational flexibility where the bearing virtually clamps the spindle like a fixed end, or almost infinite flexibility with freedom to revolve freely around a point as in a pin joint. It is seen from Fig. 10 that the spindle end deflection is dependent upon the rotational flexibility and therefore a pad geometry with very low rotational flexibility should be selected for minimum spindle end deflection.

However, a closer examination of Fig. 8 shows that while rotational flexibility can be reduced considerably by a larger axial land ratio,

the minimum practical value thus obtained, by itself makes very little reduction in the spindle end deflection. At the same time, the normal flexibility increases and the total power requirement becomes almost twice its minimum value at el = .100. Therefore, it seems that for steady loads after selecting the circumferential land ratio for higher load capacity the axial land ratio can then be selected from minimum power requirement consideration.

2.2. Dynamic Load Considerations

The main considerations in the design of the bearing system for dynamic loads are;

(i) Natural frequency

(ii) Dynamic Stiffness

(iii) Damping ratio

The natural frequency of the system depends largely on the normal and rotational flexibilities and will be discussed in greater detail later. The damping ratio is a function of the damping constant of the bearing, as well as the other parameters mentioned above.

The equations for the load capacity and stiffness of the bearing to steady uniform loads have been derived earlier. However, when the spindle is subjected to impact or a variable load, because of the lubricants resistance to instant extrusion from between the approaching surfaces, a pressure is built up and is actually capable of supporting load. This phenomenon is known as the squeeze film effect. The extent of the pressure build up depends on the oil viscosity, the area across which the flow takes place and the time factor of the dynamic load.

While the damping provided by a fluid film to dynamic loads is not entirely independent of the fluid compressibility, it is largely dependent upon the squeeze film effect and therefore this factor will

be discussed in detail as applied to compensated journal bearings.

2.2a. Squeeze Film Equation for a Hydrostatic Journal Bearing

The expressions for the damping constant of a flat rectangular pad with one dimensional and two dimensional flow are derived in Appendix II. This analysis may be extended for a journal bearing with the following assumptions;

(1) The dynamic displacement of the spindle is small, such that it can be taken to deflect parallel to the bearing and mean oil film thicknesses hold over the axial and the circumferential lands.

(2) The side pad pressures do not change with spindle deflection and the loaded and the unloaded pads can be analysed as individual pads.

(3) Oil behaves as an incompressible fluid.

(4) The depth of the pressure pad is large compared to the oil film thickness, so that the pressure is constant within the confines of the pad.

The configuration of the pad for deriving the squeeze film equation is shown in Fig. 12. Consider the spindle approach the pad 3 with a velocity $\frac{dh}{dt}$, then the flow equation in terms of a flat rectangular pad with two dimensional flow is;

$$\frac{h^3}{12\mu}\frac{d^2p}{dx^2} + \frac{h^3}{12\mu}\frac{d^2p}{dy^2} = \frac{dh}{dt} \qquad \ldots (37)$$

The equations for the pad pressure p_3' and the pressures over the axial and the circumferential lands can be solved as shown in Appendix II. It is only to be kept in mind that since the pressure in pads 2 and 4 is assumed constant, the boundary equations applicable in this case are;

$$p_c = p_3', \qquad \theta = \theta_1$$

$$p_c = p_o, \qquad \theta = \theta_2$$

$$p_a = p_3', \qquad y = y_1$$

and $$p_a = o, \qquad y = y_2 \qquad \ldots (38)$$

where p_3' = new pressure of pad 3 - psi

p_o = original pressure of pads 2 and 4 - psi

p_c = pressure over the circumferential lands - psi

and p_a = pressure over the axial lands - psi

Then the equations for the pressures over the lands are;

$$p_c = \frac{12\mu}{h_c^3} \frac{r^2}{2} \frac{dh_c}{dt} \left[\theta^2 - (\theta_2 + \theta_1)\theta + \theta_1\theta_2 \right] + \frac{p_3'}{(\theta_2 - \theta_1)} (\theta_2 - \theta) + \frac{p_o}{(\theta_2 - \theta_1)} (\theta - \theta_1) \qquad \ldots (39)$$

and $$p_a = \frac{12\mu}{h_a^3} \frac{dh_a}{2dt} \left[y^2 - (y_2 + y_1)y + y_1y_2 \right] + \frac{p_3'}{y_2 - y_1}(y_2 - y) \qquad \ldots (40)$$

If the spindle eccentricity ratio is e, then

$$h_a = h_o(1 - e \cos \beta)$$

and $$h_c = h_o(1 - e \cos \beta') \qquad \ldots (41)$$

when $$\beta' = \beta + \frac{\theta_2 + \theta_1}{2}$$

Therefore from the above equation;

$$\frac{dh_a}{dt} = - h_o \cos \beta \frac{de}{dt}$$

and $$\frac{dh_c}{dt} = - h_o \cos \beta' \frac{de}{dt} \qquad \ldots (42)$$

Substituting the above equations in equations (39) and (40), therefore;

$$p_c = -\frac{12\mu}{h_c^3} \frac{r^2}{2} \cos \beta' \, h_o \frac{de}{dt} \left[\theta^2 - (\theta_2 + \theta_1)\theta + \theta_1\theta_2 \right] + \frac{p_3'}{(\theta_2 - \theta_1)}(\theta_2 - \theta) + \frac{p_o}{(\theta_2 - \theta_1)}(\theta - \theta_1) \qquad \ldots (43)$$

$$\text{and } p_a = -\frac{12\mu}{h_a^3}\frac{\cos\beta}{2} h_o \frac{de}{dt}\left[y^2 - (y_2 + y_1)y + y_1y_2\right]$$

$$+ \frac{p_3'}{(y_2 - y_1)}(y_2 - y) \qquad \ldots (44)$$

Differentiating equations (43) and (44); therefore;

$$\left(\frac{1}{r}\frac{\partial p_c}{\partial\theta}\right)_{\theta=\theta_1} = \frac{12\mu}{h_c^3}\frac{r}{2}\cos\beta' h_o \frac{de}{dt}(\theta_2 - \theta_1) - \frac{(p_3' - p_o)}{r(\theta_2 - \theta_1)} \qquad \ldots (45)$$

$$\text{and } \left(\frac{\partial p_a}{\partial y}\right)_{y=y_1} = \frac{12\mu}{h_a^3}\frac{\cos\beta\, h_o}{2}\frac{de}{dt}(y_2 - y_1) - \frac{p_3'}{y_2 - y_1} \qquad \ldots (46)$$

For a capillary compensated journal bearing, the oil flow through the restrictor is given by

$$Q = K_c(p_s - p_3') \qquad \ldots (47)$$

$$\text{where } K_c = \frac{\pi d^4}{128\mu l} \qquad \ldots (48)$$

Then the equation of the oil flow through the pad is;

$$K_c(p_s - p_3') + \frac{h_c^3}{12\mu} 4y_1\left(\frac{1}{r}\frac{\partial p_c}{\partial\theta}\right)_{\theta=\theta_1} + \frac{h_a^3}{12\mu} 4r\theta_1\left(\frac{\partial p_a}{\partial y}\right)_{y=y_1}$$

$$= 4ry_1\theta_1\frac{dh}{dt} \qquad \ldots (49)$$

Putting in the values of $\left(\frac{1}{r}\frac{\partial p}{\partial\theta}\right)_{\theta=\theta_1}$ and $\left(\frac{\partial p_a}{\partial y}\right)_{y=y_1}$ from equations (45) and (46), the above equation becomes;

$$K_c p_s + \frac{h_c^3}{3\mu}\frac{y_1}{r(\theta_2 - \theta_1)} p_o + h_o\frac{de}{dt}\left[2\cos\beta' ry_1(\theta_2 - \theta_1)\right.$$

$$\left. + 2\cos\beta\, r\,\theta_1(y_2 - y_1) + 4ry_1\theta_1\right] = p_3'\left[K_c + \frac{h_c^3}{3\mu}\right.$$

$$\left.\frac{y_1}{r(\theta_2 - \theta_1)} + \frac{h_a^3}{3\mu}\frac{r\theta_1}{(y_2 - y_1)}\right] \qquad \ldots (50)$$

Equating the bearing pad resistance terms to K_b, and simplifying, the equation for the pad pressure is,

$$p_3' = \frac{K_c p_s + \frac{h_c^3}{3\mu} \frac{y_1}{r(\theta_2 - \theta_1)} p_o}{(K_c + K_b)} + h_o \frac{de}{dt} \left[\frac{2 \cos \beta' \, r y_1 (\theta_2 - \theta_1) + 2 r\theta_1 \{\cos \beta (y_2 - y_1) + 2y_1\}}{K_c + K_b} \right] \quad \ldots (51)$$

where $K_b = \frac{h_c^3}{3\mu} \frac{y_1}{(\theta_2 - \theta_1)} + \frac{h_a^3}{3\mu} \frac{r\theta_1}{(y_2 - y_1)}$ ... (52)

The load capacity of the pad can now be calculated from the equations of the pressure distribution over the axial and the circumferential lands, neglecting the load carried by the corners made up of the intersection of the lands.

The total load capacity is the sum of that carried by the pressure pad, the axial and the circumferential lands.

(i) Pressure Pad

The load carried by the pad is;

$$W_p = 2y_1 \int_{-\theta_1}^{\theta_1} p_3' \cos \theta \, r \, d\theta$$

or $$= 4ry_1 \, p_3' \sin \theta_1 \quad \ldots (53)$$

(ii) Circumferential Land

The load carried by the circumferential land is given by;

$$W_c = 4y_1 \int_{\theta_1}^{\theta_2} p_c \cos \theta \, r \, d\theta$$

or $$W_c = -24ry_1 \frac{u}{h_c^3} \cos \beta' \, h_o \frac{de}{dt} \int_{\theta_1}^{\theta_2} \left[\theta^2 - (\theta_1 + \theta_2)\theta + \theta_1\theta_2\right] \cos \theta \, d\theta + 4ry_1 \int_{\theta_1}^{\theta_2} \frac{p_3(\theta_2 - \theta) + p_o(\theta - \theta_1)}{\theta_2 - \theta_1} \cos \theta \, d\theta \quad \ldots (54)$$

Which on integration and simplification gives;

$$W_c = \frac{-24\mu y_1 r^3}{h_c^3} \cos \beta' \, h_o \frac{de}{dt} \left[(\cos \theta_2 + \cos \theta_1)(\theta_2 - \theta_1) - 2(\sin \theta_2 - \sin \theta_1) \right] - 4y_1 r p_3' \left[\sin \theta_1 + \frac{\cos \theta_2 - \cos \theta_1}{\theta_2 - \theta_1} \right]$$

$$+ 4y_1 rp_o \left[\sin\theta_2 + \frac{\cos\theta_2 - \cos\theta_1}{\theta_2 - \theta_1}\right] \quad \ldots (55)$$

(iii) Axial Lands

The load carried by the axial lands is given by;

$$W_a = 2\int_{-\theta_1}^{\theta_1}\int_{y_1}^{y_2} p_a \, dy \cos\theta \, rd\theta \quad \ldots (56)$$

or

$$= -24r \sin\theta_1 \frac{\mu}{h_a^3} \cos\beta \, h_o \frac{de}{dt} \int_{y_1}^{y_2}\left[y^2 - (y_2 + y_1)y + y_1y_2\right] dy + \frac{4r \sin\theta_1 p_3'}{y_2 - y_1}\int_{y_1}^{y_2}(y_2 - y)dy$$

On integration and simplification, this gives;

$$W_a = 4r \sin\theta_1\left[\frac{\mu}{h_a^3}\cos\beta \, h_o \frac{de}{dt}(y_2 - y_1)^3 + p_3'\frac{(y_2 - y_1)}{2}\right] \quad \ldots (57)$$

Therefore, the total load capacity is;

$$W = W_p + W_c + W_a$$

Putting in the values of W_p, W_c and W_a from equations (53), (55) and (57)

$$W = p_3'\left[2r \sin\theta_1(y_2 - y_1) - 4ry_1\frac{(\cos\theta_2 - \cos\theta_1)}{(\theta_2 - \theta_1)}\right] + 4y_1 rp_o\left[\sin\theta_2 + \frac{\cos\theta_2 - \cos\theta_1}{\theta_2 - \theta_1}\right] - \mu h_o \frac{de}{dt}\left[\frac{24r^3 \cos\beta' y_1}{h_c^3}\left\{(\cos\theta_2 + \cos\theta_1)(\theta_2 - \theta_1) - 2(\sin\theta_2 - \sin\theta_1)\right\} - \frac{4r \sin\theta_1 \cos\beta}{h_a^3}(y_2 - y_1)^3\right] \quad \ldots (58)$$

Substituting the value of p_3' from equation (51), the load capacity of the pad is given by;

$$W = \frac{\left[K_c p_s + \frac{h_c^3}{3\mu} \cdot \frac{y_1}{r(\theta_2 - \theta_1)} p_o\right]\left[2r \sin\theta_1(y_2 - y_1) - 4ry_1\frac{\cos\theta_2 - \cos\theta_1}{\theta_2 - \theta_1}\right]}{(K_c + K_b)} + 4y_1 rp_o\left[\sin\theta_2 + \frac{(\cos\theta_2 - \cos\theta_1)}{(\theta_2 - \theta_1)}\right] - \mu h_o \frac{de}{dt}\left[\frac{2\cos\beta' \, ry_1(\theta_2 - \theta_1) + 2r\theta_1\left\{\cos\beta(y_2 - y_1) + 2y_1\right\}}{(K_c + K_b)}\right] x$$

$$\left[4ry_1 \frac{(\cos\theta_2 - \cos\theta_1)}{\theta_2 - \theta_1} - 2r \sin\theta_1 (y_2 - y_1)\right]$$

$$- \mu h_o \frac{de}{dt}\left[\frac{24}{h_c^3} r^3 \cos\beta' y_1\left\{(\cos\theta_2 + \cos\theta_1)(\theta_2 - \theta_1) - 2(\sin\theta_2 - \sin\theta_1)\right\}\right.$$

$$\left. - \frac{4r \sin\theta_1 \cos\beta}{h_a^3} (y_2 - y_1)^3\right] \qquad \ldots (59)$$

The load capacity consists of the load carried by an equivalent steady pressure and that due to the squeeze film effect, and is of the form;

$$W = W_{static} + K_d \frac{dh}{dt} \qquad \ldots (60)$$

where K_d = damping constant - lb/in/sec.

Using the notations of Fig. 1, as in the analysis for the steady load;

$$\frac{y_2 - y_1}{L} = el$$

$$y_2 = \frac{L}{2}$$

$$\frac{\theta_2 + \theta_1}{2} = \alpha_2$$

$$\theta_1 = e\alpha.\alpha_2$$

$$\theta_2 = \alpha_2(2 - e\alpha)$$

$$Z_1 = \frac{K_c}{K_b}$$

and $$p_o = \left(\frac{Z}{\pi + Z}\right)p_s \qquad \ldots (61)$$

The equation (59) can therefore be expressed as;

$$W_{static} = \frac{p_s}{1 + \frac{1}{Z_1}}\left[L\ el\ D \sin(e\alpha.\alpha_2) - \frac{LD(1 - 2\ el)}{2\alpha_2(1 - e\alpha)}\right.$$

$$\left.\left\{\cos\alpha_2(2 - e\alpha) - \cos e\alpha.\alpha_2\right\}\right]$$

$$\frac{p_s Z h_o (1 - e\cos\beta')^3 L(1 - 2\ el)}{6\mu D \alpha_2(1 - e\alpha)(Z_1 + 1)(Z + \pi)K_b}\left[Lel\ D \sin(e\alpha.\alpha_2) - \frac{LD(1 - 2\ el)}{2\alpha_2(1 - e\alpha)}\right.$$

$$\left\{\cos\alpha_2(2-e\alpha)-\cos e\alpha.\alpha_2\right\}\Big]$$

$$+\frac{p_s Z}{(Z+\pi)}\,LD(1-2\,el)\left[\sin\alpha_2(2-e\alpha)+\frac{\cos\alpha_2(2-e\alpha)-\cos e\alpha.\alpha_2}{2\alpha_2(1-e\alpha)}\right] \qquad \ldots (62)$$

and the damping constant is;

$$K_d=\frac{12\mu}{h_o^3}\left\{\frac{DL\,\alpha_2(1-2el)(1-e\alpha)\cos\beta'+LD\,\alpha_2 e\alpha\left[\cos\beta.el+1-2el\right]}{(Z_1+1)}\right\}x$$

$$\frac{(Lel)\left[2\alpha_2(1-e\alpha)\,DLel\,\sin(\alpha_2 e\alpha)-LD(1-2el)\left\{\cos\alpha_2(2-e\alpha)-\cos\alpha_2 e\alpha\right\}\right]}{2L^2(1-2el)el(1-e\cos\beta')^3+4D\,\alpha_2^2\,e\alpha(1-e\alpha)(1-e\cos\beta)^3}$$

$$+\frac{D\sin(\alpha_2 e\alpha)}{6(1-e\cos\beta)^3}(Lel)^3\cos\beta$$

$$+\frac{D^3L}{8}\frac{(1-2el)}{(1-e\cos\beta')^3}\cos\beta'\left[2\left\{\sin\alpha_2(2-e\alpha)-\sin\alpha_2 e\alpha\right\}\right.$$

$$\left.-\left\{\cos\alpha_2(2-e\alpha)+\cos\alpha_2 e\alpha\right\}\left\{2\,\alpha_2(1-e\alpha)\right\}\right]\Big\} \qquad \ldots (63)$$

The effect of the pad geometry factor on the damping constant of a journal bearing is shown in Fig. 13. It is clear that the damping constant increases rapidly by increasing both the axial and the circumferential land ratios. As shown in Fig. 14a, the damping constant drops with a larger ratio of the resistances of the pad and the capillary restrictor, Z_1. It is interesting to see that for a given pad goemetry, both the normal stiffness and the damping constant decrease with larger radial clearance and a lower oil film thickness offers advantage for both the steady and the dynamic loads.

2.2b. Dynamic Load Analysis of a Hydrostatic Bearing System

As for the static deflection curves, computer programmes have been prepared for determining the natural frequencies, modal shapes, modal damping ratios and the general response to the dynamic load of three

dimensional structures. The distributed mass of the elements is replaced by set concentrated masses located at the station points. The bearing is converted into a helical and torsional spring as before, and a single dashpot damper is included in the system in the directions of loading (Fig. 9.).

The variation of natural frequency and damping ratio with rotational flexibility is shown in Figs. 15 and 16 respectively. It is seen, once again, that a lower flexibility is desirable for dynamic loads as well as the steady loads considered earlier. As shown in Fig. 16, the damping ratio is lower for higher bearing stiffness and it is here that the two important parameters are in direct conflict. It would therefore be necessary, to establish a compromise criterion for selection of the bearing stiffness and damping constant.

The effect of the damping constant on the damping ratio of the system is shown in Fig. 17, where it is obvious that the concept of increasing the damping ratio by increasing the damping constant can be misleading. The shape of the curve could be explained by considering first zero damping in the system which would result in zero damping ratio, and then a very large value of the damping constant - which implies zero spindle deflection at the bearing, hence again a zero damping ratio. It follows therefore, that finite damping ratios must appear for intermediate values of damping constant and an optimum for which the damping ratio is a maximum depending on the equivalent spring stiffness of the bearing.

Hence, for a particular normal stiffness of the bearing, determined from static deflection programmes, a damping constant can be selected to give the best damping ratio, and taken to its logical conclusion, a pad geometry can be selected to give this damping constant.

The resonant frequency is not appreciably affected by the damping constant as shown in Fig. 18. Similarly the damping ratio does not vary

considerably with the rotational flexibility over the whole range of the damping constants of the bearing pad. Fig. 19 shows the variation of the damping ratio for rotational flexibilities of 500 x 10^{-9} and 10,000 x 10^{-9} rad/lb in. The variation of resonant frequency shows higher value for stiffer bearing, the two curves following almost identical pattern for various values of the damping constant.

2.3. Hydrostatic Thrust Bearing

The analysis of an anular thrust bearing with capillary compensation for steady loads has been covered in the earlier thesis and only the results of that will be included here.

2.3a. Oil Flow

The oil flow in the bearing is given by the equation;

$$Q = \frac{\pi p h^3}{6\mu} K_f \qquad \ldots (64)$$

where $K_f = \frac{1}{\log \frac{r_2}{r_1}} + \frac{1}{\log \frac{r_4}{r_3}}$ ... (65)

For capillary compensation, the pad pressure is given by

$$p = \frac{p_s}{1 + \frac{\pi h^3 K_f}{6K_c}} \qquad \ldots (66)$$

where $K_c = \frac{\pi d^4}{128\mu l}$; as for a journal bearing.

2.3b. Load Capacity and Stiffness

The load capacity is given by the equation;

$$W = \frac{p_s}{\frac{2}{\pi K_1} + \frac{h^3 K_f}{3K_1 K_c}} \qquad \ldots (67)$$

where $K_1 = \frac{r_4^2 - r_3^2}{\log \frac{r_4}{r_3}} - \frac{r_2^2 - r_1^2}{\log \frac{r_2}{r_1}}$ ... (68)

Therefore, the stiffness of the bearing is;

$$S = - \frac{K_f K_1 K_c p_s}{\left[\frac{K_f h^2}{3} + \frac{2K_c}{\pi h} \right]^2} \qquad \ldots (69)$$

2.3c. Total Power Requirement

The total power requiremrnt is given by the equation;

$$P = \frac{1}{6600} \left[\frac{2}{3\pi} \frac{K_f W^2 h^3}{\mu K_1^2} + \frac{\mu N^2 K_p}{58.05h} \right] \qquad \ldots (70)$$

where $K_p = (r_4^4 - r_3^4) + (r_2^4 - r_1^4)$ ... (71)

By differentiating equation (70) and equating to zero, the optimum oil film thickness for minimum total power requirement is;

$$h_{opt} = 0.406 \sqrt{\frac{\mu N}{W}} \left[\frac{K_p K_1^2}{K_f} \right]^{\frac{1}{4}} \qquad \ldots (72)$$

The design of the thrust bearing pad is subject to the same discussion as the journal bearing, and hence will not be covered in detail here. The variation of the oil flow and the total power requirement with the width of the land is shown in Fig. 21. It is noticed again that for a particular oil film thickness, one value of the land width requires minimum total power, while each of the lines shows constant stiffness characteristics. Hence, an oil film thickness can first be chosen for a required stiffness, and consequently a pad geometry selected for minimum power requirement.

CHAPTER III

EXPERIMENTATION AND RESULTS

The performance of the hydrostatic bearing system was mainly investigated to determine the following three characteristics;

1. Temperature distribution and heat balance
2. Steady load deflection
3. Dynamic response

3.1. Tempeature Distribution and Heat Balance

The hydrostatic bearing system for this investigation consisted of two journal bearings to support the main spindle and carry the radial loads, and a double film thrust bearing to take axial loads in either direction. The spindle could be loaded radially through another journal bearing, connected to a hydraulic cylinder supplied with oil under high pressure.

3.1a. Journal Bearing

The design features of the hydrostatic journal bearing are shown in Fig. 22. The main feature of the bearing was the interchangeable brass bush, which was screwed on to the main housing with the pad geometry machined on it, to enable bearings of different geometrical configurations and radial clearances to be employed without any major alteration in the assembly.

Sixteen $\frac{1}{4}$ BSF screws were mounted radially in one bearing to carry thermocouples for measuring the temperature of the oil film along the bush circumference. In the other bearing eight screws were fixed up to the bush internal diameter, while alternately eight more were mounted at a distance of $\frac{3}{8}$ in. from the bush. The bush internal diameters of both the bearings were finish bored in one operation with these screws in position for accurate alignment and consistent tolerances on both bearings.

3.1b. Thrust Bearing

Fig. 23 shows the main design features of the hydrostatic thrust bearing. As for the journal bearing, the annular pad configuration is machined on a brass disc and is screwed to the main body. The brass pads are then finish machined with the main body to give the correct clearance between the bearing and the thrust face of the main spindle and such that the two faces are parallel to one another and coaxial.

3.1c. The Hydraulic Circuit

A closed hydraulic circuit was designed for the system and a schematic diagram is shown in Fig. 24. High pressure oil was supplied to the bearings by a pump through a filter and the pressure was controlled by the combination of the pressure relief and control valves. All the pressure pads in one bearing were supplied from an oil distributor through identical capillary restrictors and the pressure was regulated with valves.

The outlet oil was collected in a drip tray placed around the table and was pumped back to the manifold through another filter.

3.1d. Capillary Restrictors

The compensating elements consisted of cold drawn stainless steel capillary tubing, .033 in. by .048 in. o.d. for the journal bearings and .084 in. by .112 in. o.d. for the thrust bearings. These were sealed with araldite in special $\frac{3}{8}$ in. diameter adaptors and were mounted in the pressure line to the bearings as shown in Fig. 24.

3.1e. Temperature Measurement

Thermocouples were mounted around the bearing bush to measure the circumferential and the radial temperature distribution in the journal bearing. The $\frac{1}{4}$ BSF screws were drilled and the thermocouples were inserted in them and sealed with araldite, which held them in position and insulated them from the screws and the bearing body. The thermo-

couple bead was carefully adjusted in line with the end of the screw which had been finish machined earlier with the internal diameter of the bearing bush, thus ensuring that all the thermocouples were flush with the bush diameter, when mounted in the housing. In one of the bearings sixteen thermocouples were mounted around the bush circumference to give the circumferential temperature distribution of the oil film, while in the other eight of them were fixed $\frac{3}{8}$ in. from the bush to give the radial temperature gradient in the bearing housing.

A thermocouple was also fixed in the inlet pipe to the bearing for accurate determination of the rise of temperature of the oil in the bearing.

The electric circuit employed for the temperature measurement is shown in Fig. 25. The thermocouples were grouped together in blocks of eight and through a selector switch were connected to a four channel U.V. recorder. To eliminate any error in individual block circuits, one thermocuple in each block was taken as reference and put in ice cooled water along with the cold junction.

The experimental set up of the bearing system with the thermocouple leads to the distribution box and the U.V. recorder is shown in Fig. 26. The experiments were performed by slightly preloading the spindle, to offset the effects of the belt tension and the thrust face load, such that the pressures in the four pads of the first journal bearing were approximately the same and the spindle could be assumed concentric in the bearing. The thermocouples along the bearing bush circumference and the ones radially displaced were at first connected to different galvanometer circuits respectively, but to eliminate any error in calibration, the thermocouples in the two halves of the bearing circumference were separately connected to two galvanometer circuits. Thus the temperature readings for thermocouples along the

bush circumference and radially displaced in one half of the bearing were taken by the same galvanometer, which also recorded the inlet oil temperature.

Temperature readings were obtained for spindle speeds of 500, 1050 and 1900 rpm and maximum temperature rise was observed to be 3.6 , 6 and 10.4°C, while the radial temperature difference between the two sets of thermocouples was found to be 1.0, 1.5 and 2.5°C respectively.

The procedure for the calculation of the heat dissipated to the oil and the bearing housing is outlined in Appendix III. The oil flow was determined from the average pad pressure and the viscosity at the mean oil temperature, and the heat carried away by the oil from the average temperature rise of the oil in the bearing. For the estimation of the heat given to the bearing housing, heat flow was assumed only from the bearing axial lands and approximately between cylindrical surfaces composed of the brass bush and the mild steel housing. It is realized that the heat flow from the housing will follow a more complex pattern and the estimate presented is likely to be lower than the actual heat conduction, but with the distance between the two sets of thermocouples only $\frac{3}{8}$ in., straight path heat flow was assumed to simplify the calculations.

The heat dissipated to the oil and the bearing housing is shown in Fig. 27. It was found that while the ratio of the two was nearly the same for various spindle speeds, the oil accounted for almost twice as much heat dissipated as the bearing housing.

3.1f. Torque Measurement

The technique of measuring torque on spindles by fixing strain gauges at 45° to the axis and diametrically opposite each other to form a Wheatstone bridge is fairly standard[28] and shall not be discussed in great detail here. An improvement on this procedure is the use of torque gauges which are available as one or more paired elements,

consisting of a single Vee formation of an active and dummy element. Multiple paired elements can be employed to increase the bridge resistance, the gauge area and therefore the heat dissipating capacity and to measure the average strain in the spindle. The gauges can be mounted diametrically opposite each other, with their centre lines in an axial or circumferential direction (Fig. 29).

For the present work four Saunders Roe torque foil gauges were employed[29] in series to increase the resistance of the arms of the bridge, and were mounted diametrically opposite each other circumferentially, with strain gauge adhesive and hardener. The usual precautions were taken while fixing the strain guages, i.e. no air bubbles were trapped between the bonding surface of the strain gauge and the steel coupling.

The Wheatstone bridge circuit employed for measuring the torque is shown in Fig. 30. The output from the bridge was taken through slip rings mounted over an insulation ring of synthetic resin bonded paper, to an amplifier and the signal was transmitted to a U.V. recorder.

To eliminate the inaccuracies of contact resistance of the brushes and the slip rings, a mercury pool was at first tested for transmitting the output current from the slip rings. The performance of the mercury pool commutator was found satisfactory electrically and the calibration of the gauges was done on a torque calibrating equipment shown in Fig. 31., while the calibration curves for both clockwise and anticlockwise torque are shown in Fig. 32.

However, during experimentation, the mercury tended to fly off with the slip rings, most generally shorting the circuit and this method, therefore, had to be abandoned.

A brush assembly was then mounted, with three brushes at 120^{o} intervals around each slip ring, to compensate any contact error on one

brush by the other two around the periphery. Considerable difficulty was encountered while taking the measurements with this assembly. The contact resistance across the brushes and the slip rings tended to vary with spindle rotation at different speeds from the static condition. The brushes heated up at higher speeds even with very small spring pressures and the heating and the change in contact resistance invariably upset the static balance of the bridge. Hence satisfactory results over long periods of performance could not be obtained, and the effects of speed on power loss and oil viscosity could not be studied. It was later felt that the oil temperature in the various bearings would be different due to the spindle inclination even at no load, and it would be difficult to analyse individual bearings and study the effect of speed on power loss in journal bearings accurately. Therefore the experiments were not carried any further.

3.2. Steady Load Deflection

To establish the validity of the theoretical analysis on the rotational flexibility of the journal bearing this investigation was carried out with the system consisting of the main spindle and two journal bearings. The spindle deflection shape was obtained by applying load to the pulley mounted on the spindle end, with dial gauges placed at various places along the spindle as shown in Fig. 33. Experiments were performed with supply pressures to the bearings ranging between 25 and 600 p.s.i. and maximum load of 90 lbs. The spindle deflection shape, as determined from the readings of the dial gauges for loads of 10 lbs and 90 lbs. for different supply pressures is shown in Fig. 34. The spindle end deflection was simulated from these curves and is shown in Fig. 35 for various supply pressures.

It was found that for low bearing pressures, the spindle deflection depended more on the bearing stiffness, while for higher pressures the

spindle end deflection was dependant on the spindle stiffness. Thus there was little difference in the spindle end deflection for bearing pressures of 400 p.s.i. and 600 p.s.i. and there would virtually be no advantage in increasing the bearing pressure any further.

3.3. Dynamic Response

To determine the dynamic characteristics of the journal bearing including the damping ratio, the experiments were performed at first with the main spindle and the two journal bearings as shown in Fig. 36, by applying harmonic force to the spindle and obtaining the frequency response curves. The circuit employed for the experiments is shown in Fig. 38. A Solartron Oscillator model CO 546 operating on a Wien network was employed to drive the vibrator motor through an amplifier model PP 250 VAP. The frequency of oscillation is selected by the range switch and calibrated dial on the oscillator from 25 c/s to 500 kc/s. By making use of the calibrated scale and the vernier any frequency can be set with an accuracy of 1 in 3000.

The amplifier is designed to produce an output of 250 VA over a frequency range of 20 Hz to 10,000 Hz with an anode dissipator capacity of 500 watts. An input signal of 0.7 volts r m s is required for full output.

Four illuminating on/off switch push buttons are fitted to the front panel, two marked 'HEATER' and the other two marked 'P.A.'. The green 'HEATER' button switches on the driver stages while the green 'P.A.' button switches on the power amplifier or the output stage. During normal operation the lamps show a steady light but in case of a fault or overload, the lamp monitoring the faulty circuit flashes warning of a fault indicating the affected circuit.

The displacement of the spindle was obtained with a quartz accelerometer which gives the acceleration of the point under test.

The signal from the accelerometer is transformed to a proportional output voltage in the charged amplifier and fed to the oscilloscope. The displacement can then be calculated by the relation;

$$d = \frac{a}{(2\pi f)^2} \qquad \ldots (73)$$

where d = displacement

a = acceleration

f = applied frequency

A force transducer was mounted between the vibrator and the pulley to determine the force applied to the spindle. The transducer was a quartz load washer type, which converts the mechanical force into an electrostatic charge signal. The signal is transformed into a proportional output voltage in a Kistler charged amplifier and transmitted to the oscilloscope.

3.3a. Frequency Response Curves

The frequency response characteristics were obtained for various bearing supply pressures and the curve for p_s = 100 p.s.i. is shown in Fig. 40 where the acceleration output obtained on the oscilloscope for various forced frequencies is directly plotted. It was noticed that the first mode amplitude of the spindle end was the only significant one as all the other values become small when converted into actual displacements from the acceleration plot of Fig. 40. The absolute displacement is given by the equation (73), therefore compared to the first mode displacement amplitude, the value at any subsequent mode is;

$$d_n = a_n \left(\frac{f_1}{f_n}\right)^2 \qquad \ldots (74)$$

where d_n and a_n are the displacement and acceleration amplitudes respectively at nth mode frequency.

The frequency response curves for higher supply pressures were nearly the same and to avoid overlapping of these curves they have not

been included in Fig. 40. However larger scale plots for supply pressures of 100, 200 and 400 p.s.i. in the vicinity of the first resonant frequency are shown in Fig. 41 to determine the damping ratio of the system.

3.3b. Damping Ratio

The procedure for determining the damping ratio of the system from the frequency response characteristics for acceleration is outlined in Appendix IV. For the present work, the two frequencies before and after the resonant to give 85% of the peak acceleration amplitude were found from Fig. 41 and the damping ratios were then calculated. It was found that the displacment and the resonant frequency for supply pressures of 100, 200 and 400 p.s.i. were not very different but the damping ratio was higher for the lower pressure bearings. The variation in the damping ratio and the modal displacement of the spindle end is shown in Fig. 42.

Experiments were also performed with spindle end preload and the enlarged frequency response curves for p_s = 200 p.s.i. are shown in Fig. 43 while the variation in the damping ratio, resonant frequency and displacement amplitude as compared to no preload is shown in Fig. 44. It was found that both the damping ratio and the resonant frequency increase slightly with spindle deflection in the bearing due to the preload.

3.3c. Modal Shapes

The modal shapes of the spindle at the first three resonant frequencies were obtained by placing the accelerometer along specially made flat surfaces on the spindle in line with the axis of vibration, and determining the amplitude and the phase of the signal on a Resolved Component Indicator. This instrument displays the 'in phase' and 'quadrature' components of an A.C. signal with respect to the related

reference voltage.

It consists of two thermocouple wattmeters and the associated electronic circuits to drive them. Two signal inputs are required, a constant amplitude from phase reference signal and the signal to be measured. The 0^{o} and 180^{o} phases of the reference signal energise one wattmeter, and the 90^{o} and 270^{o} phases energies the other. The signal to be measured is amplified and fed to the two wattmeters, one of which indicates that component of the test signal in phase with the 0^{o} and the 180^{o} reference phases, while the other indicates that component at 90^{o} to them.

The output points are plotted on cartesian co-ordiantes and define the signal in amplitude and phase.

Figs. 45, 46 and 47 show the three modal shapes of the spindle with the respective phase difference between the spindle end and the various other points on the spindle. Results obtained from the computer programmes are also shown in each case for the purpose of comparison.

In the second stage of the experimentation, frequency response curve was obtained with the thrust bearing in position as shown in Fig. 37 and is drawn in Fig. 40. It was found that the thrust bearing made almost nelgigible difference to the resonant frequency of the system but the damping ratio was higher and the displacement amplitude at the first resonant frequency was lower and almost indistinguishable for second and third frequencies. However, the amplitude of vibration for the other points on the spindle, away from the thrust bearing, was not significantly different as shown in Fig. 45.

CHAPTER IV

DISCUSSION

4.1. Temperature Distribution and Heat Balance

A similar investigation on a hydrodynamic journal bearing by COLE[18] has been taken as the basis for discussing the results of the present work. It has already been reported in the earlier thesis[23] that the temperature along the bearing bush circumference was quite uniform when the spindle was concentric in the bearing, while the profile of the temperature rise followed the spindle deflection in the bearing due to radial loads. The maximum rise occurred along the line of load and the minimum film thickness, and hence for the maximum eccentricity ratio of .70 and speed of 1900 r.p.m. encountered in the present experimentation, the hydrodynamic effect in the bearing was found to be negligible.

The profile of the temperature rise along the bearing circumference was quite smooth and there were no sharp temperature changes as in hydrodynamic lubrication. Perhaps the conditions of load and speed in the present work were not severe enough to cause large variations in temperature along the bush circumference but it seems that the bearing was kept at a more uniform temperature due to large oil flow. Hence there would not be any large local variations in oil viscosity in the hydrostatic journal bearings caused by these temperature differences, and the dangers of bearing failure due to this critical factor seem considerably reduced.

It was found that the oil carried away approximately 65% of the heat dissipated to the oil and the bearing housing and this high percentage was probably due to large oil flow. Since the temperature was higher for higher speeds, the larger reduction in oil viscosity due to this temperature rise caused greater oil flow and this seemed to help in keeping the ratio of the heat dissipation to the two

elements the same for various spindle speeds. Heat flow to the spindle was not determined experimentally and in the absence of power loss measurements in the journal bearing, no approximate estimation was possible, and hence the complete heat balance of the bearing could not be prepared either.

Though the maximum temperature in the bearings was by no means high, yet assuming constant viscosity of the oil as at room temperature is likely to cause error in the design of optimum parameters for the bearing system, especially for orifice compensation where the oil density is also a variable factor. In the present case it was found that as the temperature increased after starting the experiment, it caused a much higher oil flow to the thrust bearing and since all the bearings were being supplied oil from the same pump through different control valves (one each for the thrust bearing and the journal bearings, Fig. 24.) this ultimately upset the balance in the system with consequent drop in the journal bearing pressure. Hence, a more practical value of temperature and oil viscosity should be considered for designing the hydraulic system, pump capacity etc., especially for large oil flow systems.

It is appropriate to mention that the temperature of the inlet oil continued to rise during experimentation, partly due to the inefficiency of the cooler in the system. The temperature build up in the bearing is shown in Fig. 28 and it was found that while the bulk of the temperature increased during the first hour, the temperature continued to rise even after three hours of running. Due to this cumulative effect the oil temperature in the bearing went up to about $50^{\circ}C$ even though the maximum rise in the bearing itself was only about $10^{\circ}C$ for spindle speed of 1900 r.p.m. While steady state temperature is not critical for hydrostatic bearing performance

yet it is desirable to stabilize the flow characteristics of the bearing which are so sensitive to changes in oil viscosity. The importance of the cooler in a hydraulic system is not always realized as in the present case where the wrong type of cooler was installed in a new hydraulic rig, but an efficient cooler would be able to dissipate all the heat generated and maintain the inlet oil temperature as close to the room temperature as possible and thus limit the bearing temperature rise to that caused only by the losses in the bearing itself. With a new cooler more appropriate for the present low oil flow system the maximum temperature in the bearing was about 35°C at speeds of 1900 r.p.m.

It was found that most of the temperature rise in the bearing occurred due to the spindle rotation and since the dynamic tests were performed with the spindle stationary, the effect of temperature rise on the dynamic characteristics of the bearing could not be studied. The maximum temperature with p_s = 400 p.s.i., with the spindle stationary, was only 26°C and the temperatures were not found to be very different nor critical for the range of pressures encountered.

4.2. Steady Load Deflection

It was found that greater accuracy in the results from the computer programmes could be achieved by dividing the bearing system into fourteen elements instead of eight as discussed in detail in the next section, and a comparison of the spindle deflection shape obtained from this new model and the experiments is shown in Fig. 48. It shows that the programme can be used very successfully for prediction of the spindle deflection shapes. Fig. 49 shows the comparison of the experimental results of the spindle end deflection with those determined by the computer programmes and it was found that the theoretical

expressions for the rotational flexibility could be used for very accurate computation of the spindle end deflection. The very small differences in the two results could be attributed to experimental errors with the dial gauges and approximations in the computer model. The bearing stiffness in the model was assumed linear in the programme and though this assumption is not strictly true (since the stiffness of a journal bearing is not linear, especially for high eccentricity ratios) yet the spindle end deflection was found reasonably linear for the range of loads applied in the present experimentation, as shown in Fig. 35b.

It would be quite appropriate at this stage to discuss the relative importance of the bearing and the spindle stiffnesses in a bearing system. It has been shown in section 3.2 that for the present system there would virtually be no advantage in increasing the bearing pressure from 400 to 600 p.s.i., since the spindle end deflection is not substantially reduced. It seems that beyond a certain normal and rotational stiffness of the bearing, the spindle is clamped at the bearing point and the spindle end deflection is mainly a function of the spindle stiffness and is hence nearly the same for even higher bearing stiffnesses. It can be seen in Figs. 10 and 11 that while higher stiffness of the bearing reduces the spindle deflection at the bearing point, it does not proportionately reduce the spindle end deflection and hence attention has to be paid to the spindle design as well for keeping the spindle end deflection in a bearing system as small as possible. For a given system there is no substantial reduction in the spindle end deflection by increasing the bearing stiffness beyond a particular value and this can be conveniently determined with the help of the computer programmes as outlined here.

4.3. Dynamic Response

The frequency response characteristic showed that the fundamental resonant frequencies for the three supply pressures where very close to each other, but contrary to expectations the frequency of response was lower for higher bearing pressures. Although the higher pressure in the bearing implies higher normal stiffness, yet it has a smaller damping coefficient and it is the combination of these two factors which determines the equivalent stiffness of the bearing to dynamic loads and the resonant frequency of the system. Results obtained from the computer programmes also show (Fig. 18) that for large damping constants, the first resonant frequency of the system for lower normal stiffness of the bearing is indeed higher.

The damping ratio was higher for lower supply pressures to the bearing, as expected from the analysis. Since the lower stiffness of the bearing permits larger deflection of the spindle, this increases the damping and produces a higher damping ratio of the system for dynamic loads.

The higher equivalent dynamic stiffness of lower supply pressure bearings also reduces the resonant amplitude of vibration as shown in Fig. 42, with the minimum somewhere between 100 and 200 p.s.i. The variation in the amplitude of vibration for various supply pressures at their first resonant frequencies compared to p_s = 100 p.s.i. and the phase angles determined with the Resonant Component Indicator is shown in Fig. 50. It was seen earlier that there was no substantial reduction in the spindle end deflection for steady loads with bearing pressures higher than 400 p.s.i., and it is clear now that there was in fact an increase in the amplitude of vibration for dynamic loads with pressures higher than 200 p.s.i. In a bearing system, therefore, there is no real advantage in increasing the normal stiffness beyond

a particular value even for steady loads and this higher stiffness at the same time reduces the damping ratio for dynamic loads. Hence, it seems that the spindle end amplitude of vibration, which reflects the equivalent dynamic stiffness of the bearing, could be used as the criterion for the selection of the bearing normal stiffnesses.

The resonant frequency and the damping ratio both increased with preload as shown in Fig. 44. It appears that with the spindle deflection in the bearing the equivalent dynamic stiffness of the bearing increased due to the higher damping constant for a smaller film thickness, and this increased both the resonant frequency and the damping ratio of the system while decreasing the amplitude of vibration. This suggests that during a metal cutting process in a machine tool causing preload on the spindle, the dynamic performance will be no worse than that determined from the theoretical analysis with no preload.

The results from the computer programmes are shown in Fig. 51 and these confirm the trends of the experimental work discussed above. The fundamental resonant frequency, determined from the programme was only 10% lower than the experimental value. It was also found that the amplitude of vibration was smaller for higher stiffness bearings when damping in the system was neglected in the programme, but when damping was incorporated the amplitude was higher, as in the experiments, due to the combination of the normal stiffness and the damping coefficient causing a lower equivalent dynamic stiffness. The slope of this curve would obviously depend on the damping constant of the bearings.

Although the results from the computer programmes for the resonant frequency and the modal shapes correlated well with the experimental values, yet they were not felt to be accurate enough for the present

investigation. Apart from the discrepancy in the first resonant frequency, the modal shape and the node points for the second and the third modes could not be accurately determined with an eight element model of the bearing system. Hence, it was decided to divide the bearing system into fourteen elements to take into account all the discontinuities in the spindle and eliminate the inaccuracies and approximations in the calculation of the flexibilities of the various elements in the model.

To determine the ability of the computer programmes to deal with any system of hydrostatic bearings, experiments for correlation were performed on two spindle systems. One of the systems consisted of the large pulley mounted on the main spindle as shown in Fig. 36, while the other consisted of a small pulley of $2\frac{1}{2}$ in. diameter at the spindle end as shown in Fig. 9. Since the first system was more convenient for determining the comparable performance with a thrust bearing in the system (Fig. 37) and it was also felt that a large pulley at the spindle end would closely simulate the condition of performance of a lathe spindle with a head stock, it has been discussed above. However, only one result could be obtained for the fourteen element model of the second system, with damping incorporated in the programme, and despite several attempts no further success could be achieved. This was attributed to ill conditioning in the dynamic equations and the matrix for the computer programme, a condition not apparent for the eight element model. Hence, the subsequent discussion will be confined to the results of the experimental work on the second system and the computer programme.

The modal shapes of the second system with the results of the 14 element model programme are shown in Figs. 52, 53 and 54. It was found that more accurate results could be obtained by increasing the number

of elements in the model. The first resonant frequency predicted was within 1% of the experimental value, while the modal shapes and the node points were much better defined. The computer programme predicted sharp changes in phase relationship between various station points since it only takes discrete damping at the station points into account, while the experiments showed gradual changes along the length of the spindle due to distributed material damping. Consequently the differences between the results of the experiments and the computer programme were larger near the node points and best correlation was thus obtained for the first mode. However, the results of the programme were close enough in range and magnitude to permit their application to similar systems for predicting the resonant frequency and the modal shapes.

The comparison of the results for the damping ratio was more difficult since the damping ratio is a function of the normal and rotational stiffnesses and the damping constants of the bearings and the spindle system and both the theoretical analysis and the computer programme were based on simplifying assumptions and approximations. The resonant frequency is dependent largely on the normal and rotational flexibilities of the bearing and the spindle, and since these parameters can be calculated fairly accurately, the first resonant frequency is determined very close to the experimental value. However the determination of the damping ratio, experimentally and with the computer programmes was more elusive. The forced frequency response method was employed in the present case, and though it is generallly considered quite acceptable, yet for small damping ratios, any slight variation in the drawing of the frequency response curves introduced large errors in the results. The calculation of the damping ratio for 80% and 85% acceleration amplitude ratios on the frequency response curves gave

different results and hence a direct method of determining the damping constant applicable to the bearings could not be employed. An approximate method, however, was tried, as shown in Fig. 55, by drawing the variation in the damping ratio with the bearing normal flexibilities for various damping constants from Fig. 17 and plotting the experimental values on this Fig. to get the damping constant to which these curves most closely related in slope and magnitude. It was thus found that the damping constant of the system was nearer to 400 and much lower than calculated from the equation (63) in Chapter II ($\approx$ 1600). Since the Fig. 55 was itself drawn with results for an eight element model it is not known how much inaccuracy is introduced due to this factor. However, it is clear that a more accurate theoretical analysis, computer programme and experimental procedure is required to determine the correct damping value in the system. The difficulty in the calculation of the damping ratio from the experimental results has been stated earlier. In the computer programme, no material damping has been considered and this may be contributing some error to the results. The simplifying assumptions in the theoretical analysis for the squeeze film equation of a journal bearing do not appear to adequately represent the actual conditions of performance, and hence it is felt that it will be necessary to take into account both the liquid compressibility as well as the changes in the side pad pressures due to dynamic load, for getting more accurate results. At the same time, the mean oil film thickness assumed over the axial and the circumferential lands is not true by any means. Due to the spindle curvature, the oil film thickness over the axial lands of the pad is larger towards the horizontal axis away from the vertical load line as shown in Fig. 12. and the mean oil film thickness assumed at $\theta = 0^{\circ}$ in fact is the minimum over the axial lands. This increase in the film

and the area is likely to reduce the resistance of the axial lands to oil flow. It was reported earlier[23] that for steady loads the circumferential oil flow reduces the normal stiffness of the bearing even more than determined from the analysis and it is likely that for dynamic loads too, the drop in side pad pressures would increase the oil flow in the circumferential direction. Since the film thickness increases over the circumferential lands as well, due to the spindle curvature, the lands would also offer less resistance to extrusion of the oil due to dynamic loads. Both these reductions in the resistance of the pad would therefore decrease the damping constant of the journal bearing.

It is a coincidence that this drop in the damping constant has produced near optimum conditions of damping for the present system. If the damping constant had been as high as calculated from the theoretical analysis, the damping ratio of the system would have been much smaller as shown in Fig. 17 and nearly the same for all bearing pressures.

CHAPTER V

CONCLUSION

The computing technique can be successfully employed to determine the characteristics of similar hydrostatic bearing systems, and knowing the preferential requirements of the system, i.e. stiffness, power etc., an optimum pad geometry for the journal bearings from both the steady and dynamic load considerations can be selected. Also, the range of maximum stiffnesses effective to limit the steady load deflection and the amplitude of forced vibration of the spindle in a bearing system can be assessed. The input data requirement of the bearings for the model in the program can be calculated from the theoretical analysis presented, and by dividing the system into as large a number of elements as possible, very accurate results of spindle deflection curve, resonant frequency etc. can be obtained.

A more rigorous analysis is required to determine the damping characteristics of a journal bearing, and the effects of liquid compressibility, leakage factors across the axial and the circumferential lands, location of the compensating element etc., need to be considered for an exact solution.

In machine tools, it is now considered advisable to locate the thrust bearing nearer to the spindle end, to prevent spindle distortion due to thermal expansion, and since the thrust bearing reduces the amplitude of vibration of the spindle end, it should also be considered in preparing the model of the system for the computer programs.

The effect of temperature on the performance of hydrostatic bearings is not as considerable as in hydrodynamic bearings. The

temperature rise within the bearing was not substantial and inefficient cooling contributed a large share to the actual temperature in the bearing, and hence more attention should be paid to the cooler design. Due to more uniform temperature distribution with spindle deflection, the danger of bearing failure is less likely and therefore the design of the hydrostatic journal bearing of comparable dimensions can be mainly considered from the considerations of static and dynamic stiffness outlined earlier, though a more practical value of working temperature and oil viscosity should be taken for calculating the design parameters, pump capacity etc.

BIBLIOGRAPHY

1. MANNAM, J., FOWLER, J.H., CARPENTER, A.L. - "Tapered Lands Hydrostatic Journal Bearings"; Proceedings of the Institute of Mechanical Engineers, Lubrication and Wear, Third Convention, 1965, p.78.

2. KEARNEY, G.P. - "Master and Slave Bearing Systems for Machine Tools"; Journal of Mechanical Engineering Science, Vo. 8, No. 2, 1966, p.152.

3. HIRS, G.G. - "Externally Pressurised Bearings with Inherent Friction Compensation"; Trans. ASME, Journal of Applied Mechanics, Vol.87, 1965, p.285.

4. SHINKLE, J.N., HORNUNG, K.G. - "Friction Characteristics of Liquid Hydrostatic Journal Bearings"; Trans. ASME, Journal of Basic Engineering, Vol. 87, 1965, p.163.

5. ROYLE, J.K., HOWARTH, R.B., CASELEY-HAYFORD, A.L. - "Application of Automatic Control to Pressurised Oil Film Bearings"; Proceedings of the Institute of Mechanical Engineers, 1962, 176(22), p.532.

6. SCHER, R.S. - "Theoretical and Laboratory Performance of a Pressurised Journal Bearing with Positional Feedback Control"; M.Sc. Thesis, Massachusetts Institute of Technology, Massachusetts, U.S.A., 1958.

7. BROWN, G.M. - "The Dynamic Characteristics of a Hydrostatic Thrust Bearing"; International Journal of Machine Tool Design and Research, Vol. 1, 1961, p.157.

8. MORI, H., YABE, H. - "Theoretical Investigation on Hydrostatic Bearings"; Bulletin of the Japan Society of Mechanical Engineers, Vol. 6, No. 22, 1963, p.354.

9. LICHT, L. - "Axial, Relative Motion of a Circular Step Bearing"; Trans. ASME, Journal of Basic Engineering, Vol. 81, 1959, p.109.

10. HUNT, J.B., TORBE, I. - "Characteristics of a Hydrostatic Thrust Bearing"; International Journal of Mechanical Sciences, Vol. 4, p.503.

11. DE GAST, J.G.C. - "A New Type of Controlled Restrictor for Double Film Hydrostatic Bearings and its Applications to High Precision Machine Tools"; Proceedings of the 7th International Machine Tool Design and Research Conference, 1966, p.273.

12. KINGSBURY, A. - "Heat Effects in Lubricating Films"; Mechanical Engineering, Vol. 55, 1933, p.685.

13. KARELITZ, G.B. - "Heat Dissipation in Self Contained Bearings"; Trans. ASME, Vol. 64, 1942, p.463.

14. HERSEY, M.D. - "Heat Conditions in Bearings"; Trans. ASME, Vol. 64, 1942, p.445.

15. MUSKAT, M., MORGAN, F. - "Temperature Behaviour of Journal Bearing Systems"; Journal of Applied Physics, Vol. 14, 1943, p.234.

16. BOYD, J., ROBERTSON, B.P. - "Oil Flow and Temperature Relations in Lightly Loaded Journal Bearings"; Trans. ASME, Vol. 70, 1948, p.257.

17. CLAYTON, D., WILKIE, M.J. - "Temperature Distribution in the Bush of a Journal Bearing"; Engineering, Vol. 166(4302), 1948, p.49.

18. COLE, J.A. - "An Experimental Investigation of Temperature Effects in Journal Bearings"; Proceedings of the Institute of Mechanical Engineers, Lubrication and Wear, Second Convention, 1957, p.111.

19. PINKUS, O., STERNLICHT, B. - "The Maximum Temperature Profile in Journal Bearings"; Trans. ASME, Vol. 79, 1957, p.337.

20. PURVIS, M.B., MEYER, M.E., BENTON, T.C. - "Temperature Distribution in Journal Bearing Lubricant Films"; Trans. ASME, Vol. 79, 1957, p.343.

21. ORLOFF, P.I. - "Coefficient of Friction, Oil Flow and Heat Balance of a full Journal Bearing"; Aeronautical Engineering (Moscow), Jan. 1935, p.25, NACA Technical Memorandum no. 1165.

22. CUENCA, R.M., RAYNOR, S. - "Thermal Effects on a Cylindrical Hydrostatic Bearing with Central Fluid Supply"; Trans. ASLE, Vol. 7, No. 3, 1964, p.304.

23. KHER, A.K. - "An Investigation into the Behaviour of an Externally Pressurised Oil Bearing System"; M.Sc. Thesis, University of Manchester Institute of Science and Technology, Manchester, 1966.

24. KHER, A.K., COWLEY, A. - "The Design and Performance Characteristics of a Capillary Compensated Hydrostatic Journal Bearing"; Proceedings of the 8th International M.T.D.R. Conference, 1967, p.397.

25. MIGLIARDI, G. - "Analysis of the Static and Dynamic Behaviour of a Grinding Machine Spindle"; M.Sc. Dissertation, University of Manchester Institute of Science and Technology, Manchester, 1967.

26. COWLEY, A., FAWCETT, M.A. - "The Analysis of a Machine Tool Structure by Computing Techniques "; Proceedings of the 8th International M.T.D.R. Conference, 1967.

27. MUNSON, C.D. - "Prediction of Dynamic Characteristics of Simple Structures with and without Damping"; M.Sc. Dissertation, UMIST, 1957.

28. PERRY, C.C., LISSNER, H.R. - "Strain Gauge Primers"; Second Ed., McGraw Hill, New York.

29. "Saunders Roe Foil Strain Gauges", published by the Strain Guage Department, Westland Aircraft Ltd., Publication No. SP.1191, 1966.

OTHER REFERENCES

1. FULLER, D.D. - "Hydrostatic Lubrication"; Parts I, II, III and IV, Machine Design, June - September, 1947.

2. FULLER, D.D. - "Theory and Practice of Lubrication for Engineers"; John Wiley and Sons., 1956.

3. RIPPEL, H.C. - "Design of Hydrostatic Bearings"; Parts I - X, Machine Design, August 1st, 1963 - December 5th, 1963.

4. RAIMONDI, A.A., BOYD, J. - "An Analysis of Orifice and Capillary Compensated Hydrostatic Journal Bearings"; Lubrication Engineering, Vol. 13, No. 1, Jan. 1957, p.28.

5. MAYER JR., J.E., SHAW, M.C. - "Characteristics of Externally Pressurised Bearings having Variable External Flow Restrictors"; Trans. ASME, Journal of Basic Engineering, Vol. 85, No. 2, 1963, p.291.

6. RIPPEL, H.C., LOEB, A.M. - "Determination of Optimum Proportions for Hydrostatic Bearings"; Trans. ASLE, Vol. 1, No. 2, 1958, p.241.

7. SHUKLA, J.B. - "An Externally Pressurised Bearing with Variable Film Thickness"; Applied Sci. Research, Section A, Vol. 13, No. 6, 1964, p.432.

8. LOXHAM, J., HEMP, J. - "The Application of Hydrostatic Bearings to High Precision Machine Tools"; Production Engineer, Vol. 43, 1964, p.556.

9. STANSFIELD, F.M. - "The Design of Hydrostatic Journal Bearings"; Proceedings of the 8th International M.T.D.R. Conference, 1967,

10. TOKAR, I.Y., BYALI, B.I. - "Hydrostatic Lift of Shafts in Journal Bearings"; Russian Engineering Journal, Vol. XLIII, Issue no. 7, p.6.

11. RUMBARGER, J.H. - "Hydrostatic Bearing Analysis"; Machine Design, February 18th, 1965, p.175.

12. STERNLIGHT, B. - "Elastic and Damping Properties of Cylindrical Journal Bearings"; Trans. ASME, Journal of Basic Engineering, Vol. 81, 1959, p.101.

13. BOOKER, J.F. - "Dynamically loaded Journal Bearings: Mobility Method of Solution"; Trans. ASME, Journal of Basic Engineering, Vol. 87, 1965, p.537.

14. SWIFT, H.W. - "Fluctuating Loads in Sleeve Bearings"; Journal of the Institution of Civil Engineers, Vol. 5, 1937, p.161.

15. BURWELL, J.T. - "The Calculated Performance of Dynamically loaded Sleeve Bearings"; Trans. ASME, Vol. 69, 1947, p.231.

16. BURWELL, J.T. - "The Calculated Performance of Dynamically loaded Sleeve Bearings - III"; Trans. ASME, Journal of Applied Mechanics, Vol. 73, 1951, p.393.

17. SHAWKI, G.S.A. - "Journal Bearing Performance for Combinations of Steady, Fundamental and Harmonic Components of Load"; Proceeding of the Institute of Mechanical Engineers, 1957, 171(28), p.795.

18. TAYLOR, S., TOBIAS, S.A. - "Lumped Constants Method for the Prediction of the Vibration Characteristics of Machine Tool Structures"; Proceedings of the 5th International M.T.D.R. Conference, 1964.

APPENDICES

LIST OF NOTATIONS

General

μ = oil viscosity in Reyns - lb.sec/in^2.

h = oil film thickness - in.

h_{opt} = optimum oil film thickness for minimum power requirement - in.

p = pad oil pressure - p.s.i.

p_s = supply oil pressure - p.s.i.

Q = oil flow - cu.in/sec.

W = load carrying capacity of the bearing - lbs.

S = normal stiffness of the bearing - lb/in.

F = normal flexibility of the bearing - in/lb.

h_b = bearing oil pumping power requirement - h.p.

h_s = oil shearing power loss - h.p.

P = total power requirement of the bearing - h.p.

Q_c = oil flow through the capillary restrictor - cu.in/sec.

d = internal diameter of the capillary tube - in.

l = length of the capillary tube - in.

n = number of pressure pads in the bearing.

N = R.P.M. of the spindle.

K_l = bearing load coefficient.

K_f = bearing flow coefficient.

K_p = shear power loss coefficient.

K_c = capillary coefficient.

Journal Bearing

L = length of the bearing - in.

D = diameter of the spindle - in.

r = radius of the spindle - in.

h_o = radial clearance - in.

l = length of the axial land - in.

el = axial land ratio.

$= \frac{l}{L}$

α = angle between the direction of application of the load and the beginning of the first pressure pad (Fig. 1.)

α_1 = half of the angle subtended by the edges of the pressure pad at the centre of the bearing.

α_2 = half of the angle subtended by one pressure pad at the centre of the bearing.

$e\alpha = \frac{\alpha_1}{\alpha_2}$

p_o = pad pressure with spindle concentric - p.s.i.

Q_o = oil flow with the spindle concentric - cu.in/sec.

P_o = total power requirement with the spindle concentric - h.p.

e = eccentricity ratio.

l_f = load factor.

f_f = flow factor.

m = pad geometry factor.

Z = bearing design factor.

Resistance to Tilting

α = angle of spindle tilt in the bearing.

M = moment acting on the spindle due to tilt - lb.in.

RFl = rotational flexibility of the bearing - rad/lb.in.

Squeeze Film Equation

h_a = oil film thickness over axial land - in.

h_c = oil film thickness over circumferential land - in.

p_a = pressure over axial land due to dynamic load - p.s.i.

p_c = pressure over circumferential land due to dynamic load - p.s.i.

p_3' = pressure of pad 3 due to dynamic load - p.s.i.

β = angle between the load line and the centre of the axial land.

β' = angle between the load line and the centre of the circumferential land.

θ_1 = half of the angle subtended by the edges of the pressure pad at the

centre of the bearing.

θ_2 = half of the angle subtended by the outer edges of the circumferential lands at the centre of the bearing (Fig. 12.)

W_p = dynamic load carried by the pressure pad.

W_c = dynamic load carried by the circumferential lands.

W_a = dynamic load carried by the axial lands.

K_d = damping constant.

K_b = bearing pad resistance.

Z_1 = ratio of the capillary resistance to the bearing pad resistance to oil flow

$$= \frac{K_c}{K_b}$$

Thrust Bearing

r_1, r_2 = radii of the annular thrust pad - in.

r_3, r_4

$r_2 - r_1$ = radial land width.

Heat Dissipation

H_o = heat carried away by the oil - BTU/sec.

Δt_o = oil temperature rise in the bearing - ^oF.

γ = weight density of the oil - lb/in^3.

C = specific heat of the oil - BTU/lb deg F.

H_b = heat conducted to the bearing housing - BTU/sec.

Δt_b = mean radial temperature different in the bearing - ^oF.

R_1 = inner radius of the bush - in.

R_2 = outer radius of the bush - in.

R_3 = radius of the outer thermocouple setting - in.

K_B = thermal conductivity of brass - BTU/sec/in/^oF.

K_S = thermal conductivity of steel - BTU/sec/in/^oF.

SQUEEZE FILM EQUATION FOR A RECTANGULAR PAD

The main assumptions in the derivation of the squeeze film equations are enunciated in Chapter II. Consider a rectangular pad, bounded on one side, and permitting oil flow in only one direction as shown in Fig. 12. Then the equation of the equilibrium of forces acting on a small volume of oil is;

$$\left[\left(p + \frac{\partial p}{\partial x}\,dx\right) - p\right] dydz = \left[\left(\tau + \frac{\partial \tau}{\partial z}\,dz\right) - \tau\right] dxdy \qquad \ldots (1)$$

which on simplification gives

$$\frac{\partial p}{\partial x} = \frac{\partial \tau}{\partial z} \qquad \ldots (2)$$

The shear stress, τ, can be expressed in terms of the oil viscosity and the velocity of flow; hence,

$$\tau = \mu \frac{\partial u}{\partial z} \qquad \ldots (3)$$

$$\therefore \quad \frac{\partial p}{\partial x} = \mu \frac{\partial^2 u}{\partial z^2} \qquad \ldots (4)$$

The solution of equation (4) can be obtained by applying the boundary conditions,

$u = o, \quad z = o$

$u = o, \quad z = h$

$$\therefore \quad u = -\frac{1}{2\mu} \frac{dp}{dx} (hz - z^2) \qquad \ldots (5)$$

Then the equation for the oil flow is

$$q_x = \int_o^h u\, dz$$

$$\text{or} \quad q_x = -\frac{1}{2\mu} \frac{dp}{dx} \int_o^h (hz - z^2)\, dz$$

$$\text{or} \quad q_x = -\frac{h^3}{12\mu} \frac{dp}{dx} \qquad \ldots (6)$$

The rate of oil flow is a constant

$$\therefore \quad \frac{dq_x}{dx} + \frac{dq_y}{dy} + \frac{dq_z}{dz} = o$$

or $\frac{du}{dx} + \frac{dv}{dz} = o$

or $dv = -\frac{du}{dx}\, dz$ ... (7)

Integrating both sides

$$\int_o^h dv = -\int_o^h \frac{du}{dx}\, dz$$

Since the L.H.S. is $V = \frac{dh}{dt}$

∴ the equation (7) becomes

$$\frac{h^3}{12\mu}\frac{d^2p}{dx^2} = \frac{dh}{dt} \quad \text{... (8)}$$

The equation of pressure distribution can be determined for a pad with width b, by integrating equation (8) and applying the boundary conditions;

$p_x = p, \quad x = x_1$

and $p_x = o, \quad x = x_2$

$$\therefore p_x = \frac{12\mu}{h^3} \cdot \frac{dh}{2dt}\left\{x^2 - (x_1 + x_2)x + x_1x_2\right\} + \frac{p}{(x_2 - x_1)}(x_2 - x) \quad \text{... (9)}$$

The load carried by the pad is given by the equation;

$$W = 2bx_1p + 2b\int_{x_1}^{x_2} p_x\, dx$$

Putting in the value of p_x from equation (9)

$$W = pb(x_2 + x_1) - \frac{2b\mu}{h^3}\frac{dh}{dt}(x_2 - x_1)^3 \quad \text{... (10)}$$

For a capillary compensated pad, the equation of oil flow through the restrictor is;

$$Q = K_c(p_s - p)$$

where $K_c = \frac{\pi d^4}{128\mu l}$

Therefore, the equation of the oil flow in the system is;

$$Q + \frac{2bh^3}{12\mu}\left(\frac{\partial p}{\partial x}\right)_{x=x_2} = 2bx_2\frac{dh}{dt} \quad \text{... (11)}$$

From equation (9),

$$\left(\frac{\partial p}{\partial x}\right)_{x=x_2} = \frac{12\mu}{h^3} \cdot \frac{dh}{2dt} (x_2 - x_1) - \frac{p}{x_2 - x_1} \quad \ldots (12)$$

$\therefore$ the equation (10) becomes;

$$K_c(p_s - p) - b\frac{dh}{dt}(x_2 + x_1) - \frac{bh^3}{6\mu}\frac{p}{x_2 - x_1} = 0 \quad \ldots (13)$$

$$\therefore \quad p = \frac{K_c p_s}{K_c + \frac{bh^3}{6\mu(x_2 - x_1)}} - \frac{b\frac{dh}{dt}(x_2 + x_1)}{K_c + \frac{bh^3}{6\mu(x_2 - x_1)}} \quad \ldots (14)$$

Denoting the resistance of the pad as K_b, such that;

$$K_b = \frac{bh^3}{6\mu(x_2 - x_1)}$$

The equation for the pad pressure is;

$$p = \frac{K_c p_s}{K_c + K_b} - \frac{dh}{dt} \frac{6\mu(x_2^2 - x_1^2)}{h^3\left(\frac{K_c}{K_b} + 1\right)} \quad \ldots (15)$$

Putting in the value of the pad pressure into equation (10) the load capacity is given by;

$$W = \frac{bp_s(x_2 + x_1)}{1 + \frac{K_b}{K_c}} - \mu b \frac{dh}{dt}\left[2(x_2 - x_1)^3 + \frac{6(x_2^2 - x_1^2)(x_2 + x_1)}{\left(\frac{K_c}{K_b} + 1\right)}\right] \quad \ldots (16)$$

This consists of the load carried due to the static pressure and due to the squeeze film effect. Therefore, the damping constant of the pad is;

$$K_d = \frac{2\mu b}{h^3} x_2^3 \left[(1 - \frac{x_1}{x_2})^3 \left\{1 + \frac{(1 + \frac{x_1}{x_2})^2}{(1 - \frac{x_1}{x_2})^2} \cdot \frac{1}{\left(\frac{K_c}{K_b} + 1\right)}\right\}\right] \quad \ldots (17)$$

RECTANGULAR PAD WITH TWO DIMENSIONAL FLOW

The equation of flow for a two dimensional pad shown in Fig. 12, can be derived in the same manner as shown above for a pad with one

dimensional flow. Therefore, the equation is;

$$\frac{h^3}{12\mu}\frac{\partial^2 p}{\partial x^2} + \frac{h^3}{12\mu}\frac{\partial^2 p}{\partial y^2} = \frac{dh}{dt} \qquad \ldots (18)$$

The solution of the equations is found by assuming that the equations for flow in the x and y directions can be solved independently and applying the boundary conditions

$p_x = p, \quad x = x_1$

$p_x = o, \quad x = x_2$

$p_y = p, \quad y = y_1$

and $p_y = o, \quad y = y_2$

$$\therefore p_x = \frac{12\mu}{h^3} \cdot \frac{dh}{2dt}\left\{x^2 - (x_1 + x_2)x + x_1x_2\right\} + \frac{p}{(x_2 - x_1)}(x_2 - x) \qquad \ldots (19)$$

$$\text{and } p_y = \frac{12\mu}{h^3} \cdot \frac{dh}{2dt}\left\{y^2 - (y_1 + y_2)y + y_1y_2\right\} + \frac{p_1}{(y_2 - y_1)}(y_2 - y) \qquad \ldots (20)$$

Considering the oil flow through a capillary restrictor as in the previous case, the equation of the oil flow in the system is;

$$Q + \frac{h^3}{12\mu}\, 4y_1\left(\frac{\partial p}{\partial x}\right)_{x=x_1} + \frac{h^3}{12\mu}\, 4x_1\left(\frac{\partial p}{\partial y}\right)_{y=y_1} = 4x_1y_1\frac{dh}{dt} \qquad \ldots (21)$$

The expressions for $\left(\frac{\partial p}{\partial x}\right)_{x=x_1}$ and $\left(\frac{\partial p}{\partial y}\right)_{y=y_1}$ can be obtained from equations (19) and (20) as before, and therefore the equation (21) becomes;

$$4x_1y_1\frac{dh}{dt} = K_c(p_s - p) + 4y_1\left[\frac{dh}{2dt}(x_1 - x_2) - \frac{h^3}{12\mu}\frac{p}{(x_2 - x_1)}\right]$$

$$+ 4x_1\left[\frac{dh}{2dt}(y_1 - y_2) - \frac{h^3}{12\mu}\frac{p}{(y_2 - y_1)}\right] \qquad \ldots (22)$$

The equation for pressure in the pad is therefore;

$$p = \frac{K_c p_s}{K_c + \frac{h^3}{3\mu}\left(\frac{y_1}{x_2 - x_1} + \frac{x_1}{y_2 - y_1}\right)} - \frac{2\frac{dh}{dt}(x_1y_2 + y_1x_2)}{K_c + \frac{h^3}{3\mu}\left(\frac{y_1}{x_2 - x_1} + \frac{x_1}{y_2 - y_1}\right)} \qquad \ldots (23)$$

The load capacity of the pad can now be calculated by assuming the pressure distribution as a truncated pyramid as shown in Fig. 12.

$$\therefore W = 4x_1y_1p + 4y_1\int_{x_1}^{x_2} p_x dx + 4x_1\int_{y_1}^{y_2} p_y dy + 4\int_{x_1}^{x_2} p_x(y - y_1)dx + 4\int_{y_1}^{y_2} p_y(x - x_1)dy \quad \ldots (24)$$

where $$\frac{y - y_1}{y_2 - y_1} = \frac{x - x_1}{x_2 - x_1} \quad \ldots (25)$$

Integrating the above equation and simplifying;

$$W = \frac{2}{3}p\left[2(x_2y_2 + x_1y_1) + (x_1y_2 + x_2y_1)\right] - \frac{2\mu}{h^3}\frac{dh}{dt}\left[(x_2 - x_1)^3(y_2 + y_1) + (y_2 - y_1)^3(x_2 + x_1)\right] \quad \ldots (26)$$

Putting in the value of p from equation (23), and denoting the pad resistance as K_b as before;

$$W = \frac{2}{3}p_s\frac{\left[2(x_2y_2 + x_1y_1) + x_1y_2 + x_2y_1\right]}{(1 + \frac{K_b}{K_c})} - \frac{2\mu}{h^3}\frac{dh}{dt}\left[(x_2 - x_1)^3(y_2 + y_1) + (y_2 - y_1)^3(x_2 + x_1) + 2\frac{(x_1y_2 + y_1x_2)(2x_2y_2 + 2x_1y_1 + x_1y_2 + x_2y_1)(x_2 - x_1)(y_2 - y_1)}{(\frac{K_c}{K_b} + 1)\{y_1(y_2 - y_1) + x_1(x_2 - x_1)\}}\right] \quad \ldots (27)$$

$\therefore$ the damping constant is given by the equation;

$$K_d = \frac{2\mu}{h^3}\left[(x_2 - x_1)^3(y_2 + y_1) + (y_2 - y_1)^3(x_2 + x_1) + 2\frac{(x_1y_2 + y_1x_2)(2x_2y_2 + 2x_1y_1 + x_1y_2 + x_2y_1)(x_2 - x_1)(y_2 - y_1)}{(\frac{K_c}{K_b} + 1)\{y_1(y_2 - y_1) + x_1(x_2 - x_1)\}}\right] \quad \ldots (28)$$

HEAT DISSIPATION IN HYDROSTATIC JOURNAL BEARINGS

(a) OIL FLOW

The oil flow in the journal bearing is given by the equation;

$$Q_o = \frac{K_f h_o^3}{6\mu} p \qquad \ldots (1)$$

where $K_f = \frac{\pi D}{Le}$

h_o = radial clearance - in

μ = oil viscosity at mean bearing temperature in Reyns - $lb\ sec/in^2$

and p = average pad pressure - psi

It is assumed that the journal is concentric in the bearing, the observed temperature is the average of the oil film, there is no temperature gradient along the axis and the oil viscosity is uniform over the axial land.

Then the heat carried away by the oil is given by the equation;

$$H_o = Q_o \Delta t\ \gamma C \qquad \ldots (2)$$

where γ = weight density of oil - lb/in^3

C = specific heat of the oil - BTU/lb deg F

Δt_o = oil temperature rise in the bearing

Substituting the values of K_f, h_o, r and c in the above equation;

$$H_o = \frac{\Delta t_o p}{6\mu} \left(\frac{1.8 \times 12.57 \times (.003)^3 \times .0307 \times .5}{}\right)$$

$$= 1.55 \frac{\Delta t_o p \times 10^{-9}}{\mu} \quad \text{BTU/sec} \qquad \ldots (3)$$

BEARING HOUSING

The profile of the bearing bush in the housing is shown in Fig. 22 The thermocouples are placed midway between the axial land and it is assumed that there is no temperature gradient along the axial land and the average temperatures indicated by the thermocouples are fairly

representative of the actual temperatures.

The heat transfer through the bearing can be calculated from the observed radial temperature difference across the bush and the steel housing, assuming same heat flow from both the axial lands and none from the circumferential lands.

Therefore, heat flow through the brass ring is;

$$H_B = - \frac{K_B \, 2\pi l (t_2 - t_1)}{\log \frac{R_2}{R_1}} \qquad \ldots (4)$$

Similarly, the heat flow through the steel housing is given by;

$$H_S = - \frac{K_S \, 2\pi l (t_3 - t_2)}{\log \frac{R_3}{R_2}} \qquad \ldots (5)$$

where K_B and K_S are thermal conductivities of brass and steel respectively.

Since the heat flow is the same, the equations (4) and (5) can be equated to eliminate the unknown temperature t_2. Then the heat flow in terms of the observed temperatures is given by;

$$H_b = - \frac{2\pi l (t_3 - t_1)}{\frac{\log \frac{R_2}{R_1}}{K_B} + \frac{\log \frac{R_3}{R_2}}{K_S}} \qquad \ldots (6)$$

where $t_1 - t_3 = \Delta t_b$ = the mean radial temperature difference - ^oF

l = effective length of the axial lands - ft

R_1 = inner radius of the bush - in

R_2 = outer radius of the bush - in

and R_3 = radius of the outer thermocouple setting - in

Substituting the values of R_1, R_2, R_3, l, K_S and K_B;

$$H_b = \frac{\frac{2\pi}{12} (\Delta t_b) 1.8}{\frac{\log \frac{1.25}{1}}{.28} + \frac{\log \frac{1.375}{1.25}}{.12}}$$

or $$= .0592 \, \Delta t_b \qquad \ldots (7)$$

CALCULATION OF DAMPING RATIO FROM FREQUENCY RESPONSE CHARACTERISTICS OF THE BEARING SYSTEM

When a harmonic force is applied to a damped system, the amplitude ratio is given by the equation;

$$\frac{X}{F_o/K} = \frac{1}{\sqrt{(1 - \frac{w^2}{w_n^2})^2 + (2\xi\frac{w}{w_n})^2}} \quad \ldots (1)$$

where F_o = amplitude of the force

K = stiffness of the equivalent spring

ξ = damping ratio

w = applied angular frequency

w_n = resonant angular frequency

At resonance therefore,

$$\frac{X_n}{F_o/K} = \frac{1}{2\xi} \quad \ldots (2)$$

When the frequency response characteristics are obtained for acceleration rather than displacement amplitudes for all frequencies, then any ratio of acceleration amplitudes, R at frequencies w and w_n is;

$$R = \frac{w^2}{\sqrt{(1 - \frac{w^2}{w_n^2})^2 + (2\xi\frac{w}{w_n})^2}} \cdot \frac{2\xi}{w_n^2} \quad \ldots (3)$$

Squaring both sides therefore,

$$(1 - \frac{w^2}{w_n^2})^2 + (2\xi\frac{w}{w_n})^2 = (\frac{w}{w_n})^4 \frac{4\xi^2}{R^2}$$

or $$(\frac{w}{w_n})^4 (1 - \frac{4\xi^2}{R^2}) + (\frac{w}{w_n})^2 (4\xi^2 - 2) + 1 = 0 \quad \ldots (4)$$

This is a quadratic equation in $(\frac{w}{w_n})^2$, therefore the solution is;

$$(\frac{w}{w_n})^2_{1.2} = \frac{-\frac{4\xi^2 - 2}{(1 - \frac{4\xi^2}{R^2})} \pm \sqrt{(\frac{4\xi^2 - 2}{1 - \frac{4\xi^2}{R^2}})^2 - \frac{4}{(1 - \frac{4\xi^2}{R^2})}}}{2}$$

which gives two roots of $(\frac{w}{w_n})^2$, so that

$$(\frac{w_1}{w_n})^2 + (\frac{w_2}{w_n})^2 = \frac{2 - 4\xi^2}{1 - \frac{4\xi^2}{R^2}} \quad \ldots (5)$$

From the frequency response curve, the two frequencies before and after the resonant frequency which give acceleration amplitude ratios, R, can be obtained. The value of the damping ratio, ξ, can then be calculated from equation (5).

COMPUTER PROGRAM TO DETERMINE THE EFFECT OF THE DESIGN FACTOR ON THE LOAD FACTOR AND THE FLOW FACTOR OF THE HYDROSTATIC JOURNAL BEARING

```
begin
real a,e,bl,el,ea,a2,c1,c2,m1,m2,x,m,p1,p2,p3,p4,ps,ap2,lf,ff,w,u,h,q,olf,c
off,A,hb,hs,th,d,l,L,D,N,kp,kf,ho,qo,OA,kl
integer nn,n,ll,ii,jj,xx,kk
array f(1:4,1:2)
read(a,m)

cycle ll=6,1,9
e=.lll
newlines(2);  spaces(15)
caption$$eccentricity$ratio$e$=$;   print(e,1,2)
newlines(3); spaces(18)
cycle n=1,1,4
f(n,1)=π+6e*((cos(a)+sin(a))*sin(n*π/2)+(cos(a)-sin(a))*cos(π*n/2))+3e²*c
       (π/2-cos(π*n)*sin(2a))+2/3*(e↑3)*((sin(n*π/2)*cos(a)-cos(n*π/2)*c
       sin(a))*(5/2+1/2*cos(n*π)*cos(2a))+(cos(n*π/2)*cos(a)+sin(n*π/2)*c
       sin(a))*(5/2-1/2*cos(n*π)*cos(2a)))

f(n,2)=(1+e*(cos(n*π/2)*cos(a)+sin(n*π/2)*sin(a)))↑3
repeat
select output(1)
caption$$$$z$$$$$$$$$lf$$$$$$$$$$ff; newline; spaces(18)
cycle kk=1,1,15
A=kk
5: p2=0.5
1: p3=(A+4m*p2*f(3,2))/(A+(f(3,1)+4m*f(3,2)))
p1=(A+4m*p2*f(1,2))/(A+(f(1,1)+4m*f(1,2)))
ap2=(A+2m*(p1*f(1,2)+p3*f(3,2)))/(A+f(2,1)+2m*(f(1,2)+f(3,2)))
if |(p2-ap2)/p2| ≤ .005 then ->2
p2=(p2+ap2)/2; ->1
2: p4=ap2; p2=ap2
lf=p3-p1; ff=(p1*f(1,1)+p2*f(2,1)+p3*f(3,1)+p4*f(4,1))

print(A,2,2); spaces(3); print(lf,1,3); spaces(4); print(ff,3,3); newline
spaces(18)
repeat
newlines(8); spaces(15)
repeat
stop
end of program
```

.7854 .7960

***Z

SPECIMEN RESULT

eccentricity ratio e = 0.60

z	lf	ff
1.00	0.454	2.947
2.00	0.536	4.904
3.00	0.547	6.376
4.00	0.536	7.552
5.00	0.519	8.484
6.00	0.499	9.282
7.00	0.479	9.965
8.00	0.460	10.551
9.00	0.441	11.070
10.00	0.424	11.521
11.00	0.408	11.923
12.00	0.393	12.283
13.0	0.379	12.608
14.0	0.366	12.902
15.00	0.354	13.170

eccentricity ratio e = 0.70

z	lf	ff
1.00	0.566	2.898
2.00	0.631	4.898
3.00	0.628	6.460
4.00	0.608	7.720
5.00	0.584	8.777
6.00	0.561	9.639
7.00	0.537	10.401
8.00	0.515	11.062
9.00	0.494	11.651
10.00	0.476	12.169
11.00	0.458	12.632
12.00	0.442	13.048
13.00	0.426	13.426
14.00	0.412	13.770
15.00	0.399	14.085

COMPUTER PROGRAM TO DETERMINE THE EFFECT OF THE OIL FILM THICKNESS ON THE OIL FLOW, STIFFNESS AND THE TOTAL POWER REQUIREMENT OF THE HYDROSTATIC JOURNAL BEARING

```
begin
real a,e,el,ea,a2,m,p1,p2,p3,p4,ps,ap2,lf,ff,w,u,h,q,olf,off,c
Z,hbo,hso,th,d,l,L,D,N,kp,kl,kf,ho,qo,OZ
integer n,ll,ii,jj,xx,kk
array f(1:4,1:2)
read(a,e,L,D,ps,u,N,d,a2)

cycle n=1,1,4
f(n,1)=π+6e*((cos(a)+sin(a))*sin(n*π/2)+(cos(a)-sin(a))*cos(π*n/2))+3e^2*c
       (π/2-cos(π*n)*sin(2a))+2/3*(e↑3)*((sin(n*π/2)*cos(a)-cos(n*π/2)*c
       sin(a))*(5/2+1/2*cos(n*π)*cos(2a))+(cos(n*π/2)*cos(a)+sin(n*π/2)*c
       sin(a))*(5/2-1/2*cos(n*π)*cos(2a)))

f(n,2)=(1+e*(cos(n*π/2)*cos(a)+sin(n*π/2)*sin(a)))↑3
repeat
cycle ll=1,1,4
el=ll/20
cycle ii=7,1,8
ea=ii/9
m=(L/D)^2*(1-2el)*el/(a2*(1-ea))
kl=L*D*(1-el)*sin(a2); kf=π*D/(L*el); kp=(D↑3)*L*(π-4a2*ea*(1-2el))/π

newline
spaces(18)
captionel$=$; print(el,1,3); newline; spaces(18)
captionea$=$$; print(ea,1,4); newline; spaces(18)
captionm$$=$$; print(m,1,4); newline; spaces(18)
captionkl$=$$; print(kl,1,3); newline; spaces(18)
captionkf$=$; print(kf,2,3); newline; spaces(18)
caption$kp$=$; print(kp,2,3); newlines(3); spaces(18)
caption$$$z$$$$$$$$$$lf$$$$$$$$$$ff; newline
xx=1
cycle jj=1,1,10
Z=jj
5: p2=0.5
1: p3=(Z+4m*p2*f(3,2))/(Z+(f(3,1)+4m*f(3,2)))
p1=(Z+4m*p2*f(1,2))/(Z+(f(1,1)+4m*f(1,2)))
ap2=(Z+2m*(p1*f(1,2)+p3*f(3,2)))/(Z+f(2,1)+2m*(f(1,2)+f(3,2)))
if |(p2-ap2)/p2| ≤ .005 then ->2;  p2=(p2+ap2)/2;   ->1
2: p4=ap2;   p2=ap2
lf=p3-p1;  ff=(p1*f(1,1)+p2*f(2,1)+p3*f(3,1)+p4*f(4,1)); spaces(18)
print(Z,2,2); spaces(4); print(lf,1,4); spaces(4); print(ff,3,3); newline
if xx<1.5 then ->4
OZ=Z;   olf=lf;   off=ff;   ->3
```

```
4:repeat
xx=2;   Z=π;   ->5
3:w=olf*D*L*(1-el)*ps*sin(a2)
ho=0.362sqrt(u*N/ps)*(exp(0.25log(kp*(π+OZ)/(kf*OZ))));  newline
caption$w$=$; print(w,4,2); newline
caption$$$$optimum$film$thickness$in$inches$hopt$=$; print fl(ho,3)
newlines(3)
caption$$$$$h$$$$$$$$$$hso$$$$$$$$qo$$$$$$$$hbo$$$$$$po$$$$$$$$$$l$$$c
$$$$$$$$q
newlines(2)
cycle kk=1,1,8
h=kk*5α-4
q=ps*(h↑3)*D*off/(24u*L*el);  qo=kf*(h↑3)*OZ*ps/(6u*(π+OZ))
hbo=ps*qo/6600;   hso=u*(D↑3)*N^2*L*(π-4a2*ea*(1-2el))/(766000h*π)
th=hbo+hso
l=3π*(d↑4)*L*el/(16*(h↑3)*D*OZ)
print fl(h,3); spaces(2); print(hso,2,3); spaces(2); print(qo,3,3)
spaces(2); print(hbo,2,3); spaces(2); print(th,2,3); spaces(2); print fl(l,3)
spaces(2); print(q,3,3); newline
repeat
newpage
repeat
repeat
stop
end of program
```

```
.7854    .6    2.5    2.0    400    9.96α-6    2000    3.3α-2    .7854
```

```
***Z
```

SPECIMEN RESULT

el = 0.100
ea = 0.778
m = 0.716
kl = 3.182
kf = 25.133
kp = 7.556

z	lf	ff
1.00	0.4692	2.935
2.00	0.5493	4.882
3.00	0.5578	6.356
4.00	0.5454	7.524
5.00	0.5275	8.457
6.00	0.5067	9.256
7.00	0.4858	9.940
8.00	0.4661	10.525
9.00	0.4471	11.044
10.00	0.4296	11.496
3.14	0.5568	6.536

w = 708.72
optimum film thickness in inches hopt = 2.250α -3

h	hso	qo	hbo	po	l	q
5.000α -4	0.786	0.011	0.001	0.787	2.224α 2	0.011
1.000α -3	0.393	0.084	0.005	0.398	2.780α 1	0.087
1.500α -3	0.262	0.284	0.017	0.279	8.236α 0	0.295
2.000α -3	0.196	0.673	0.041	0.237	3.474α 0	0.700
2.500α -3	0.157	1.314	0.080	0.237	1.779α 0	1.367
3.000α -3	0.131	2.271	0.138	0.269	1.029α 0	2.362
3.500α -3	0.112	3.606	0.219	0.331	6.483α -1	3.751
4.000α -3	0.098	5.383	0.326	0.424	4.343α -1	5.599

COMPUTER PROGRAM TO DETERMINE THE ROTATIONAL FLEXIBILITY OF THE HYDROSTATIC JOURNAL BEARING

```
begin
real a,h,ps,a2,L,D,Z,C,B,M,S,RF1,el
integer ii,jj,kk
read(ps,a2,L,D,Z)

cycle ii=1,1,9
el=.05*ii
newlines(2)
select output(1)
caption$$$el$=$; print(el,1,3); newlines(3)
caption$$$h$$$$$$$$$$$$$$a$$$$$$$$$M$$$$$$$$$$S$$$$$$$$$$RF1
newlines(2)
cycle jj=1,1,8
h=jj*5a-4
cycle kk=1,1,9
a=.2*h*kk/L
C=(h-.5*L*a*(1-2*el))↑2/((h-.5L*a)↑2-(h-.5L*a*(1-2el))↑2)

B=(h+.5L*a*(1-2el))↑2/((h+.5L*a)↑2-(h+.5L*a*(1-2el))↑2)

M=-((Z*ps)/((Z+π)*a)*C*((h-.5L*a)↑2/(h-.5L*a*(1-2el))-(h-.5L*a)+L*el*a)+c
   (Z*ps)/((π+Z)*a)*B*((h+.5L*a)↑2/(h+.5L*a*(1-2el))-(h+.5L*a)-L*el*a))*c
   (3-4el)*L*D*sin(a2)/3

S=M/(a*10↑3)

RF1=10↑3/S

print fl(h,3); spaces(5); print fl(a,3); spaces(5); print(M,3,2); spaces(4)
print(S,3,2); spaces(4); print(RF1,4,2)
newline
repeat
newlines(3)
repeat
newlines(5)
repeat
newpage
stop
end of program
```

```
400    .7854    2.50    2.00    3.14

***Z
```

SPECIMEN RESULT

el = 0.050

h	a	M	S	RFl
1.500α -3	1.200α -4	0.42	3.47	288.37
1.500α -3	2.400α -4	0.86	3.57	280.49
1.500α -3	3.600α -4	1.35	3.74	267.36
1.500α -3	4.800α -4	1.93	4.02	248.98
1.500α -3	6.000α -4	2.66	4.44	225.34
1.500α -3	7.200α -4	3.67	5.09	196.45
1.500α -3	8.400α -4	5.18	6.16	162.31
1.500α -3	9.600α -4	7.81	8.14	122.92
1.500α -3	1.080α -3	13.80	12.78	78.27
2.000α -3	1.600α -4	0.42	2.60	384.49
2.000α -3	3.200α -4	0.86	2.67	373.99
2.000α -3	4.800α -4	1.35	2.81	356.48
2.000α -3	6.400α -4	1.93	3.01	331.97
2.000α -3	8.000α -4	2.66	3.33	300.45
2.000α -3	9.600α -4	3.67	3.82	261.94
2.000α -3	1.120α -3	5.18	4.62	216.41
2.000α -3	1.280α -3	7.81	6.10	163.89
2.000α -3	1.440α -3	13.80	9.58	104.36

el = 0.100

h	a	M	S	RFl
1.500α -3	1.200α -4	1.54	12.87	77.71
1.500α -3	2.400α -4	3.17	13.19	75.81
1.500α -3	3.600α -4	4.96	13.77	72.63
1.500α -3	4.800α -4	7.04	14.66	68.19
1.500α -3	6.000α -4	9.60	16.01	62.48
1.500α -3	7.200α -4	12.97	18.02	55.50
1.500α -3	8.400α -4	17.78	21.16	47.25
1.500α -3	9.600α -4	25.44	26.50	37.73
1.500α -3	1.080α -3	40.08	37.12	26.94
2.000α -3	1.600α -4	1.54	9.65	103.61
2.000α -3	3.200α -4	3.17	9.89	101.08
2.000α -3	4.800α -4	4.96	10.33	96.85
2.000α -3	6.400α -4	7.04	11.00	90.92
2.000α -3	8.000α -4	9.60	12.00	83.31
2.000α -3	9.600α -4	12.97	13.51	74.00
2.000α -3	1.120α -3	17.78	15.87	63.00
2.000α -3	1.280α -3	25.44	19.88	50.31
2.000α -3	1.440α -3	40.08	27.84	35.92

COMPUTER PROGRAM TO DETERMINE THE DAMPING CONSTANT OF THE JOURNAL BEARING

```
begin
real u,h,el,ea,b,ps,a2,L,D,B,W,Kd,e,Z,Kb,Kc,d,l
integer ii,jj,kk,ll
read(u,b,ps,a2,L,D,B,Z)

cycle ll=0,1,3
e=.1*ll
newlines(3)
caption$$$e$=$; print(e,1,3); newlines(3)
cycle ii=1,1,4
el=ii/20
caption$$$el$$$$$$$$$ea$$$$$$$$$$h$$$$$$$$$$$$$W$$$$$$$$$$K
newlines(2)
cycle jj=7,1,8
ea=jj/9
cycle kk=2,1,6
h=kk*5α-4

W=ps*((D*sin(ea*a2)*(L*el))/(1+1/(Z))-(D*L*(1-2el)*(cos(a2*(2-ea))-cos(a2*c
  ea)))/((1+1/(Z))*2*(1-ea)*a2))
Kd=12*u/(h↑3*(Z+1))*((L*(1-2el)*D^2*cos(B)*(1-ea)*a2)/(2)+(D*a2*ea*(cos(b)*c
   L*el+L*(1-2el)))/(1))*(el*L)*(D*sin(ea*a2)*L*el*a2*(1-ea)*2-(D*L*(1-2el)*c
   (cos(a2*(2-ea))-cos(a2*ea))))/(2*L^2*(1-2*el)*el*(1-e*cos(B))↑3+4*ea*D*c
   a2*a2*(1-e*cos(b))↑3*(1-ea))-12u*L*D↑3*(1-2el)*cos(B)*((cos(a2*ea)+cos(a2*c
   (2-ea)))*(1-ea)*2a2-2*(sin(a2*(2-ea))-sin(ea*a2)))/(h↑3*8*(1-e*cos(B))↑3)+c
   (2u*D*sin(ea*a2)*cos(b)*(L*el)↑3)/(h↑3*(1-e*cos(b))↑3)

print(el,1,3); spaces(5); print(ea,1,3); spaces(5); print fl(h,3); spaces(5)
print(W,4,1); spaces(5); print(Kd,5,1)

newline
repeat
newlines(3)

repeat
newpage
repeat
newpage
repeat
stop
end of program
```

5.000α-6 0.00 400 0.7854 2.50 2.00 0.7854 1.00

***Z

SPECIMEN RESULT

θ = 0.000

θ_1	θ_a	h	W	K
0.050	0.778	1.000α -3	661.9	11079.2
0.050	0.778	1.500α -3	661.9	3282.7
0.050	0.778	2.000α -3	661.9	1384.9
0.050	0.778	2.500α -3	661.9	709.1
0.050	0.778	3.000α -3	661.9	410.3
0.050	0.889	1.000α -3	667.7	7564.7
0.050	0.889	1.500α -3	667.7	2241.4
0.050	0.889	2.000α -3	667.7	945.6
0.050	0.889	2.500α -3	667.7	484.1
0.050	0.889	3.000α -3	667.7	280.2

θ_1	θ_a	h	W	K
0.100	0.778	1.000α -3	620.2	14809.6
0.100	0.778	1.500α -3	620.2	4388.0
0.100	0.778	2.000α -3	620.2	1851.2
0.100	0.778	2.500α -3	620.2	947.8
0.100	0.778	3.000α -3	620.2	548.5
0.100	0.889	1.000α -3	629.2	9636.2
0.100	0.889	1.500α -3	629.2	2855.2
0.100	0.889	2.000α -3	629.2	1204.5
0.100	0.889	2.500α -3	629.2	616.7
0.100	0.889	3.000α -3	629.2	356.9

θ_1	θ_a	h	W	K
0.150	0.778	1.000α -3	578.5	16860.2
0.150	0.778	1.500α -3	578.5	4995.6
0.150	0.778	2.000α -3	578.5	2107.5
0.150	0.778	2.500α -3	578.5	1079.1
0.150	0.778	3.000α -3	578.5	624.5
0.150	0.889	1.000α -3	590.8	10981.2
0.150	0.889	1.500α -3	590.8	3253.7
0.150	0.889	2.000α -3	590.8	1372.7
0.150	0.889	2.500α -3	590.8	702.8
0.150	0.889	3.000α -3	590.8	406.7

COMPUTER PROGRAM TO DETERMINE THE STEADY LOAD DEFLECTION OF THE SPINDLE IN A HYDROSTATIC BEARING SYSTEM

```
begin
integer elements, dimensions, cuts, n, runs, f
read(elements); read(dimensions); read(cuts); read(runs)
n=(elements-cuts)*dimensions
400: begin
integer i,j,k,h
array H,X,Y,Z(1:elements,1:elements)
array F(1:12,1:elements)
cycle i=1,1,elements
cycle j=1,1,12
read(F(j,i)); F(j,i)=F(j,i)*1α-9
repeat
read(X(1,i)); read(Y(1,i)); read(Z(1,i))
repeat
cycle i=2,1,elements
cycle j=i,1,elements
k=i-1
X(i,j)=X(k,j)-X(k,i);  Y(i,j)=Y(k,j)-Y(k,i);  Z(i,j)=Z(k,j)-Z(k,i)
repeat
repeat
begin
real N
integer R,r
null(H)
cycle i=1,1,elements
read(N) ; if N > 100 then ->7
R=int(mod(N))+i-1; ->8
7: R=int(N)-100+i-1
8: r=i;  ->5
3: r=R+1
read(N); if N>100 then ->9
R=R+int(mod(N)) ; ->5
9: R=R+int(N)-100
5: cycle j=r,1,R
if N<0 then ->2; if N>100 then ->6
H(i,j)=1 ; ->4
2: H(i,j)=0;->4
6: H(i,j)=-1
4: repeat
if R<elements then ->3
repeat
end

begin
real  det
integer  p,q,g,b,c,e,d
array a(1:n)
```

```
if cuts=0 then ->50
array inv,F''(1:cuts*dimensions,1:cuts*dimensions)
array F'''(1:n,1:cuts*dimensions)
null(F'')
cycle q=1,1,elements
cycle p=1,1,cuts
cycle g=p,1,cuts
b=elements-cuts+p; c=elements-cuts+g;  ->100 unless g=p
if H(q,b)=0 then ->110;  ->115
100: if H(q,c)=0  or H(q,b)=0 then ->110
115: cycle i=6*g-5,1,6*g
cycle j=6*p-5,1,i+(g-p)*(6-i)

if i=6g-5 then ->1;  if i=6g-4 then ->2;  if i=6g-3 then ->3
if i=6g-2 then ->4;  if i=6g-1 then ->5;  ->6

1:if j=6p-5 then ->7;  if j=6p-4 then ->8;  if j=6p-3 then ->9
if j=6p-1 then ->10;  if j=6p then ->11;  ->31
2: if j=6p-5 then ->12;  if j=6p-4 then ->13;  if j=6p-3 then ->14
if j=6p-2 then ->15;  if j=6p  then ->16;  ->31
3:  if j=6p-5 then ->17;  if j=6p-4 then ->18;  if j=6p-3 then ->19
if j=6p-2 then ->20;  if j=6p-1 then ->21;  ->31
4: if j=6p-4 then ->22;  if j=6p-3 then ->23;  if j=6p-2 then ->24;  ->31
5:if j=6p-5 then ->25;  if j=6p-3 then ->26;  if j=6p-1 then ->27;  ->31
6:if j=6p-5 then ->28;  if j=6p-4 then ->29;  if j=6p then ->30;  ->31

7: F''(i,j)=F''(i,j)+(F(1,q)+F(2,q)*Z(q,c)-F(3,q)*Y(q,c)+(F(2,q)+F(11,q)*c
          Z(q,c))*Z(q,b)-(F(3,q)-F(12,q)*Y(q,c))*Y(q,b))*H(q,c)*H(q,b); ->32
8: F''(i,j)=F''(i,j)+(-F(6,q)*Y(q,c)+(F(3,q)-F(12,q)*Y(q,c))*X(q,b))*H(q,c)*c
          H(q,b); ->32
9: F''(i,j)=F''(i,j)+(F(9,q)*Z(q,c)-(F(2,q)+F(11,q)*Z(q,c))*X(q,b))*H(q,c)*c
          H(q,b); ->32
10:F''(i,j)=F''(i,j)+(F(2,q)+F(11,q)*Z(q,c))*H(q,c)*H(q,b);->32
11:F''(i,j)=F''(i,j)+(F(3,q)-F(12,q)*Y(q,c))*H(q,c)*H(q,b);->32
12:F''(i,j)=F''(i,j)+(F(3,q)*X(q,c)-(F(6,q)+F(12,q)*X(q,c))*Y(q,b))*H(q,c)*c
          H(q,b); ->32
13: F''(i,j)=F''(i,j)+(F(4,q)-F(5,q)*Z(q,c)+F(6,q)*X(q,c)-(F(5,q)-F(10,q)*c
          Z(q,c))*Z(q,b)+(F(6,q)+F(12,q)*X(q,c))*X(q,b))*H(q,c)*H(q,b); ->32
14: F''(i,j)=F''(i,j)+(-F(8,q)*Z(q,c)+(F(5,q)-F(10,q)*Z(q,c))*Y(q,b))*H(q,c)*c
          H(q,b);->32
15: F''(i,j)=F''(i,j)+(F(5,q)-F(10,q)*Z(q,c))*H(q,c)*H(q,b);->32
16: F''(i,j)=F''(i,j)+(F(6,q)+F(12,q)*X(q,c))*H(q,c)*H(q,b);->32
17: F''(i,j)=F''(i,j)+(-F(2,q)*X(q,c)+(F(9,q)-F(11,q)*X(q,c))*Z(q,b))*H(q,c)*c
          H(q,b);->32
18: F''(i,j)=F''(i,j)+(F(5,q)*Y(q,c)-(F(8,q)+F(10,q)*Y(q,c))*Z(q,b))*H(q,c)*c
          H(q,b); ->32
19: F''(i,j)=F''(i,j)+(F(7,q)+F(8,q)*Y(q,c)-F(9,q)*X(q,c)+(F(8,q)+F(10,q)*c
          Y(q,c))*Y(q,b)-(F(9,q)-F(11,q)*X(q,c))*X(q,b))*H(q,c)*H(q,b); ->32
20: F''(i,j)=F''(i,j)+(F(8,q)+F(10,q)*Y(q,c))*H(q,c)*H(q,b); ->32
21: F''(i,j)=F''(i,j)+(F(9,q)-F(11,q)*X(q,c))*H(q,c)*H(q,b); ->32
22: F''(i,j)=F''(i,j)+(F(5,q)-F(10,q)*Z(q,b))*H(q,c)*H(q,b); ->32
23: F''(i,j)=F''(i,j)+(F(8,q)+F(10,q)*Y(q,b))*H(q,c)*H(q,b); ->32
24: F''(i,j)=F''(i,j)+F(10,q)*H(q,c)*H(q,b); ->32
25: F''(i,j)=F''(i,j)+(F(2,q)+F(11,q)*Z(q,b))*H(q,c)*H(q,b); ->32
26: F''(i,j)=F''(i,j)+(F(9,q)-F(11,q)*X(q,b))*H(q,c)*H(q,b); ->32
27: F''(i,j)=F''(i,j)+F(11,q)*H(q,c)*H(q,b); ->32
28: F''(i,j)=F''(i,j)+(F(3,q)-F(12,q)*Y(q,b))*H(q,c)*H(q,b); ->32
29: F''(i,j)=F''(i,j)+(F(6,q)+F(12,q)*X(q,b))*H(q,c)*H(q,b); ->32
30: F''(i,j)=F''(i,j)+F(12,q)*H(q,c)*H(q,b); ->32
```

```
31: F''(i,j)=0
32:F''(j,i)=F''(i,j)
repeat
repeat
110: repeat
repeat
repeat
repeat
comment BtFB is input

begin
cycle i=1,1,cuts*dimensions
cycle j=1,1,cuts*dimensions
print fl(F''(i,j),3); spaces(2)
repeat
newline
repeat
end


invert(inv,F'',det)
newlines(2)
print fl(det,3)
newlines(2)


null (F''')
cycle q=1,1,elements-cuts
cycle p=1,1,cuts
cycle g=q,1,elements-cuts
b=elments-cuts+p
if  H(q,g)=0 or H(q,b)=0 then ->200
cycle i=6*g-5,1,6*g
cycle j=6*p-5,1,6*p


if i=6g-5 then ->41;  if i=6g-4 then ->42;  if i=6g-3 then ->43
if i=6g-2 then ->44;  if i=6g-1 then ->45;  -> 46
41:if j=6p-5 then ->71;  if j=6p-4 then ->81;  if j=6p-3 then ->91
if j=6p-1 then ->101;  if j=6pthen ->111;  ->311
42: if j=6p-5 then ->121;  if j=6p-4 then ->131;  if j=6p-3 then ->141
if j=6p-2 then ->151;  if j=6p   then ->161
->311
43:  if j=6p-5 then ->171;  if j=6p-4 then ->181;  if j=6p-3 then ->191
if j=6p-2 then ->201;  if j=6p-1 then ->211;  ->311
44: if j=6p-4 then ->221;  if j=6p-3 then ->231;  if j=6p-2 then ->241;  ->311
45:if j=6p-5 then ->251;  if j=6p-3 then ->261;  ifj=6p-1 then ->271;  ->311
46:if j=6p-5 then ->281;  if j=6p-4 then ->291;  if j=6p then ->301;  ->311


71: F'''(i,j)=F'''(i,j)+(F(1,q)+F(2,q)*Z(q,g)-F(3,q)*Y(q,g)+(F(2,q)+F(11,q)*c
              Z(q,g))*Z(q,b)-(F(3,q)-F(12,q)*Y(q,g))*Y(q,b))*H(q,b) ;->321
81: F'''(i,j)=F'''(i,j)+(-F(6,q)*Y(q,g)+(F(3,q)-F(12,q)*Y(q,g))*X(q,b))*c
              H(q,b) ;->321
91: F'''(i,j)=F'''(i,j)+(F(9,q)*Z(q,g)-(F(2,q)+F(11,q)*Z(q,g))*X(q,b))*c
              H(q,b);->321
101:F'''(i,j)=F'''(i,j)+(F(2,q)+F(11,q)*Z(q,g))*H(q,b) ;->321
111:F'''(i,j)=F'''(i,j)+(F(3,q)-F(12,q)*Y(q,g))*H(q,b);->321
121:F'''(i,j)=F'''(i,j)+(F(3,q)*X(q,g)-(F(6,q)+F(12,q)*X(q,g))*Y(q,b))*c
              H(q,b);->321
```

```
131:F'''(i,j)=F'''(i,j)+(F(4,q)-F(5,q)*Z(q,g)+F(6,q)*X(q,g)-(F(5,q)-F(10,q)*c
              Z(q,g))*Z(q,b)+(F(6,q)+F(12,q)*X(q,g))*X(q,b))*H(q,b) ;->321
141: F'''(i,j)=F'''(i,j)+(-F(8,q)*Z(q,g)+(F(5,q)-F(10,q)*Z(q,g))*Y(q,b))*c
              H(q,b);->321
151:F'''(i,j)=F'''(i,j)+(F(5,q)-F(10,q)*Z(q,g))*H(q,b);->321
161:F'''(i,j)=F'''(i,j)+(F(6,q)+F(12,q)*X(q,g))*H(q,b);->321
171:F'''(i,j)=F'''(i,j)+(-F(2,q)*X(q,g)+(F(9,q)-F(11,q)*X(q,g))*Z(q,b))*c
              H(q,b);->321
181:F'''(i,j)=F'''(i,j)+(F(5,q)*Y(q,g)-(F(8,q)+F(10,q)*Y(q,g))*Z(q,b))*c
              H(q,b);->321
191:F'''(i,j)=F'''(i,j)+(F(7,q)+F(8,q)*Y(q,g)-F(9,q)*X(q,g)+(F(8,q)+F(10,q)*c
              Y(q,g))*Y(q,b)-(F(9,q)-F(11,q)*X(q,g))*X(q,b))*H(q,b);->321
201:F'''(i,j)=F'''(i,j)+(F(8,q)+F(10,q)*Y(q,g))*H(q,b);->321
211:F'''(i,j)=F'''(i,j)+(F(9,q)-F(11,q)*X(q,g))*H(q,b);->321
221:F'''(i,j)=F'''(i,j)+(F(5,q)-F(10,q)*Z(q,b))*H(q,b);->321
231:F'''(i,j)=F'''(i,j)+(F(8,q)+F(10,q)*Y(q,b))*H(q,b);->321
241:F'''(i,j)=F'''(i,j)+F(10,q)*H(q,b);->321
251:F'''(i,j)=F'''(i,j)+(F(2,q)+F(11,q)*Z(q,b))*H(q,b);->321
261:F'''(i,j)=F'''(i,j)+(F(9,q)-F(11,q)*X(q,b))*H(q,b);->321
271:F'''(i,j)=F'''(i,j)+F(11,q)*H(q,b);->321
281:F'''(i,j)=F'''(i,j)+(F(3,q)-F(12,q)*Y(q,b))*H(q,b);->321
291:F'''(i,j)=F'''(i,j)+(F(6,q)+F(12,q)*X(q,b))*H(q,b);->321
301:F'''(i,j)=F'''(i,j)+F(12,q)*H(q,b);->321
311:F'''(i,j)=0
321: repeat
repeat
200: repeat
repeat
repeat
comment  Bot F B  is input

50: read(e)
cycle f=1,1,e
read(d)
cycle i=1,1,n
a(i)=0
repeat
->51 if cuts=0
cycle i=1,1,n
cycle p=1,1,dimensions*cuts
cycle q=1,1,dimensions*cuts
a(i)=a(i)-F'''(i,q)*inv(q,p)*F'''(d,p)
repeat
repeat
repeat
51:cycle q=1,1, elements-cuts
cycle p=q,1, elements-cuts
g=intpt((d+dimensions-1)/dimensions)
if H(q,p)=0or H(q,g)=0 then ->330
cycle j=6p-5,1,6p
->510 if fracpt((d-1)/6)<0.001
->52 if fracpt((d-2)/6)<0.001
->53 if fracpt((d-3)/6)<0.001
->54 if fracpt((d-4)/6)<0.001
->55 if fracpt((d-5)/6)<0.001
->56
```

```
510: if j=6p-5 then->72;  if j=6p-4 then ->82;  if j=6p-3 then ->92
if j=6p-1 then ->102;  if j=6p  then ->112;  ->312
52: if j=6p-5 then ->122;  if j=6p-4 then ->132;  if j=6p-3 then ->142
if j=6p-2 then ->152;  if j=6p   then ->162
->312


53:  if j=6p-5 then ->172;  if j=6p-4 then ->182;  if j=6p-3 then ->192
if j=6p-2 then ->202;  if j=6p-1 then ->212;  ->312
54: if j=6p-4 then ->222;  if j=6p-3 then ->232;  if j=6p-2 then ->242
->312
55:if j=6p-5 then ->252;  if j=6p-3 then ->262;  if j=6p-1 then ->272
->312
56:if j=6p-5 then ->282;  if j=6p-4 then ->292;  if j=6p then ->302
->312


72:a(j)=a(j)+F(1,q)+F(2,q)*Z(q,g)-F(3,q)*Y(q,g)+(F(2,q)+F(11,q)*Z(q,g))*c
       Z(q,p)-(F(3,q)-F(12,q)*Y(q,g))*Y(q,p) ;->322
82:a(j)=a(j)-F(6,q)*Y(q,g)+(F(3,q)-F(12,q)*Y(q,g))*X(q,p) ;->322
92:a(j)=a(j)+F(9,q)*Z(q,g) -(F(2,q)+F(11,q)*Z(q,g)) *X(q,p) ;->322

102:a(j)=a(j)+ F(2,q)+ F(11,q)*Z(q,g) ;->322
112:a(j)=a(j)+ F(3,q)- F(12,q)*Y(q,g) ;->322
122:a(j)=a(j)+(F(3,q)*X(q,g)-(F(6,q)+F(12,q)*X(q,g))*Y(q,p));->322
132:a(j)=a(j)+ F(4,q)-F(5,q)*Z(q,g)+F(6,q)*X(q,g) -(F(5,q)-F(10,q)*Z(q,g))*c
        Z(q,p)+(F(6,q)+F(12,q)*X(q,g))*X(q,p);->322
142:a(j)=a(j)-F(8,q)*Z(q,g)+(F(5,q)-F(10,q)*Z(q,g))*Y(q,p);->322
152:a(j)=a(j)+ F(5,q)-F(10,q)*Z(q,g) ;->322
162:a(j)=a(j)+ F(6,q)+F(12,q)*X(q,g) ;->322
172:a(j)=a(j)- F(2,q)*X(q,g)+(F(9,q)-F(11,q)*X(q,g))*Z(q,p);->322
182:a(j)=a(j)+ F(5,q)*Y(q,g)-(F(8,q)+F(10,q)*Y(q,g))*Z(q,p) ;->322
192:a(j)=a(j)+F(7,q)+F(8,q)*Y(q,g)-F(9,q)*X(q,g)+(F(8,q)+F(10,q)*Y(q,g))*c
        Y(q,p)-(F(9,q)-F(11,q)*X(q,g))*X(q,p);->322
202:a(j)=a(j)+F(8,q)+F(10,q)*Y(q,g);->322
212:a(j)=a(j)+F(9,q)-F(11,q)*X(q,g);->322
222:a(j)=a(j)+F(5,q)-F(10,q)*Z(q,p);->322
232:a(j)=a(j)+F(8,q)+F(10,q)*Y(q,p);->322
242:a(j)=a(j)+F(10,q);->322
252:a(j)=a(j)+F(2,q)+F(11,q)*Z(q,p);->322
262:a(j)=a(j)+F(9,q)-F(11,q)*X(q,p);->322
272:a(j)=a(j)+F(11,q);->322
282:a(j)=a(j)+F(3,q)-F(12,q)*Y(q,p);->322
292: a(j)=a(j)+F(6,q)+F(12,q)*X(q,p);->322
302:a(j)=a(j)+F(12,q);->322
312:a(j)=a(j)+0
322: repeat
 330:repeat

repeat

comment   input is  Bot F Bo - Bot F B * inv * ( Bot F B )t
cycle i=1,1,elements-cuts
cycle j=6i-5,1,6i-3
print fl(a(j),3); space
repeat
spaces(2)
```

```
if fracpt(i/3)<0.001 then newline
repeat
newlines(2)
repeat
end
end
runs=runs-1
->400 if runs>0
stop
end of program
```

```
14  6  1  1

0  0  0  4000  0  0  8000  0  0  100000  160000  320000
0  0  0

21.2  0  0  166.2  0  -84.9  166.2  0  84.9  106.1  84.9  84.9
-2.0  0  0

67.8  0  0  3639.1  0  -867.4  3639.1  0  867.4  361.4  289.1  289.1
-8.0  0  0

0.80  0  0  2.00  0  -0.10  2.00  0  0.10  0.60  0.40  0.40
-8.5  0  0

39.6  0  0  787.6  0  -295.2  787.6  0  295.2  210.8  168.7  168.7
-12.0  0  0

75.2  0  0  1608.9  0  -1065.7  1608.9  0  1065.7  1332.1  1065.7  1065.7
-14.0  0  0

21.2  0  0  166.2  0  84.9  166.2  0  -84.9  106.1  84.9  84.9
2.00  0  0

62.2  0  0  2827.9  0  728.8  2827.9  0  -728.8  331.3  265.0  265.0
7.50  0  0

42.4  0  0  1011.5  0  339.5  1011.5  0  -339.5  212.2  169.8  169.8
11.5  0  0

62.2  0  0  2827.9  0  728.8  2827.9  0  -728.8  331.3  265.0  265.0
17.0  0  0

21.2  0  0  166.2  0  84.9  166.2  0  -84.9  106.1  84.9  84.9
19.0  0  0

21.2  0  0  166.2  0  84.9  166.2  0  -84.9  106.1  84.9  84.9
21.0  0  0

33.9  0  0  518.5  0  216.8  518.5  0  -216.8  180.7  144.6  144.6
24.0  0  0

0  0  0  4000  0  0  8000  0  0  100000  160000  320000
19.0  0  0
```

14 5 -8 4 -8 3 -8 2 -8 1 -8 8 7 6 5 4 2 -1 1 -1 1

3
31
32
33

***Z

SPECIMEN RESULT

0.000α-99	0.000α-99	0.000α-99	2.120α -2	0.000α-99	0.000α-99
8.900α -2	0.000α-99	0.000α-99	8.980α -2	0.000α-99	0.000α-99
1.294α -1	0.000α-99	0.000α-99	2.046α -1	0.000α-99	0.000α-99
0.000α-99	0.000α-99	0.000α-99	0.000α-99	0.000α-99	0.000α-99
0.000α-99	0.000α-99	0.000α-99	0.000α-99	0.000α-99	0.000α-99
0.000α-99	0.000α-99	0.000α-99	0.000α-99	0.000α-99	0.000α-99
0.000α-99	0.000α-99	0.000α-99			

0.000α-99	3.473α 0	0.000α-99	0.000α-99	1.331α 1	0.000α-99
0.000α-99	5.472α 1	0.000α-99	0.000α-99	5.874α 1	0.000α-99
0.000α-99	8.824α 1	0.000α-99	0.000α-99	1.072α 2	0.000α-99
0.000α-99	-3.991α 0	0.000α-99	0.000α-99	-1.333α 1	0.000α-99
0.000α-99	-1.238α 1	0.000α-99	0.000α-99	-4.990α 0	0.000α-99
0.000α-99	-1.473α 0	0.000α-99	0.000α-99	2.046α 0	0.000α-99
0.000α-99	7.324α 0	0.000α-99			

0.000α-99	0.000α-99	6.947α 0	0.000α-99	0.000α-99	1.730α 1
0.000α-99	0.000α-99	6.028α 1	0.000α-99	0.000α-99	6.443α 1
0.000α-99	0.000α-99	9.483α 1	0.000α-99	0.000α-99	1.143α 2
0.000α-99	0.000α-99	-1.038α 0	0.000α-99	0.000α-99	-1.181α 1
0.000α-99	0.000α-99	-1.190α 1	0.000α-99	0.000α-99	-5.943α 0
0.000α-99	0.000α-99	-2.947α 0	0.000α-99	0.000α-99	5.167α -2
0.000α-99	0.000α-99	4.549α 0			

COMPUTER PROGRAM TO DETERMINE THE DYNAMIC RESPONSE OF THE HYDROSTATIC BEARING SYSTEM- WITH DAMPING

```
begin
integer elements, dimensions, cuts, n, runs, f, R, B,i,j,k,h,t,p,q,e,aa,c
bb,cc,ss,times,u
real e'
read (elements, cuts, B, R)
n=(elements-cuts)*3; dimensions=6
array A(1:2n,1:2n),X,Y(1:R+1,1:2*elements),l(1:2*elements,1:2)
array A'(1:2*elements,1:2*elements)
routine spec solve eigenvalue problem(arrayname A,l,X,Y, integer n,c
integername  R)
begin
real C
array a(1:n,1:n),m(1:n)
array H,X,Y,Z(1:elements,1:elements)
array F(1:12,1:elements)
cycle i=1,1,elements
cycle j=1,1,12
read(F(j,i)); F(j,i)=F(j,i)*10-9
repeat
read(X(1,i)); read(Y(1,i)); read(Z(1,i))
repeat
if elements=1 then ->1
cycle i=2,1,elements
k=i-1
cycle j=i,1,elements
X(i,j)=X(k,j)-X(k,i);  Y(i,j)=Y(k,j)-Y(k,i);  Z(i,j)=Z(k,j)-Z(k,i)
repeat
repeat

1:begin
real N
integer R,r
null(H)
cycle i=1,1,elements
read(N) ; if N > 100 then ->7
R=int(mod(N))+i-1; ->8
7: R=int(N)-100+i-1
8: r=i; ->5
3: r=R+1
read(N); if N>100 then ->9
R=R+int(mod(N)) ; ->5
9: R=R+int(N)-100
5: cycle j=r,1,R
```

```
if N<0 then ->2; if N>100 then ->6
H(i,j)=1 ; ->4
2: H(i,j)=0;->4
6: H(i,j)=-1
4: repeat
if R<elements then ->3
repeat
end
```

```
begin
real  det
integer  p,q,g,b,c,e,d,m,l
if cuts=0 then ->50
array inv,F'''(1:cuts*dimensions,1:cuts*dimensions)
array F'''(1:2*n,1:cuts*dimensions)
switch  A(1:6), C(1:3), D'(0:8), D(0:35)
cycle times=1,1,2
null (F''')
aa=0;  bb=0;  cc=1
if times=1 then aa=1; if times=2 then bb=1; if times=2 then cc=-1
cycle q=1,1,elements-bb*cuts
cycle  p=1,1,cuts
b=elements-cuts+p;  ->47 if H(q,b)=0
cycle g=aa*p+bb*q,1,bb*elements+cuts*cc
h=int((g-p)/(g-p+0.1));  c=g+(elements-cuts)*aa
if H(q,c)=0 then -> 110
cycle i=6g-5,1,6g
d=i-6g+6
cycle j=6p-5,1,6p*(h*aa+bb)+i*aa*(1-h)
->A(d)
A(1): f=j-6p+5; ->D(f);  A(2): f=j-6p+11; ->D(f);  A(3): f=j-6p+17; ->D(f)
A(4): f=j-6p+23; ->D(f);  A(5): f=j-6p+29; ->D(f);  A(6): f=j-6p+35; ->D(f)

D(0): F'''(i,j)=F'''(i,j)+(F(1,q)+F(2,q)*Z(q,c)-F(3,q)*Y(q,c)+(F(2,q)+F(11,q)*c
                Z(q,c))*Z(q,b)-(F(3,q)-F(12,q)*Y(q,c))*Y(q,b))*H(q,c)*H(q,b)
                ->32
D(1): F'''(i,j)=F'''(i,j)+(-F(6,q)*Y(q,c)+(F(3,q)-F(12,q)*Y(q,c))*X(q,b))*c
                H(q,c)*H(q,b);   ->32
D(2):  F'''(i,j)=F'''(i,j)+(F(9,q)*Z(q,c)-(F(2,q)+F(11,q)*Z(q,c))*X(q,b))*c
                 H(q,c)*H(q,b);   ->32
D(4): F'''(i,j)=F'''(i,j)+(F(2,q)+F(11,q)*Z(q,c))*H(q,c)*H(q,b);  ->32

D(5): F'''(i,j)=F'''(i,j)+(F(3,q)-F(12,q)*Y(q,c))*H(q,c)*H(q,b);  ->32

D(6): F'''(i,j)=F'''(i,j)+(F(3,q)*X(q,c)-(F(6,q)+F(12,q)*X(q,c))*Y(q,b))*c
                H(q,c)*H(q,b);   ->32
D(7): F'''(i,j)=F'''(i,j)+(F(4,q)-F(5,q)*Z(q,c)+F(6,q)*X(q,c)-(F(5,q)-F(10,q)*c
                Z(q,c))*Z(q,b)+(F(6,q)+F(12,q)*X(q,c))*X(q,b))*H(q,c)*H(q,b)
                ->32
D(8): F'''(i,j)=F'''(i,j)+(-F(8,q)*Z(q,c)+(F(5,q)-F(10,q)*Z(q,c))*Y(q,b))*c
                H(q,c)*H(q,b);   ->32
D(9): F'''(i,j)=F'''(i,j)+(F(5,q)-F(10,q)*Z(q,c))*H(q,c)*H(q,b);  ->32

D(11): F'''(i,j)=F'''(i,j)+(F(6,q)+F(12,q)*X(q,c))*H(q,c)*H(q,b); ->32

D(12): F'''(i,j)=F'''(i,j)+(-F(2,q)*X(q,c)+(F(9,q)-F(11,q)*X(q,c))*Z(q,b))*c
                 H(q,c)*H(q,b);  ->32

D(13): F'''(i,j)=F'''(i,j)+(F(5,q)*Y(q,c)-(F(8,q)+F(10,q)*Y(q,c))*Z(q,b))*c
                 H(q,c)*H(q,b);   ->32
```

```
D(14):F'''(i,j)=F'''(i,j)+(F(7,q)+F(8,q)*Y(q,c)-F(9,q)*X(q,c)+(F(8,q)+F(10,q)*c
                Y(q,c))*Y(q,b)-(F(9,q)-F(11,q)*X(q,c))*X(q,b))*H(q,c)*H(q,b)
                ->32
D(15): F'''(i,j)=F'''(i,j)+(F(8,q)+F(10,q)*Y(q,c))*H(q,c)*H(q,b);  ->32
D(16): F'''(i,j)=F'''(i,j)+(F(9,q)-F(11,q)*X(q,c))*H(q,c)*H(q,b);  ->32
D(19): F'''(i,j)=F'''(i,j)+(F(5,q)-F(10,q)*Z(q,b))*H(q,c)*H(q,b);  ->32
D(20): F'''(i,j)=F'''(i,j)+(F(8,q)+F(10,q)*Y(q,b))*H(q,c)*H(q,b);  ->32
D(21): F'''(i,j)=F'''(i,j)+F(10,q)*H(q,c)*H(q,b);  ->32
D(24): F'''(i,j)=F'''(i,j)+(F(2,q)+F(11,q)*Z(q,b))*H(q,c)*H(q,b);  ->32
D(26): F'''(i,j)=F'''(i,j)+(F(9,q)-F(11,q)*X(q,b))*H(q,c)*H(q,b);  ->32
D(28): F'''(i,j)=F'''(i,j)+F(11,q)*H(q,c)*H(q,b);  ->32
D(30): F'''(i,j)=F'''(i,j)+(F(3,q)-F(12,q)*Y(q,b))*H(q,c)*H(q,b);  ->32
D(31): F'''(i,j)=F'''(i,j)+(F(6,q)+F(12,q)*X(q,b))*H(q,c)*H(q,b);  ->32
D(35): F'''(i,j)=F'''(i,j)+F(12,q)*H(q,c)*H(q,b);  ->32
D(10): ->D(3); D(17): ->D(3); D(18): ->D(3); D(22): ->D(3); D(23): ->D(3)
D(25): ->D(3); D(27): ->D(3); D(29):->D(3); D(32): ->D(3); D(33): ->D(3)
D(34): ->D(3)
D(3): F'''(i,j)=0

32:repeat
repeat
110:repeat
47:repeat
repeat
->50 if times=2
cycle i=1,1,6*cuts
cycle j=1,1,i
F''(i,j)=F'''(i,j);  F''(j,i)=F''(i,j);  repeat
repeat
cycle i=1,1,6*cuts
cycle j=1,1,6*cuts
print fl(F''(i,j),3);  spaces(2)
repeat
newline
repeat
invert(inv,F'',det);  newlines(2)
print fl(det,3); newlines(2)
->2
50:null(a)
->51if cuts=0
cycle i=1,1,n
p=i+3*(intpt(i/3.001))
cycle j=1,1,i
q=j+3*(intpt(j/3.001))
cycle l=1,1,6*cuts
cycle e=1,1,6*cuts
a(i,j)=a(i,j)-F'''(p,e)*inv(e,l)*F'''(q,l)
repeat
repeat
repeat
repeat
2:repeat
51:cycle q=1,1,elements-cuts
cycle p=q,1,elements-cuts
```

```
if H(q,p)=0 then ->331
cycle g=p,1,elements-cuts
if H(q,g)=0 then ->330
m=int((g-p)/(g-p+0.1))
cycle l=6g-5,1,6g-3
i=int(l-1.5*(intpt(l/3.001))); c=l-6*g+6
cycle e=6p-5,1,m*(6p-l-3)+1
j=int(e-1.5*(intpt(e/3.001)))

->C(c)
C(1): f=e-6*p+5; ->D'(f);  C(2): f=e-6*p+8; ->D'(f);  C(3): f=e-6*p+11; ->D'(f)

D'(0): a(i,j)=a(i,j)+F(1,q)+F(2,q)*Z(q,g)-F(3,q)*Y(q,g)+(F(2,q)+F(11,q)*Z(q,g))*c
              Z(q,p)-(F(3,q)-F(12,q)*Y(q,g))*Y(q,p);  ->322
D'(1): a(i,j)=a(i,j)-F(6,q)*Y(q,g)+(F(3,q)-F(12,q)*Y(q,g))*X(q,p);  ->322
D'(2): a(i,j)=a(i,j)+F(9,q)*Z(q,g) -(F(2,q)+F(11,q)*Z(q,g)) *X(q,p);  ->322
D'(3):a(i,j)=a(i,j)+(F(3,q)*X(q,g)-(F(6,q)+F(12,q)*X(q,g))*Y(q,p));  ->322
D'(4): a(i,j)=a(i,j)+ F(4,q)-F(5,q)*Z(q,g)+F(6,q)*X(q,g)-(F(5,q)-F(10,q)*c
              Z(q,g))*Z(q,p)+(F(6,q)+F(12,q)*X(q,g))*X(q,p);  ->322
D'(5): a(i,j)=a(i,j)-F(8,q)*Z(q,g)+(F(5,q)-F(10,q)*Z(q,g))*Y(q,p);->322

D'(6): a(i,j)=a(i,j)-F(2,q)*X(q,g)+(F(9,q)-F(11,q)*X(q,g))*Z(q,p);  ->322
D'(7): a(i,j)=a(i,j)+ F(5,q)*Y(q,g)-(F(8,q)+F(10,q)*Y(q,g))*Z(q,p);  ->322
D'(8):a(i,j)=a(i,j)+F(7,q)+F(8,q)*Y(q,g)-F(9,q)*X(q,g)+(F(8,q)+F(10,q)*c
            Y(q,g))*Y(q,p)-(F(9,q)-F(11,q)*X(q,g))*X(q,p);  ->322
322: repeat
repeat

330: repeat
331: repeat
repeat
end
comment a contains lower triangle of 3*3 flex matrix

cycle i=1,1,n
cycle j=1,1,n
a(i,j)=a(j,i)
repeat
repeat
cycle i=0,3,n-3
read(e')
cycle j=1,1,3
m(i+j)=e'
repeat
repeat
null(A)
cycle p=1,1,n
i=n+p
cycle j=1,i,n
A(j,i)=-a(j,p)*m(p)
repeat
repeat
cycle i=1,1,B
u=1
read(C,p,q)
->333 unless p=0
u=0; p=1
333: cycle j=1,1,n
A(j,p)=A(j,p)-u*C*(a(j,p)-a(j,q));  A(j,q)=A(j,q)-C*(a(j,q)-u*a(j,p))
```

```
repeat
repeat
cycle j=1,1,n
A(n+j,j)=1
repeat
end

n=2*n
cycle ss=1,1,3
cycle i=ss,3,(n-3+ss)
p=1+intpt(i/3.001)
cycle j=ss,3,(n-3+ss)
q=1+intpt(j/3.001);  A'(p,q)=A(i,j)
repeat
repeat
n=(elements-cuts)*2
solve eigenvalue problem(A',l,X,Y,n,R)
newline
cycle i=1,1,n
print fl(l(i,1),3); spaces(2)
if fracpt(i/10)<.001 then newline
repeat
newlines(3)
cycle i=1,1,n
print fl(l(i,2),3); spaces(2)
if fracpt(i/10)<.001 then newline
repeat
newlines(4)
n=(elements-cuts)*6
if R=0 then -> 423
newlines(2)

cycle i=1,1,R
cycle j=1,1,(elements-cuts)*2
print fl(X(i,j),3);  spaces(2)
if fracpt(j/9) < 0.001 then newline
repeat
newlines(2)

cycle  j=1,1,(elements-cuts)*2
print fl(Y(i,j),3);  spaces(2)
if fracpt(j/9) < 0.001 then newline
repeat
newlines(3)
repeat
e'=0
cycle i=1,1,R
cycle j=1,1,(elements-cuts)*2
A(j,1)=(X(i,j))^2+(Y(i,j))^2;  e'=e'+A(i,j)
repeat
newline
print fl(e',6);  newline
repeat
423:repeat


routine solve eigenvalue problem(arrayname A,l,X,Y, integer n,integername R)
real norm ; array b,c,d(1:n)
```

```
routine Lanczos tridiagonalization (array name A,b,c,d, integer n)
array B(1:n+1,1:n), BB(1:n+1,1:n), bb(1:n), e(1:n), ee(1:n)
integer i,j,r; real sum,sum1,sum2,sum3,x,y,br,cr
x = sqrt(1/n)
cycle i = 1,1,n ; B(1,i) = x; BB(1,i) = x ; repeat; b(1) = 0 ; c(1) = 0

cycle r = 1,1,n
cycle i = 1,1,n
sum = 0; sum1 = 0
cycle j = 1,1,n ; sum = sum+ A(i,j)*B(r,j); sum1 = sum1 + A(j,i)*BB(r,j)
repeat
B(r + 1,i) = sum ; BB(r + 1,i) = sum1
repeat
sum=0
cycle i = 1,1,n; sum = sum + B(r,i)*BB(r,i)
repeat
bb(r) = sum ;sum = 0
-> 2 if r = 1 ; br = bb(r)/bb(r-1) ; b(r) = cr*br ; br = c(r)*br

2: cycle i = 1,1,n; sum = sum + BB(r,i)*B(r + 1,i)
repeat

d(r) = sum/bb(r) ; -> 3 if r = n
cycle i = 1,1,n
sum = B(r + 1,i); sum1 = BB(r + 1,i)
sum = sum - d(r)*B(r,i); sum1 = sum1 - d(r)*BB(r,i); -> 1 if r = 1
sum = sum - b(r)*B(r - 1,i); sum1 = sum1 - br*BB(r - 1,i)
1:  B(r + 1,i) = sum ; BB(r + 1,i) = sum1
repeat
cycle i = 1,1,r
sum = 0; sum1 = 0
cycle j = 1,1,n
sum = sum + BB(i,j)*B(r + 1,j); sum1 = sum1 + B(i,j)*BB(r + 1,j)
repeat
e(i) = sum/bb(i) ; ee(i) = sum1/bb(i)
repeat
sum2 = 0; sum3=0
cycle i = 1,1,n
sum = 0; sum1 = 0
cycle j = 1,1,r
sum = sum + e(j)*B(j,i); sum1 = sum1 + ee(j)*BB(j,i)
repeat
x = B(r + 1,i) - sum; B(r + 1,i) = x ; y = BB(r + 1,i) - sum1; BB(r + 1,i) = y
sum2 = sum2 + x^2; sum3 = sum3 + y^2
repeat
sum2 = sqrt(sum2); c(r + 1) = sum2; sum2 = 1/sum2 ; cr = sqrt(sum3)
sum3 = 1/cr
cycle i = 1,1,n
B(r + 1,i) = B(r + 1,i)*sum2 ;BB(r + 1,i) = BB(r + 1,i)*sum3
repeat
repeat
3: cycle r = 1,1,n
cycle i = 1,1,n
A(r,i) = B(r,i)
repeat
repeat
return
end
```

```
routine eigenvalues(arrayname b,c,d,l, integer n, realname norm)
integer i,j,k,N,L,t,rev ; real p,q,D,M,dp,dq,K,KO,r,dr,s,S
array a(0:1,0:n),A,Q,T,E,F(0:m),pa,qa(0:1)
-> 18 if n > 1 ; l(1,1) = d(1) ; l(1,2) = 0 ; norm = |d(1)| ; -> 17
18: norm = |d(1)| + |b(2)|
    cycle i = 2,1,n-1
    s = |c(i)| + |d(i)| + |b(i+1)| ; norm = s if s > norm ; repeat
    s = |c(n)| + |d(n)| ;norm = s if s > norm ; s = 1/norm
    a(0,0) = 1 ; a(1,0) = d(1)*s ; a(1,1) = - 1
    cycle i = 2,1,n
    M = -b(i)*c(i)*s² ; D = d(i)*s
    A(0) = D*a(1,0) + M*a(0,0) ; A(i-1) =  -a(1,i-2) + D*a(1,i-1)
    A(i) = - a(1,i-1) ; a(1,i) = 0 ; -> 19 if i < 3
    cycle j = 1,1,i-2
    A(j) = -a(1,j-1) + D*a(1,j) + M*a(0,j)
    repeat
19: cycle j = 0,1,i
    a(0,j) = a(1,j) ; a(1,j) = A(j)
    repeat
    repeat
    N = n ; t = 1 ; k = 1 ; KO = 1α-11
1:  -> 2 if A(0) ≠ 0 ; N = N-1 ; l(N,1) = 0 ; l(N,2) = 0
    cycle i = 0,1,N
    A(i) = A(i+1)
    repeat
    -> 1
2:  pa(0) = 0 ; pa(1) = 0 ; qa(0) = 0 ; qa(1) = 0 ; r = 0
3:  -> 7 if N = 0 ; -> 11 if N = 1 ; L = 0 ; -> 4 if N > 2 ; p = -A(1)/A(2)
    q = -A(0)/A(2)
    -> 10
11: r = - A(0)/A(1) ; -> 5
4:  K = KO ; s = 0 ; rev = 1
    cycle j = 0,1,N
    s = s + log(|A(j)|) if A(j) ≠ 0;   repeat
    s = exp(-s/(N+1))
    cycle  j = 0,1,N
    A(j) = A(j)*s
    repeat
    -> 6 if |A(N-1)A(0)| > |A(1)A(N)|
15: t = -t ; k = k + t ; r = 1/r if r ≠ 0
    cycle i = 0,1,intpt(½N-0.1)
    s = A(i) ; A(i) = A(N-i) ; A(N-i) = s
    repeat
6:  p = pa(k) ; q = qa(k)
21: cycle i = 1,1,20
    Q(N) = A(N) ; Q(N-1) = A(N-1) + p*Q(N) ; T(N) = 0 ; T(N-1) = 0
    cycle j = N-2,-1,0
    Q(j) = A(j) + p*Q(j+1) + q*Q(j+2) ; T(j) = Q(j+2) + p*T(j+1) + q*T(j+2)
    repeat
    -> 8 if |Q(1)| ≤ K ; -> 12 if |A(1)*K| ≤ |Q(1)| ; Q(0) = A(0) + q*Q(2)
8:  -> 10 if |Q(0)| ≤ K ; -> 10 if |Q(0)| ≤ |A(0)*K|
12: E(N) = A(N) ; F(N) = 0
    cycle j = N-1,-1,0
    E(j) = A(j) + r*E(j+1) ; F(j) = E(j+1) + r*F(j+1)
    repeat
    -> 5 if |E(0)| ≤ K ; -> 5 if |E(0)| ≤ |A(0)*K| ; M = p*T(0) + q*T(1)
```

```
D = T(0)^2 - M*T(1)
    D = K0 if D = 0 ; D = 1/D
    dp = (Q(0)*T(1) - T(0)*Q(1))*D ; dq = (M*Q(1) - T(0)*Q(0))*D
    -> 10 if |p*dp| + |dq| ≤ 5K*(p^2 + |q|) ; p = p + dp ; q = q + dq
    F(0) = K0 if F(0) = 0 ; dr = -E(0)/F(0) ; -> 5 if |dr| ≤ 5K*|r| ; r = r + dr
    repeat
    pa(k) = p ; qa(k) = q ; s = |Q(0)/A(0)| ;s = s + |Q(1)/A(1)| if A(1) ≠ 0
    -> 6 if s ≤ 10K ; K = 10K if rev < 0 ; rev = -rev ; -> 15
5:  r = 1/r if t < 0 ; 1(N,1) = r*norm ; 1(N,2) = 0 ; N = N-1
    cycle j = 0,1,N
    A(j) = E(j+1)
    repeat
    -> 3
10: s = ½p ;-> 13 if L = 1 and i = 1 ; D = s^2 ; S = D+q ; -> 13 if L = 1
    -> 13 if|S|≥1α-10*D
                    S = 0 ; L = 1 ; q = -D ; r = s ; -> 21
13: -> 14 if t > 0 ; q = 1/q ; s = -s*q ; S = S*q^2
14: p = s ; L = 1 ; L = 0 if S≥ 0 ; s = sqrt(|S|)
    switch C(0:1) ; -> C(L)
    C(0): 1(N,1) = norm*(p + s); 1(N,2) = 0; 1(N-1,1) = norm*(p - s)
    1(N-1,2) = 0 ; -> 16
    C(1): D = norm*p ; s = norm*s ; 1(N,1) = D ; 1(N,2) = s ; 1(N-1,1) = D
    1(N-1,2) = - s
16: N = N-2
    cycle j = 0,1,N
    A(j) = Q(j+2)
    repeat
    -> 3
7:  cycle i = 1,1,n
    A(i) = 1(i,1)^2 + 1(i,2)^2
    repeat
    N = n
9:  M  = A(N) ; k = N
   cycle i = N-1,-1,1
    -> 20 if A(i) ≥ M ; M = A(i) ; k = i
20: repeat
    p = 1(N,1) ; 1(N,1) = 1(k,1) ; 1(k,1) = p ; A(k) = A(N)
    p = 1(N,2) ; 1(N,2) = 1(k,2) ; 1(k,2) = p ; N = N-1 ; -> 9 if N > 1
17: return
    end


    routine tridiinverse iteration(arrayname b,c,d,1,X,Y,integer n,real norm)
    integer i,j,k
real s,h,eps,bi,bi1; complex lambda,u,v,w,eta
    array r,int(1:n) ;complex array m,p,q(1:n),x(1:n+2),y(1:n)
    eps = 1α-11*norm ; norm = norm*sqrt(0.5) ; lambda = norm*(1+i)
    R = n if R > n
    cycle j = 1,1,R
    w = 1(j,1) + i*1(j,2)  ; u = w-lambda
    -> 13 if |im(w)| > 0 and mag(u- 2i*im(w)) = 0
    -> 15 if mag(u) < eps ; lambda = w ; -> 16
   15:  lambda = lambda*(1 - eps/mag(lambda)) ; lambda = re(lambda) if im(w) = 0
16:  u = d(1) - lambda ; v = b(2) ; v = eps if b(2) = 0
    cycle i = 2,1,n
    bi = c(i) ; bi = eps if bi = 0 ; -> 3 if i = n
    bi1 = b(i+1) ; bi1 = eps if bi1 = 0
```

```
 3: -> 1 if |bi| ≥ mag(u)
    m(i) = bi/u ; p(i-1) = u ; q(i-1) = v ;  r(i-1) = 0
    u = d(i) - lambda - m(i)*v ; v = bi1 ; int(i) = -1 ; -> 2
 1: m(i) = u/bi ; m(i) = 1 if mag(m(i)) = 0 and bi ≤ eps
    p(i-1) = bi ; q(i-1) = d(i) - lambda ; r(i-1) = bi1
    u = v - m(i)*q(i-1) ; v = -m(i)*r(i-1) ; int(i) = 1
 2: repeat
      p(n) = u ; q(n) = 0 ; r(n) = 0 ; x(n+1) = 0 ; x(n+2) = 0 ; h = 0

    eta = 1/n ; eta = eta*(1+i) if im(lambda) ≠ 0 ; s = 0
    cycle i = n,-1,1
    u = eta - q(i)*x(i+1) - r(i)*x(i+2)
    bi1 = mag(p(i)) ; -> 6 if bi1 = 0 ; x(i) = u/p(i) ; -> 7
 6: x(i) = u/eps
 7: bi = mag(x(i)) ; -> 11 if bi ≤ s ; s = bi ; v = x(i)
11: h = h + mag(x(i))^2
    repeat
      h = 1/sqrt(h) ; v = h*conj(v)/s
    cycle  i = 1,1,n
      y(i) = x(i)*v ; x(i) = y(i)
      repeat
    cycle k = 1,1,5 ; s = 0
    cycle i = 2,1,n
    -> 4 if int(i) > 0; x(i) = x(i) - m(i)*x(i-1) ; -> 5
 4: u = x(i-1) ; x(i-1) = x(i) ; x(i) = u - m(i)*x(i-1)
 5: repeat
      h = 0
    cycle i = n,-1,1
    u = x(i) - q(i)*x(i+1) - r(i)*x(i+2)
    bi1 = mag(p(i)) ; -> 8 if bi1 = 0 ; x(i) = u/p(i) ; -> 9
 8: x(i) = u/eps
 9: bi = mag(x(i)) ; -> 12 if bi ≤ s ; s = bi ; v = x(i)
12: h = h + bi^2
    repeat
      h = 1/sqrt(h) ; v = h*conj(v)/s ; s = 0
    cycle i = 1,1,n
      u = x(i)*v ; s = s + mag(y(i)-u)^2 ; y(i) = u ; x(i) = u
    repeat
      -> 10 if s < n*1α-11
    repeat
      -> 10
13: cycle i = 1,1,n
      X(j,i) = X(j-1,i) ; Y(j,i) = -Y(j-1,i)
      repeat
      -> 14
10: cycle i = 1,1,n
      X(j,i) = re(y(i)) ; Y(j,i) = im(y(i))
      repeat
14: repeat
    return
      end

    routine backtransformation (arrayname A,X,Y,integer n)
    integer i,j,r ; complex sum,z ; complex array  y(1:n)
    cycle r = 1,1,R
    cycle i = 1,1,n
      sum = 0
    cycle j = 1,1,n
      sum = sum + A(j,i)*(X(r,j) + i*Y(r,j))
```

```
      repeat
      y(i) = sum
    repeat
    cycle i = 1,1,n ; X(r,i) = re(y(i)) ; Y(r,i) = im(y(i))
      repeat
    repeat
    return
      end

Lanczos tridiagonalization(A,b,c,d,n)
eigenvalues(b,c,d,1,n,norm)

-> 1 if R ≤ 0
tridiinverse iteration(b,c,d,1,X,Y,n,norm)
backtransformation(A,X,Y,n)
   1: return
      end

      end of program
```

```
8  1  4  9

0  0  0  4000  0  0  8000  0  0  100000  160000  320000
0  0  0

89.9  0  0  9050  0  -1525  9050  0  1525  452  360  360
-8.5  0  0

39.7  0  0  842  0  -299  842  0  299  199  159  159
-12.25  0  0

13.6  0  0  80.5  0  -34.7  80.5  0  34.7  43.5  34.7  34.7
-14.25  0  0

100.6  0  0  12420  0  1910  12420  0  -1910  505  402  402
9.50  0  0

100.6  0  0  12420  0  1910  12420  0  -1910  505  402  402
19.0  0  0

50.3  0  0  1652  0  476  1652  0  -476  230  201  201
23.755  0  0

0  0  0  4000  0  0  8000  0  0  100000  160000  320000
19.0  0  0

8  3 -4  2 -4  1 -4  4  3  1 -1  1

.02051  .02161  .00784  .00356  .02161  .01620  .00540

400  0  2
400  0  3
400  0  17
400  0  18

***Z
```

SPECIMEN RESULT

-3.117α -3	-2.733α -3	-1.866α -4	-1.866α -4	-1.147α -5	-1.147α -5
-1.114α -5	-1.114α -5	-1.593α -5	-1.593α -5	-5.550α -5	-4.388α -5
-7.157α -9	-7.157α -9				
0.000α-99	0.000α-99	-2.353α -3	2.353α -3	-3.323α -4	3.323α -4
-1.818α -4	1.818α -4	-1.346α -4	1.346α -4	0.000α-99	0.000α-99
-2.817α -5	2.817α -5				
7.471α -4	2.193α -4	-1.057α -5	-1.328α -4	1.356α -3	1.997α -3
2.316α -3	-2.397α -1	-7.035α -2	3.391α -3	4.262α -2	-4.350α -1
-6.408α -1	-7.430α -1				
0.000α-99	0.000α-99	0.000α-99	0.000α-99	0.000α-99	0.000α-99
0.000α-99	0.000α-99	0.000α-99	0.000α-99	0.000α-99	0.000α-99
0.000α-99	0.000α-99				
-9.943α -4	-1.154α -3	-1.169α -3	-1.173α -3	-4.292α -4	3.673α -4
7.804α -α	3.638α -1	4.224α -1	4.278α -1	4.293α -1	1.571α -1
-1.344α -1	-2.856α -1				
0.000α-99	0.000α-99	0.000α-99	0.000α-99	0.000α-99	0.000α-99
0.000α-99	0.000α-99	0.000α-99	0.000α-99	0.000α-99	0.000α-99
0.000α-99	0.000α-99				
1.122α -4	2.204α -4	2.728α -4	3.010α -4	2.376α -5	-4.649α -5
-8.068α -5	-2.999α -2	-3.475α -1	-5.252α -1	-6.225α -1	7.357α -2
1.272α -2	-3.090α -2				
6.212α -5	8.053α -4	1.222α -3	1.450α -3	-1.761α -4	-2.643α -5
7.957α -5	4.532α -2	6.612α -2	7.427α -2	7.854α -2	1.593α -2
-1.875α -2	-3.674α -2				
1.122α -4	2.204α -4	2.728α -4	3.010α -4	2.376α -5	-4.649α -5
-8.068α -5	-2.999α -2	-3.475α -1	-5.252α -1	-6.225α -1	7.357α -2
1.272α -2	-3.090α -2				
-6.212α -5	-8.053α -4	-1.222α -3	-1.450α -3	1.761α -4	1.643α -5
-7.957α -5	-4.532α -2	-6.612α -2	-7.427α -2	-7.854α -2	-1.593α -2
1.875α -2	3.674α -2				
4.047α -7	3.762α -6	-5.809α -8	-2.600α -6	-1.592α -5	9.317α -8
1.572α -5	-5.864α -3	-3.967α -3	-8.570α -4	1.116α -3	-5.608α -3
-5.768α -4	2.287α -3				

CALCULATION OF THE RESONANT FREQUENCY, DAMPING RATIO ETC. FROM THE COMPUTER PROGRAM PRINT OUT.

The dynamic equations of motion are formulated in the program, from the data supplied on the flexibility, damping and inertial properties of the system. The program calculates the roots of the system characteristic equations from which the various resonant frequencies and the damping ratios may be determined. Referring to the print out on page xxxix, the first block contains the real part and the second block the imaginary part of the n roots of the equation. Therefore, the first root is;

$$= 1.866\alpha \quad = 4 \pm j\, 2.353 \quad = 3 \tag{1}$$

Consider a system with a single degree of freedom expressed by the equation

$$\frac{1}{s^2} + \frac{2\xi}{w_n s} + \frac{1}{w_n^2} = 0 \tag{2}$$

where s is the Laplace Operator.

Then the roots of the equation are

$$\frac{1}{s} = -\frac{\xi}{w_n} \pm j \sqrt{\frac{1-\xi^2}{w_n^2}} \tag{3}$$

Therefore equating the equations (1) and (3)

$$\frac{\xi}{w_1} = 1.866 \times 10^{-5}$$

and

$$\sqrt{\frac{1-\xi^2}{w_1^2}} = 2.353 \times 10^{-3} \tag{4}$$

The solution of the equation gives;

$f_1 = 68.0$ c/s

and $\xi = .0791$

Similarly, the next block gives the modal shape information, i.e. the real and imaginary parts of the velocity (first seven figures) and acceleration (next seven figures) vectors of the various points on the spindle. From these values the modal shape of the spindle can be drawn at each resonance frequency as shown in Figs. 45, 46, 47, etc.

SPECIMEN CALCULATION OF THE SYSTEM FLEXIBILITIES FOR THE COMPUTER PROGRAM

14 - Element Model for Static Load Deflection

$E = 30 \times 10^6$ lb/in

$G = 12 \times 10^6$ lb/in^2

Element	L	D	$\frac{L}{EA}$ $= \frac{4L}{\pi d^2 E}$	$\frac{L^3}{3EI_z}(1+\alpha)$ $= \frac{64L^3}{3E\pi d^4}(1+\frac{3Ed^2}{1bGL^2})$	$\frac{L^2}{2EI_z}$ $= \frac{32L^2}{\pi Ed^4}$	$\frac{L^3}{3EI_y}(1+\alpha)$ $= \frac{64L^3}{3\pi Ed^4}(1+\frac{3Ed^2}{1bGL^2})$	$\frac{L^2}{2EI_y}$ $= \frac{32L^2}{\pi Ed^4}$	$\frac{L}{GJ}$ $= \frac{32L}{\pi Ed^4}$	$\frac{L}{EI_y}$ $= \frac{64L}{\pi Ed^4}$	$\frac{L}{EI_z}$ $= \frac{64L}{\pi Ed^4}$
1-2	2.00	2.000	21.2	166.2	84.9	166.2	84.9	106.1	84.9	84.9
2-3	6.00	1.937	67.8	3639.1	867.4	3639.1	867.4	361.4	289.1	289.1
3-4	0.50	5.250	0.8	2.0	0.1	2.0	0.1	0.6	0.4	0.4
4-5	3.50	1.937	39.6	787.6	195.2	787.6	295.2	210.8	168.7	168.7
5-6	2.00	1.062	75.2	1608.9	1065.7	1608.9	1065.7	1332.1	1065.7	1065.7
1-7	2.00	2.000	21.2	166.2	84.9	166.2	84.9	106.1	84.9	84.9
7-8	5.50	1.937	62.2	2827.9	728.8	2827.9	728.8	331.3	265.0	265.0
8-9	4.00	2.000	42.4	1011.5	339.5	1011.5	339.5	212.2	169.8	169.8
9-10	5.50	1.937	62.2	2827.9	728.8	2827.9	728.8	331.3	265.0	265.0
10-11	2.00	2.000	21.2	166.2	84.9	166.2	84.9	106.1	84.9	84.9
11-12	2.00	2.000	21.2	166.2	84.9	166.2	84.9	106.1	84.9	84.9
12-13	3.00	1.937	33.9	518.5	216.8	518.5	216.8	180.7	144.6	144.6

COMPUTER PROGRAM TO STUDY THE EFFECT OF RADIAL LAND WIDTH RATIO ON THE OIL FLOW AND THE TOTAL POWER REQUIREMENT OF THE HYDROSTATIC THRUST BEARING

```
begin
real s,R1, R2, R3, R4, Kf,Kl,Kc,Kp,u,w,hop,hs,p,hb,q,P,n,h,N,d,l
integer i,j,11
array aa,bb,cc(0:16)
read(R1,R4,u,w,n,N,d)

R2=R1;  R3=R4
select output(1)
cycle i=1,1,12
R2=R2+1/32
R3=R3-1/32

Kf=(1/log(R2/R1)+1/log(R4/R3))
Kl=((R4^2-R3^2)/log(R4/R3)-(R2^2-R1^2)/log(R2/R1))
Kp=(R4↑4-R3↑4)÷(R2↑4-R1↑4)
p=2w/(π*Kl)
newlines(4)
caption$$R2$=$; print(R2,1,4); spaces(8)
caption$R3$=$; print(R3,1,4); newline
caption$$Kf$=$; print fl(Kf,4); spaces(4)
caption$Kl$=$; print fl(Kl,4); newline
caption$$Kp$=$; print fl(Kp,4); newline
caption$$pocket$pressure$in$psi$=$; print(p,2,3); newline
hop=.406*sqrt(u*N/w)*(exp(.25*log(Kp*Kl^2/Kf)))
caption$$optimum$film$thickness$in$inches$hopt$=$; print fl(hop,3)
newlines(2)
caption$$$$$h$$$$$$$$$$$$$$hs$$$$$$$$$$$q$$$$$$$$$$$hb$$$$$$$$$$Pp
newline
cycle j=0,1,16;   h=j*1α-3
if j< 0.5  then h=hop
hs=N^2*u*((R2↑4-R1↑4)÷(R4↑4-R3↑4))/(58.05*h)/6600
q=π*p*Kf*h↑3/(6*u);   hb=p*q/6600;   P=(hs+hb)
print fl(h,3); spaces(5); print(hs,2,3); spaces(5); print(q,3,3)
spaces(5); print(hb,2,3); spaces(5); print(P,2,3)
4: Kc=(π*Kf*h↑3)/(6u*n)
s=-.75*π*Kl*p/h;   l=π*(d↑4)/(128u*Kc);   newline
3:aa(j)=Kc;   bb(j)=s;   cc(j)=l
repeat
newlines(4)
caption$$$$Kc$$$$$$$$$$$$$$$$s$$$$$$$$$$$$$$$l
newline
cycle j=0,1,16
print fl(aa(j),3); spaces(5); print fl(bb(j),3); spaces(5)
print fl(cc(j),3)
newline
```

repeat
newpage
repeat

stop
end of program

1.125 2.625 9.96α-6 500 4.00 2000 8.4α-2

...

***Z

SPECIMEN RESULT

R2 = 1.1875 R3 = 2.5625
Kf = 5.9993α 1 Kl = 1.0781α 1
Kp = 4.7498α 0
pocket pressure in psi = 29.524
optimum film thickness in inches hopt = 4.463α -3

h	hs	q	hb	P
4.463α -3	0.111	8.280	0.037	0.148
1.000α -3	0.494	0.093	0.000	0.494
2.000α -3	0.247	0.745	0.003	0.250
3.000α -3	0.165	2.514	0.011	0.176
4.000α -3	0.123	5.959	0.027	0.150
5.000α -3	0.099	11.640	0.052	0.151
6.000α -3	0.082	20.113	0.090	0.172
7.000α -3	0.071	31.939	0.143	0.213
8.000α -3	0.062	47.675	0.213	0.275
9.000α -3	0.055	67.882	0.304	0.359
1.000α -2	0.049	93.116	0.417	0.466
1.100α -2	0.045	123.937	0.554	0.599
1.200α -2	0.041	160.904	0.720	0.761

Kc	s	l
7.011α -2	-1.680α 5	1.750α 0
7.885α -4	-7.500α 5	1.556α 2
6.308α -3	-3.750α 5	1.945α 1
2.129α -2	-2.500α 5	5.763α 0
5.046α -2	-1.875α 5	2.431α 0
9.856α -2	-1.500α 5	1.245α 0
1.703α -1	-1.250α 5	7.204α -1
2.704α -1	-1.071α 5	4.536α -1
4.037α -1	-9.375α 4	3.039α -1
5.748α -1	-8.333α 4	2.134α -1
7.885α -1	-7.500α 4	1.556α -1
1.049α 0	-6.818α 4	1.169α -1
1.362α 0	-6.250α 4	9.005α -2

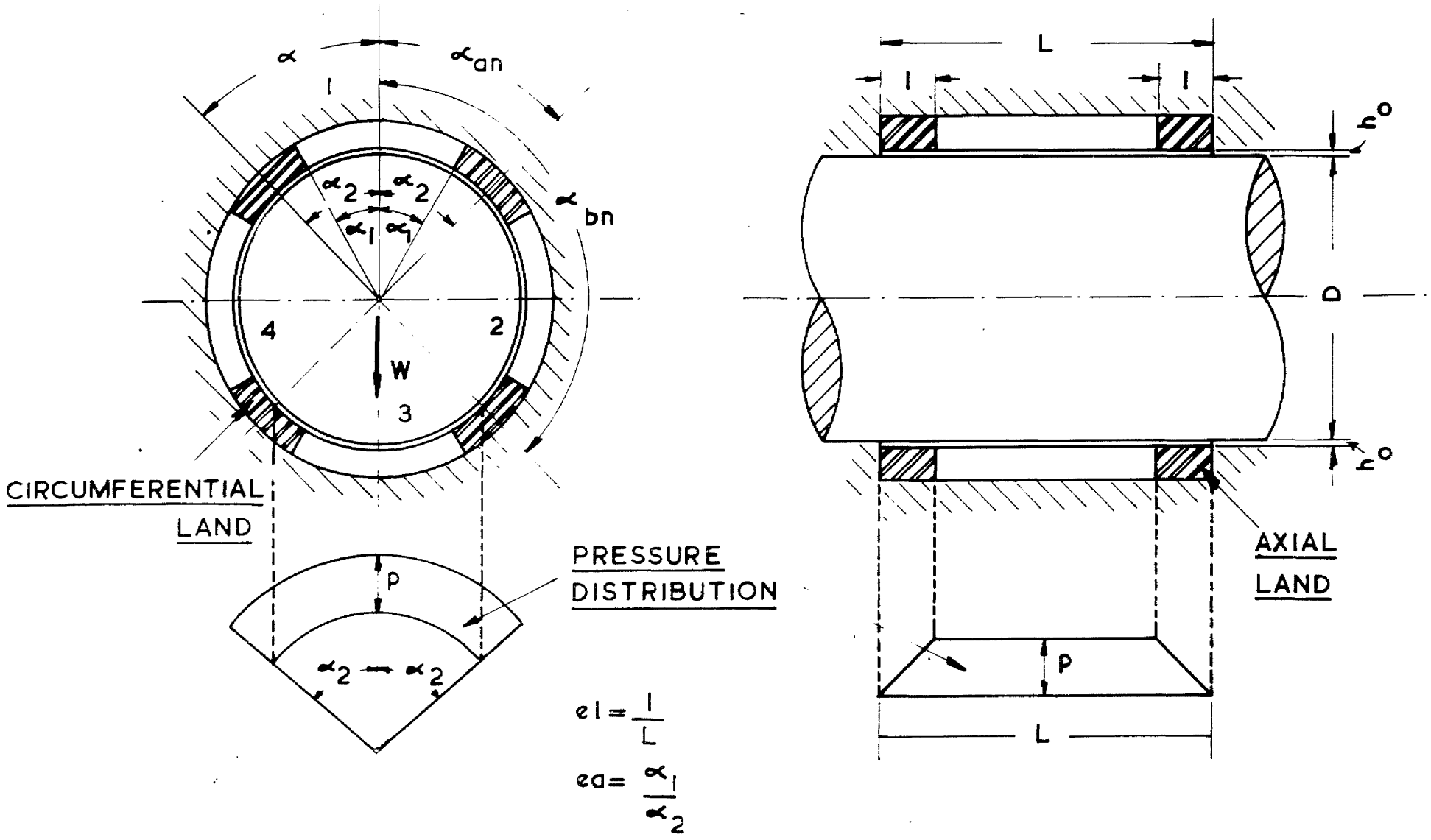

FIG. 1 4-PAD JOURNAL BEARING CONFIGURATION

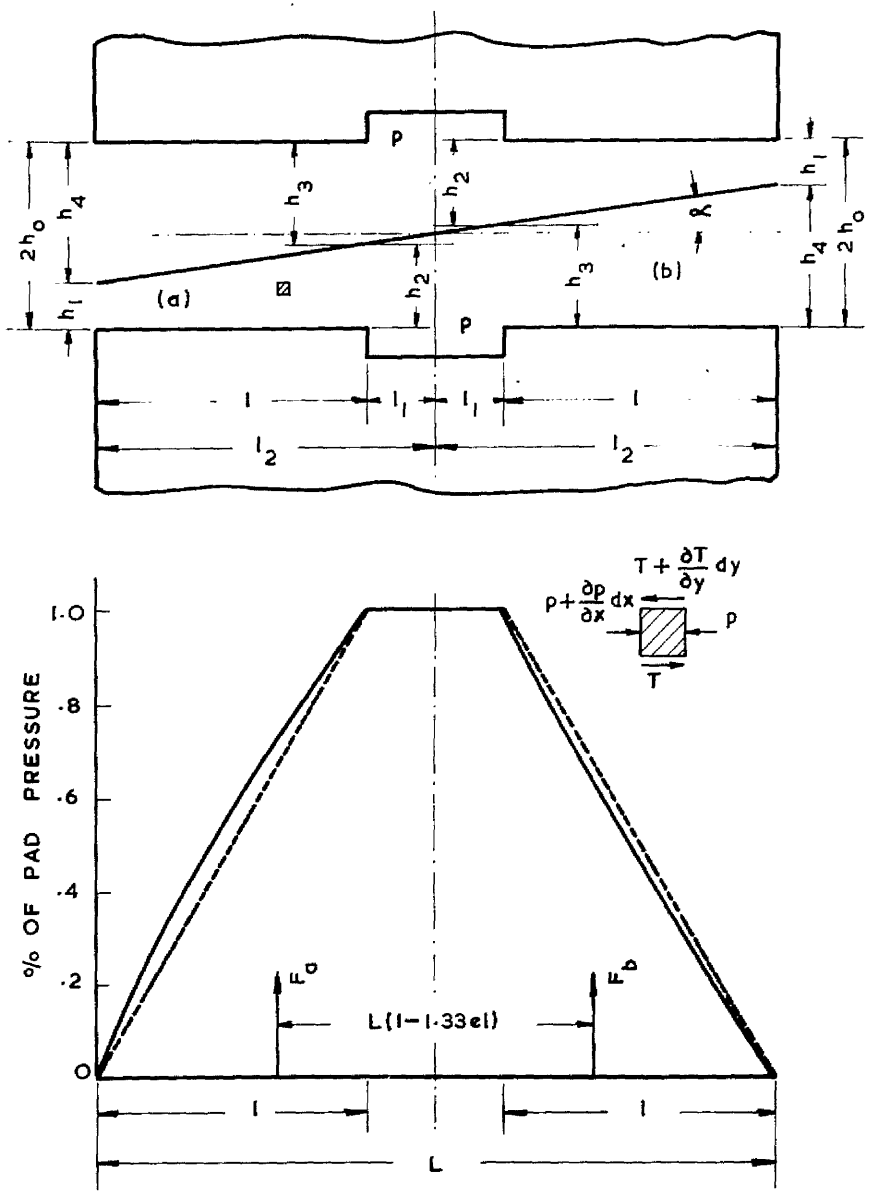

FIG.2 TYPICAL PRESSURE DISTRIBUTION OVER THE AXIAL LAND WITH SPINDLE TILT

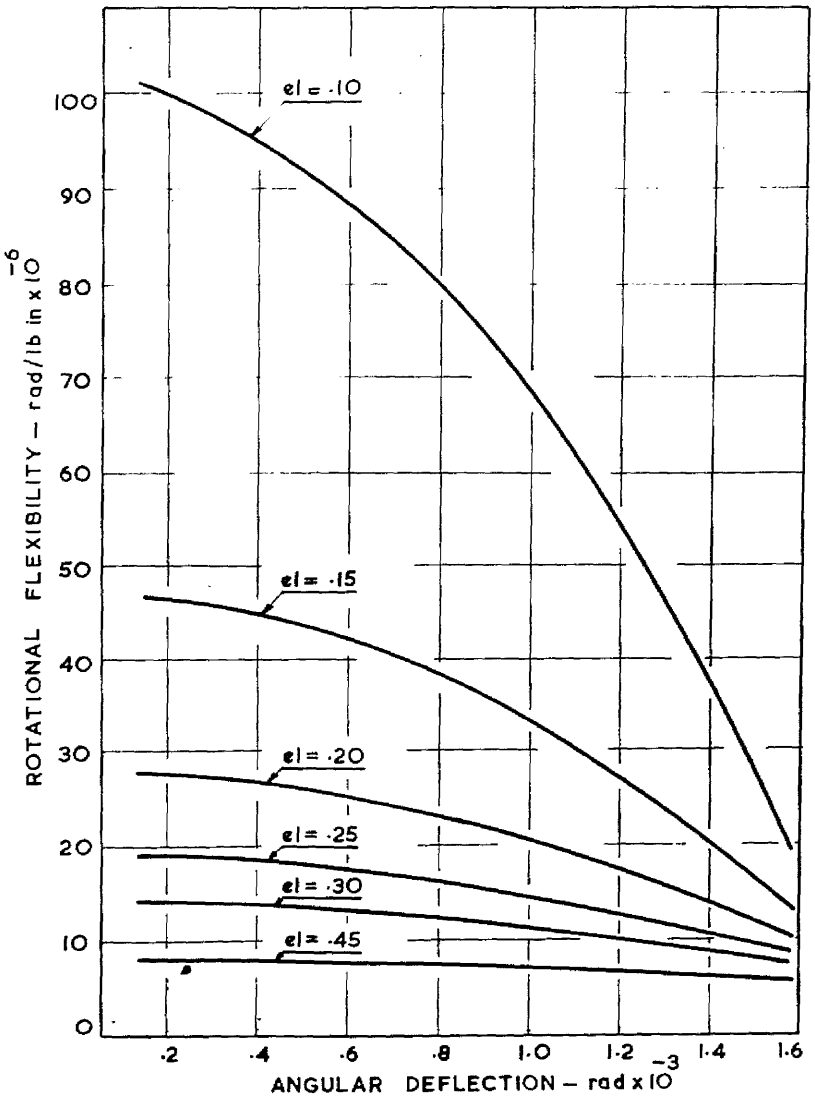

FIG.3 VARIATION IN ROTATIONAL FLEXIBILITY WITH ANGULAR DEFLECTION OF THE SPINDLE

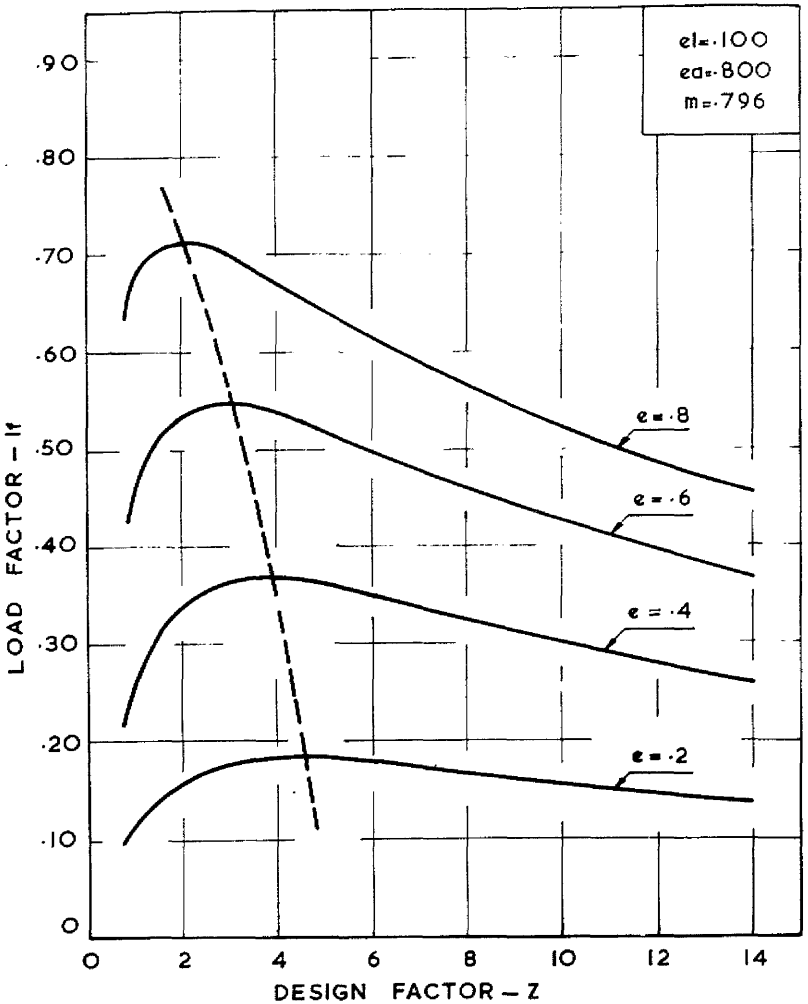

FIG.4 VARIATION OF LOAD FACTOR WITH DESIGN FACTOR

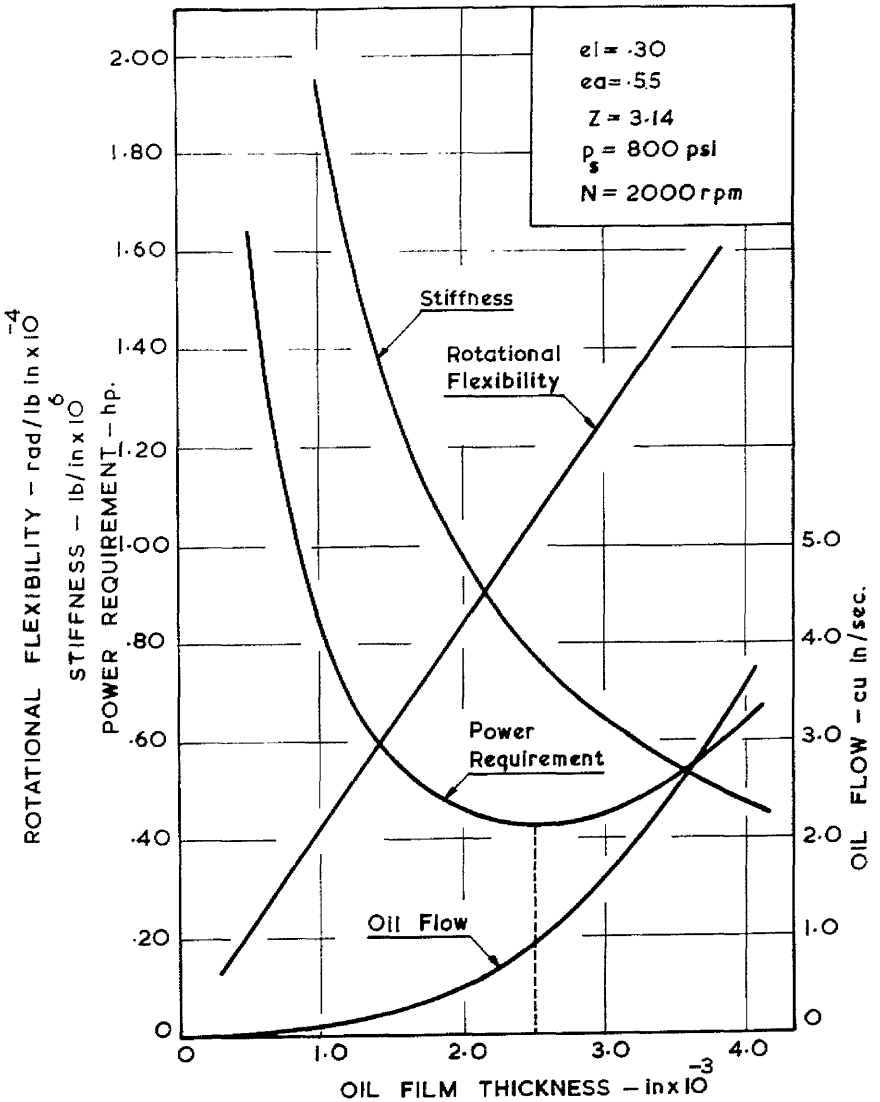

FIG.5 VARIATION OF ROTATIONAL FLEX., STIFFNESS, POWER REQUIREMENT AND OIL FLOW WITH FILM THICKNESS

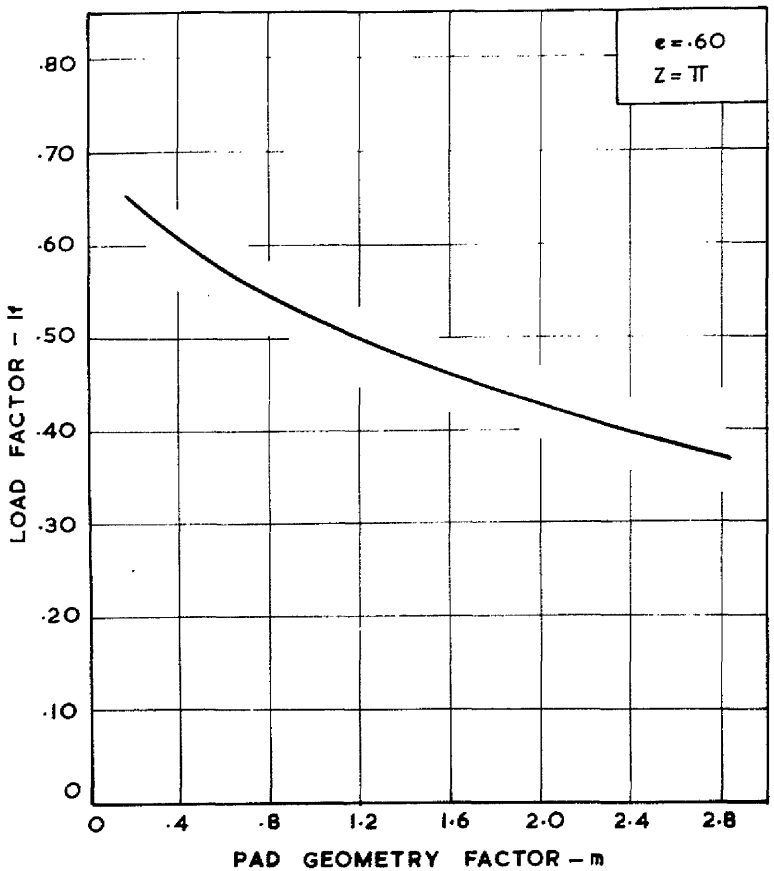

FIG.6 VARIATION OF LOAD FACTOR WITH PAD GEOMETRY FACTOR

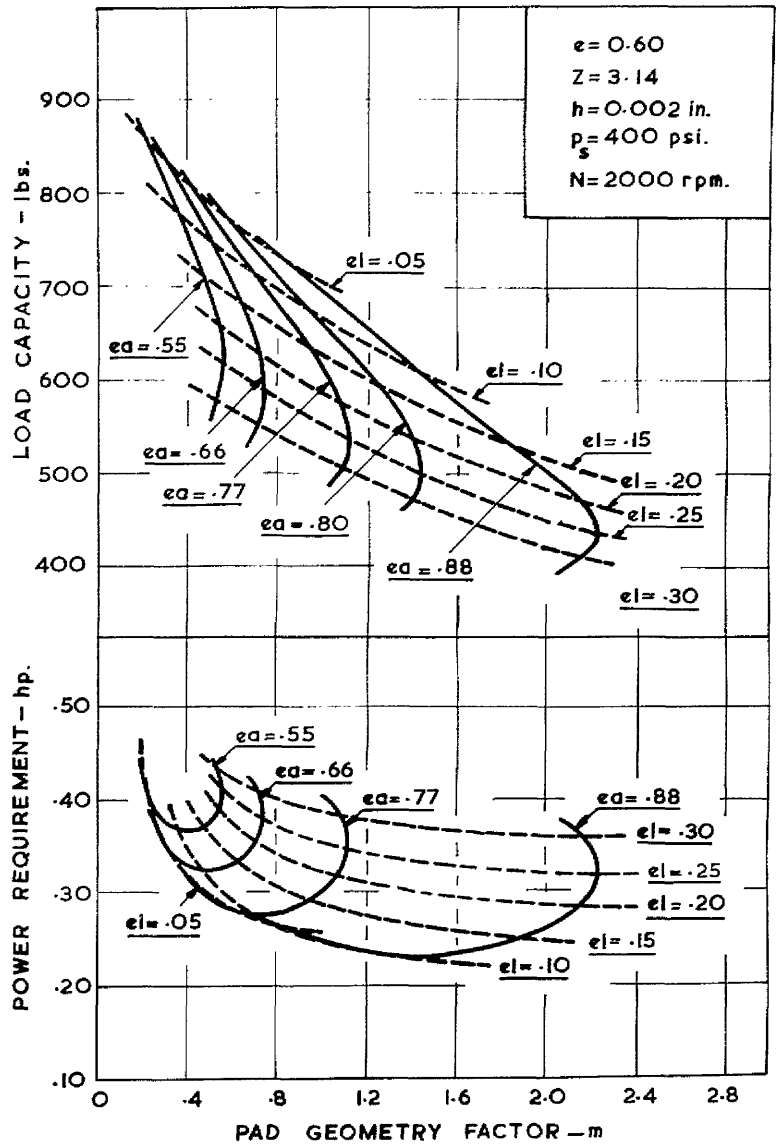

FIG.7 VARIATION OF LOAD CAPACITY AND POWER REQUIREMENT WITH PAD GEOMETRY FACTOR

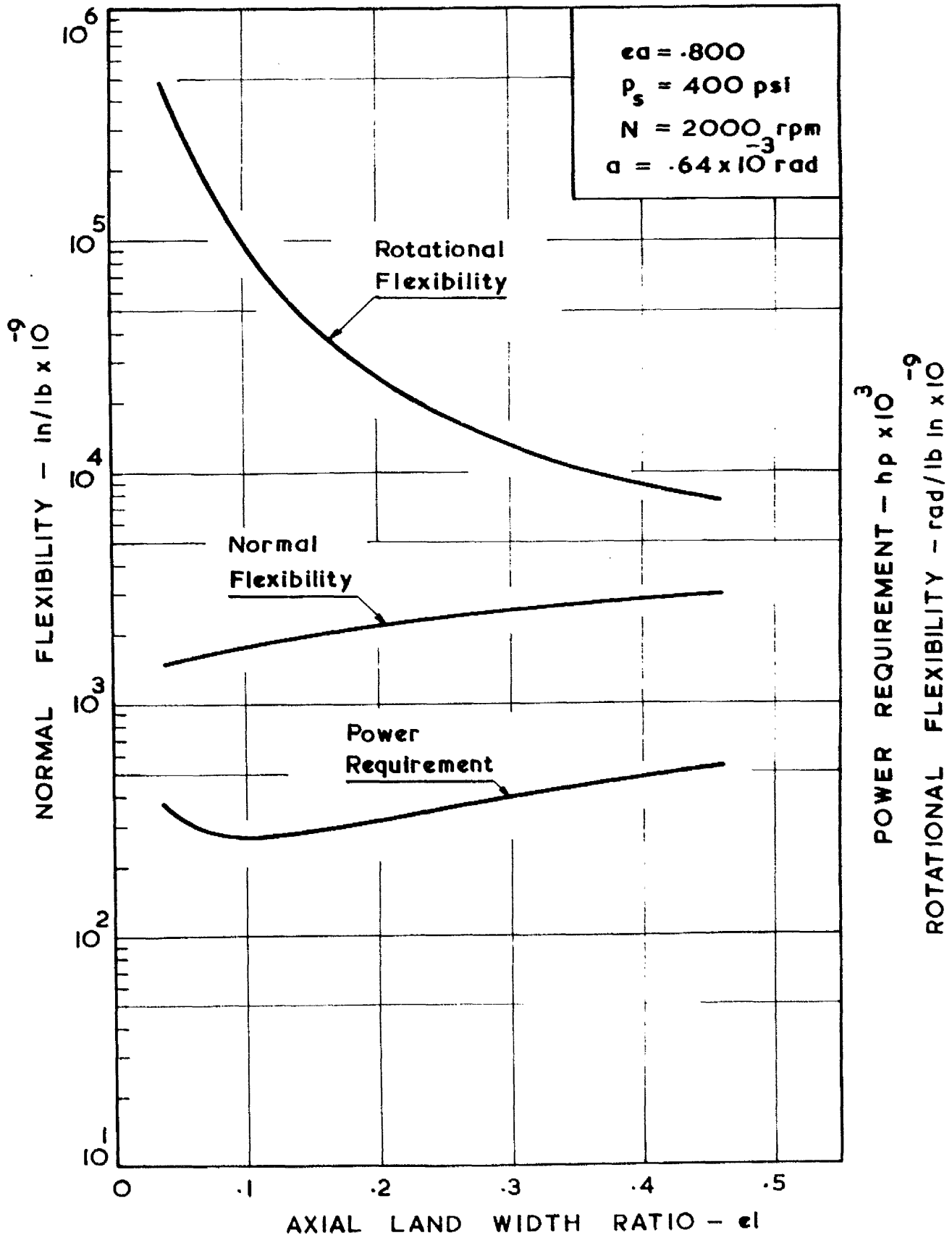

FIG. 8 VARIATION OF NORMAL AND ROTATIONAL FLEXIBILITIES AND POWER REQUIREMENT WITH AXIAL LAND WIDTH RATIO

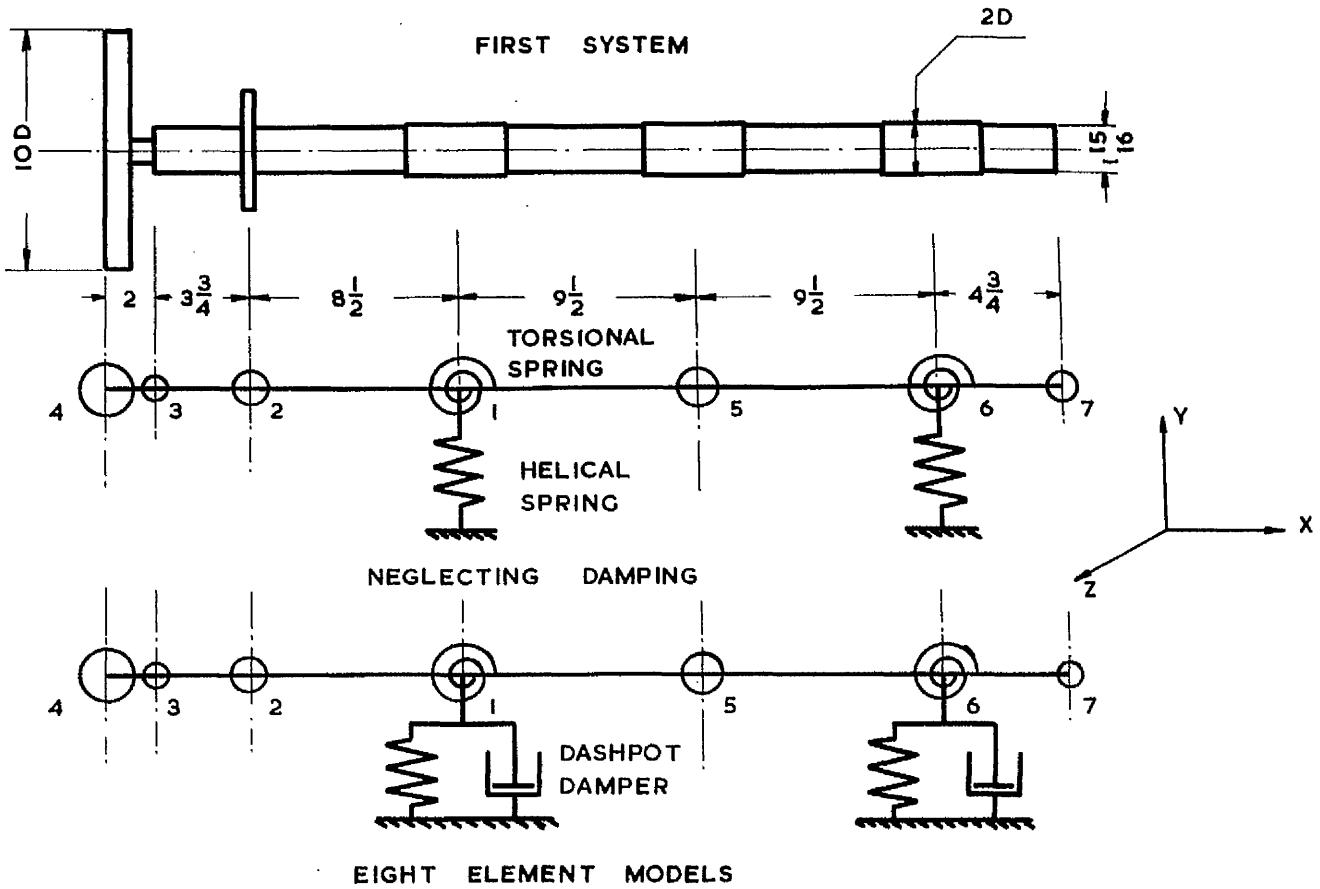

EIGHT ELEMENT MODELS

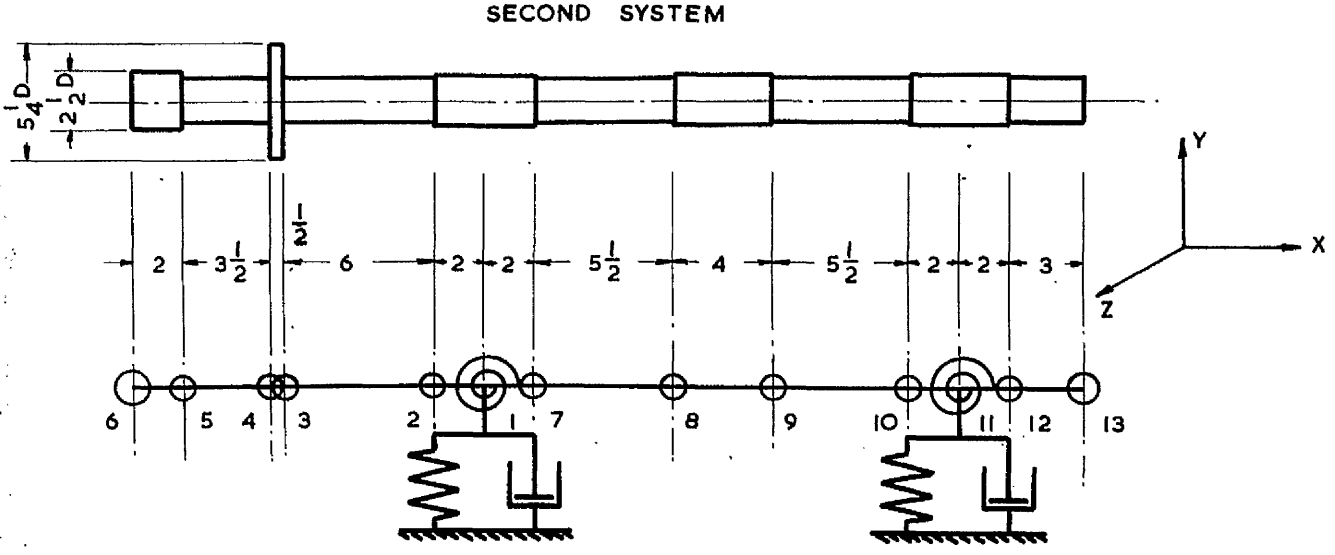

FOURTEEN ELEMENT MODEL
ALL DIMENSIONS IN INCHES

FIG.9 MODELS OF THE BEARING SYSTEM FOR THE COMPUTER PROGRAM

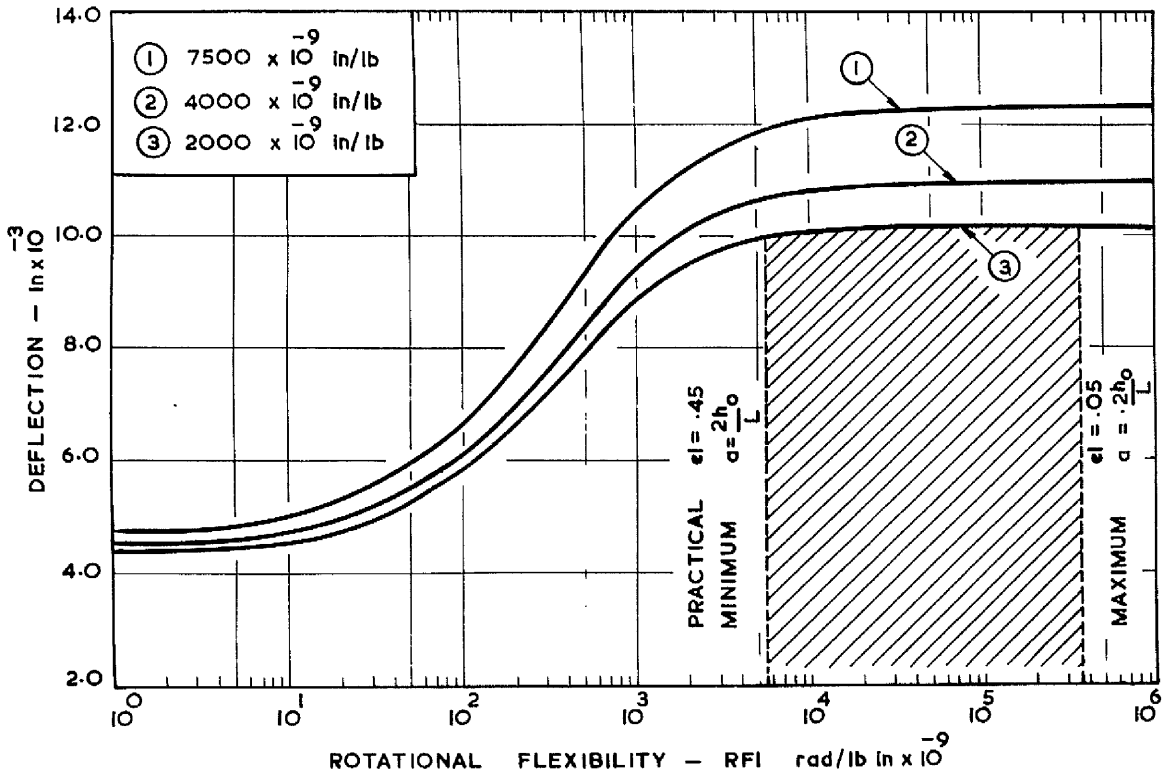

FIG.10 VARIATION OF SPINDLE END DEFLECTION WITH ROTATIONAL FLEXIBILITY FOR VARIOUS NORMAL FLEXIBILITIES

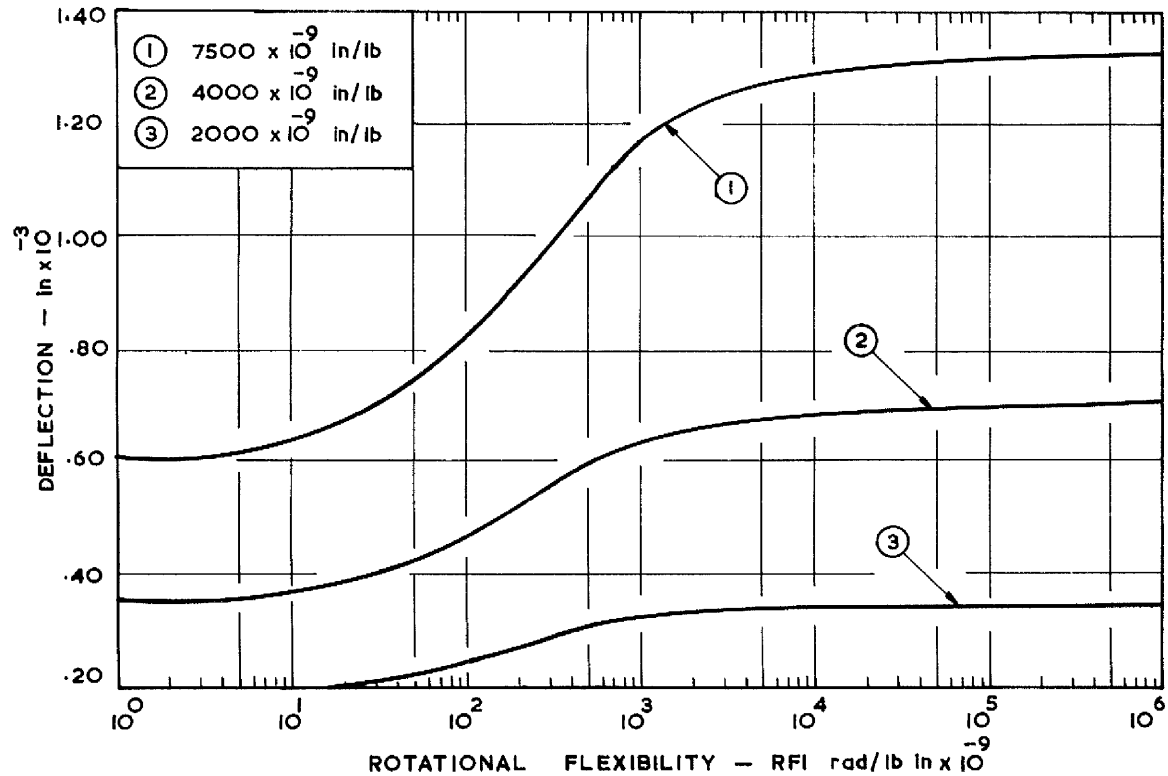

FIG.11 VARIATION OF BEARING POINT DEFLECTION WITH ROTATIONAL FLEXIBILITY FOR VARIOUS NORMAL FLEXIBILITIES

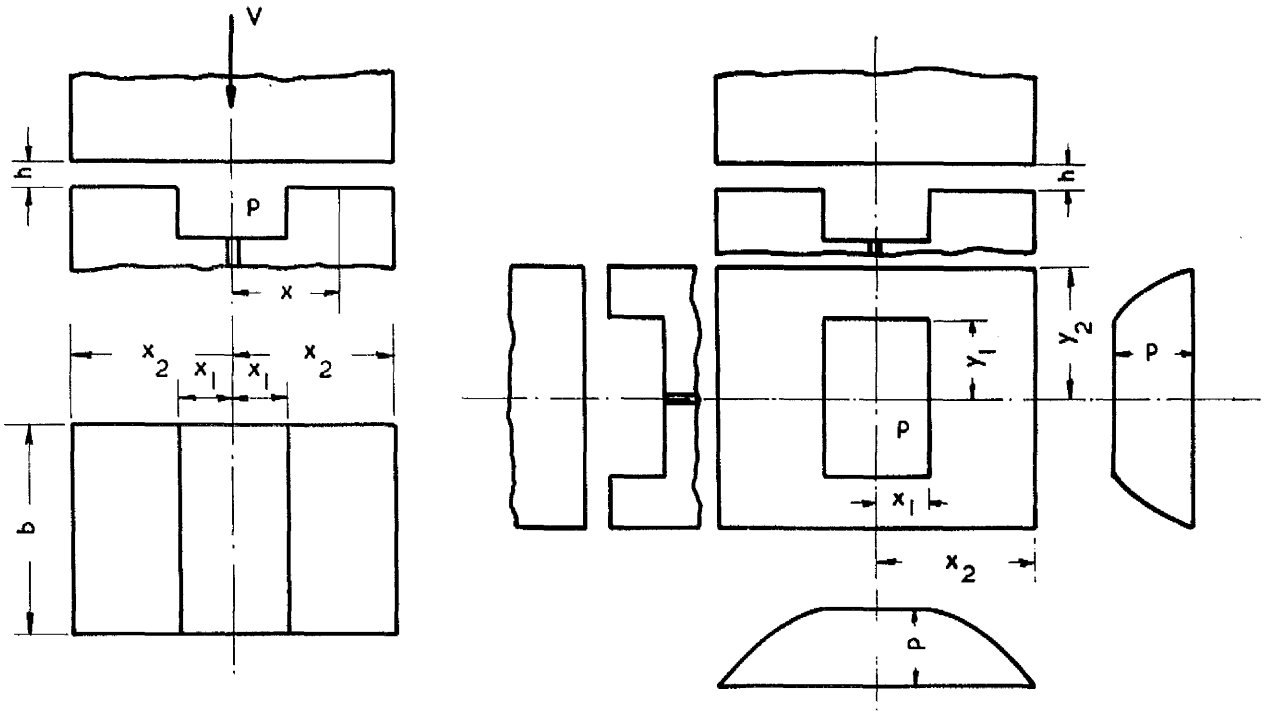

ONE DIMENSIONAL FLOW

TWO DIMENSIONAL FLOW

RECTANGUR PADS

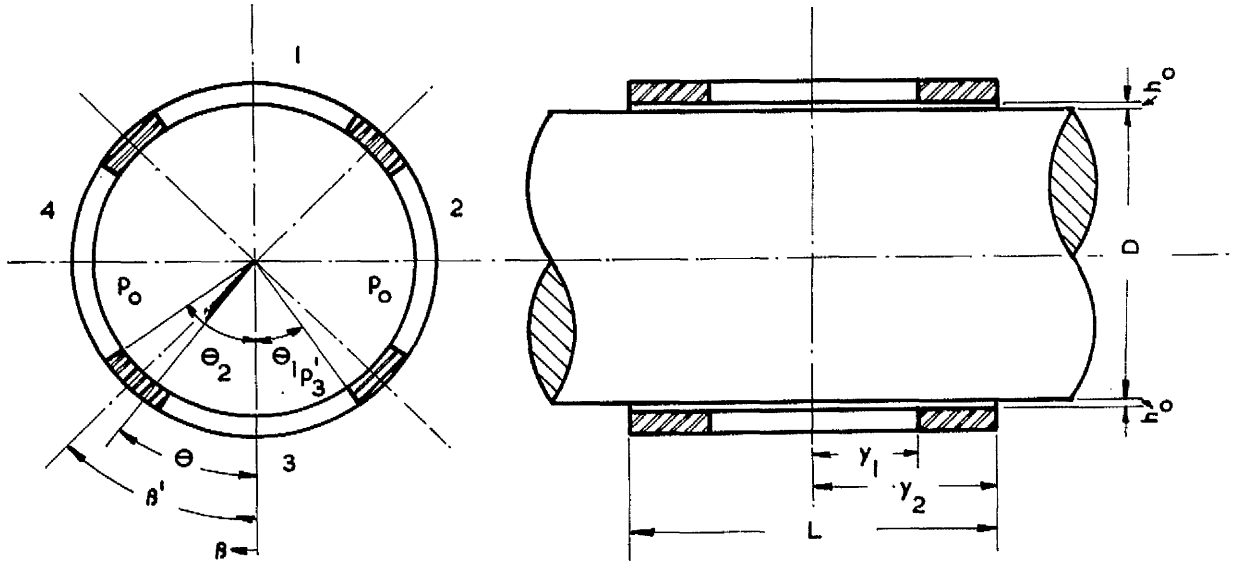

JOURNAL BEARING

FIG.12 HYDROSTATIC BEARING PAD CONFIGURATIONS FOR SQUEEZE FILM EQUATIONS

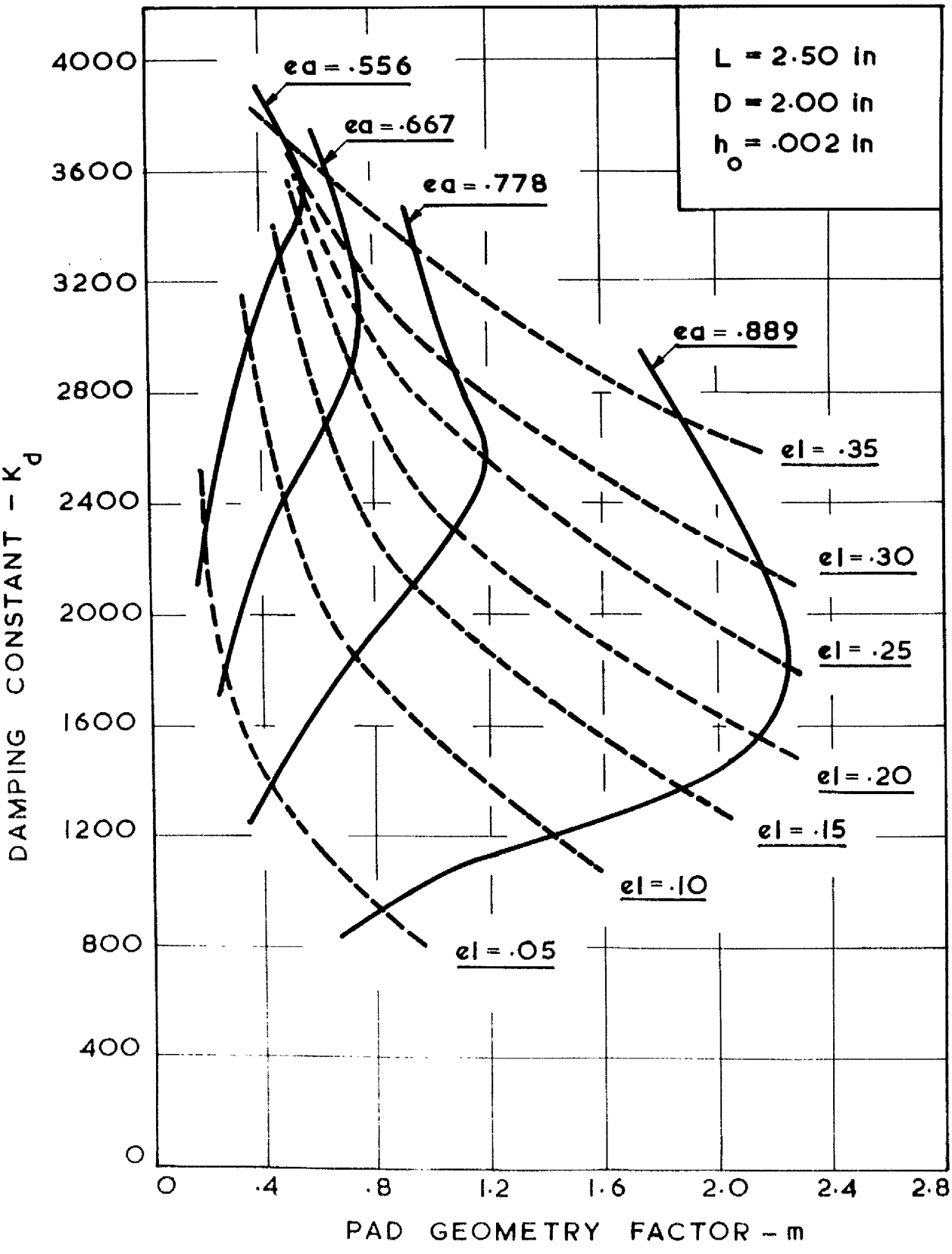

FIG.13 VARIATION OF DAMPING CONSTANT WITH PAD GEOMETRY FACTOR

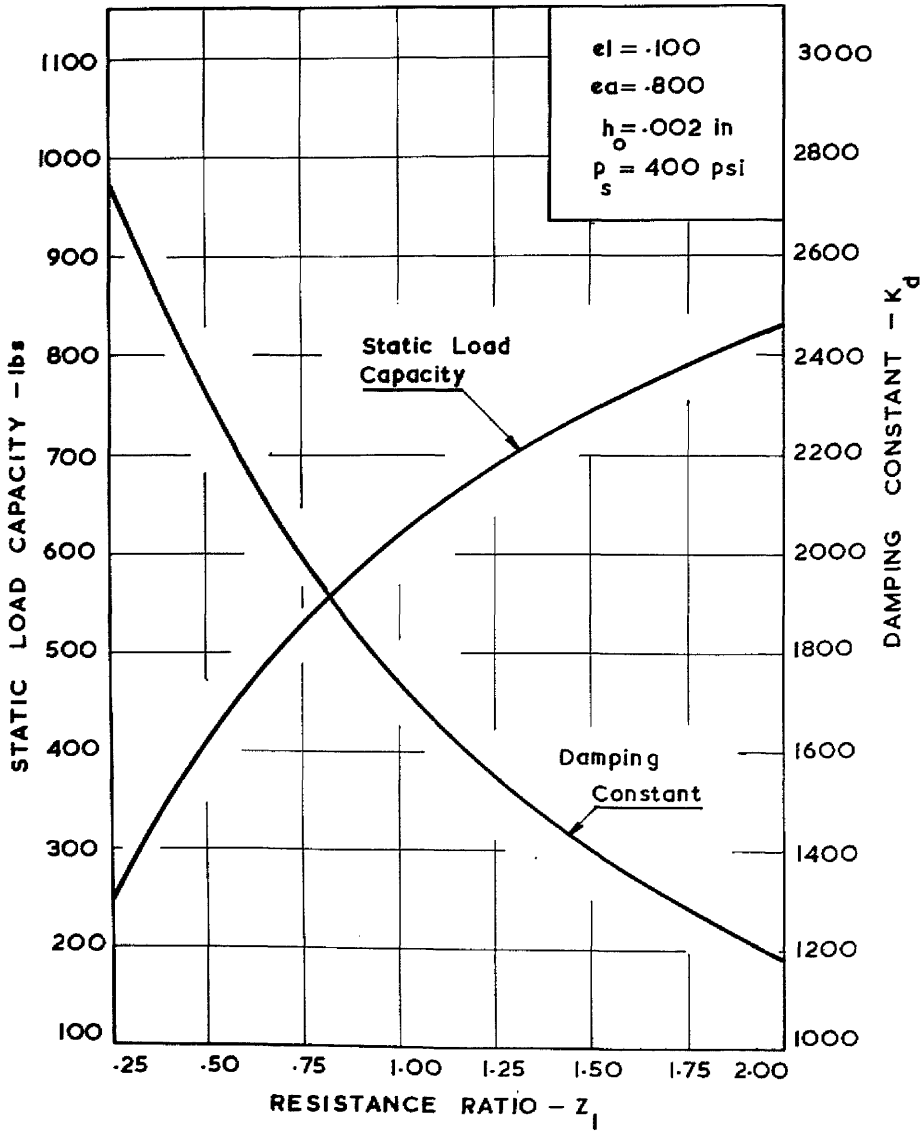

FIG. 14a VARIATION OF STATIC LOAD CAPACITY AND DAMPING CONSTANT WITH RESISTANCE RATIO

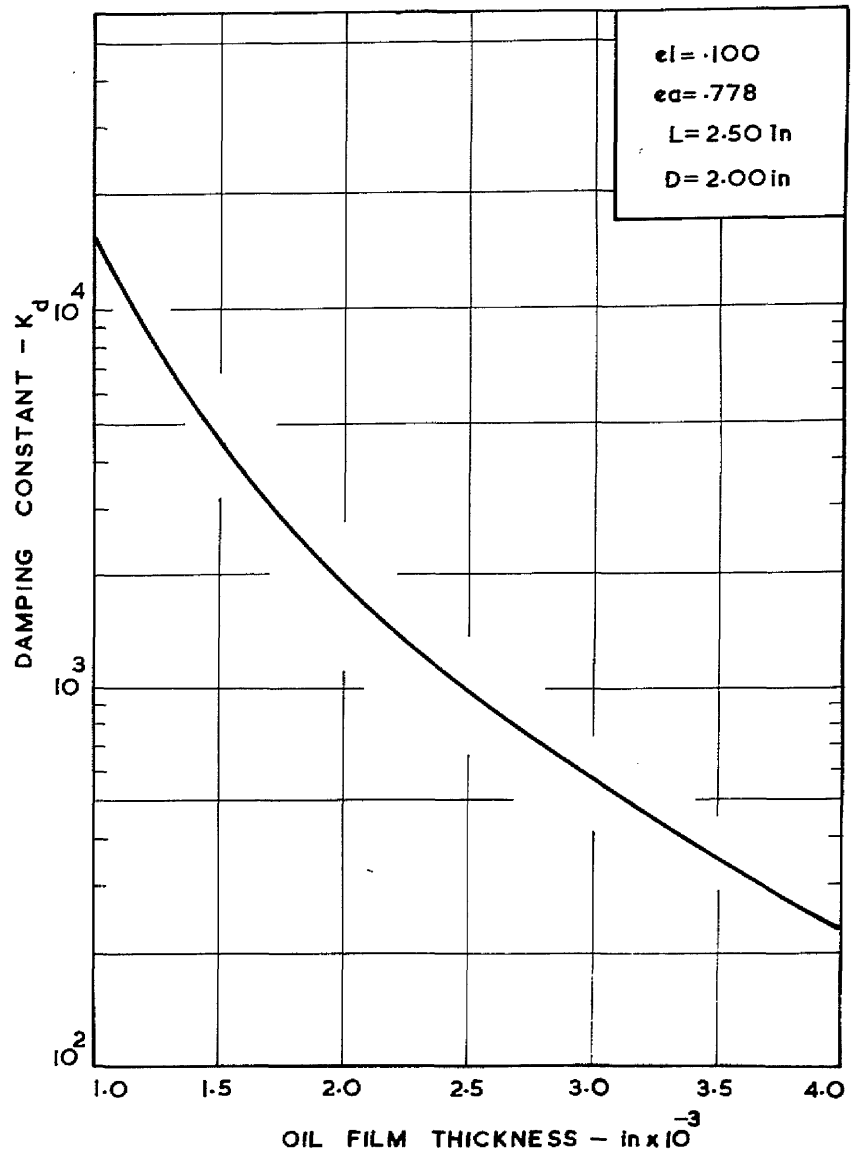

FIG. 14b VARIATION OF DAMPING CONSTANT WITH OIL FILM THICKNESS

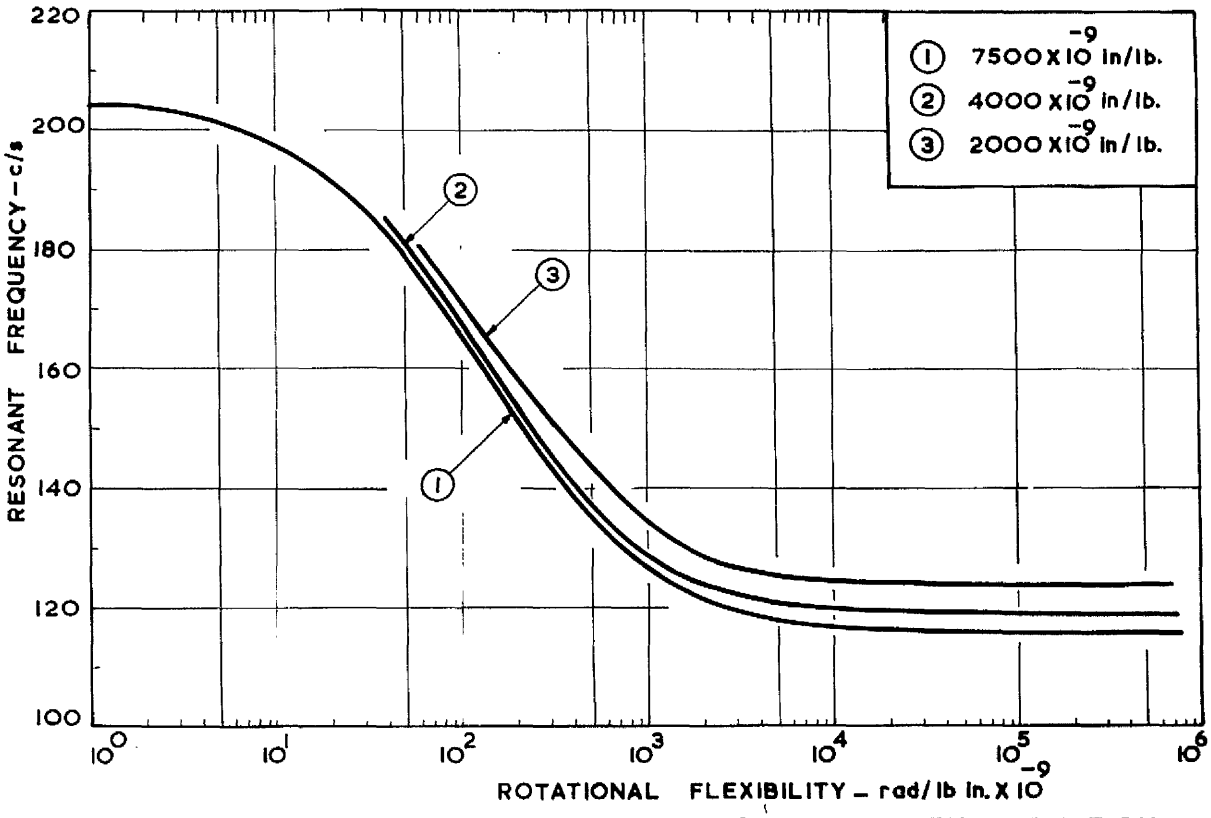

FIG.15 VARIATION OF RESONANT FREQUENCY WITH ROTATIONAL FLEXIBILITY FOR VARIOUS NORMAL FLEXIBILITIES

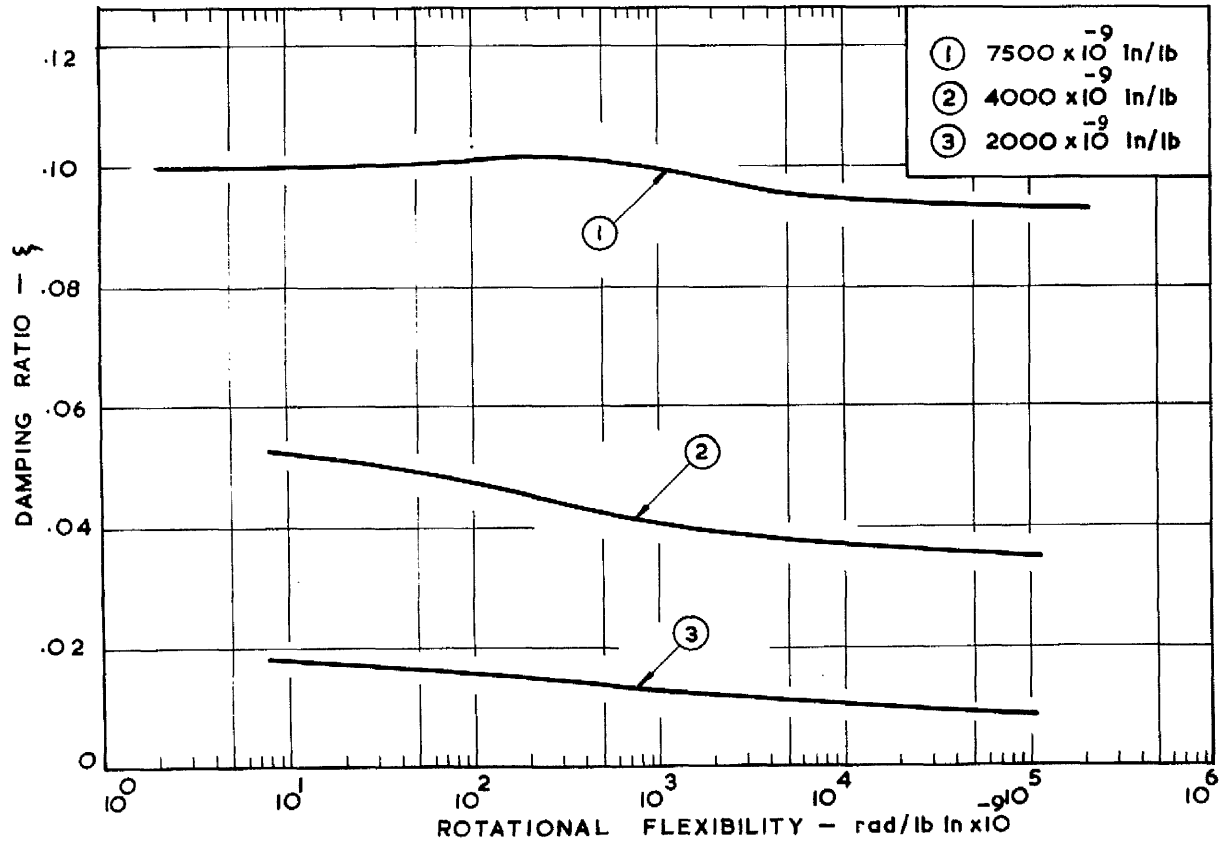

FIG.16 VARIATION OF DAMPING RATIO WITH ROTATIONAL FLEXIBILITY FOR VARIOUS NORMAL FLEXIBILITIES

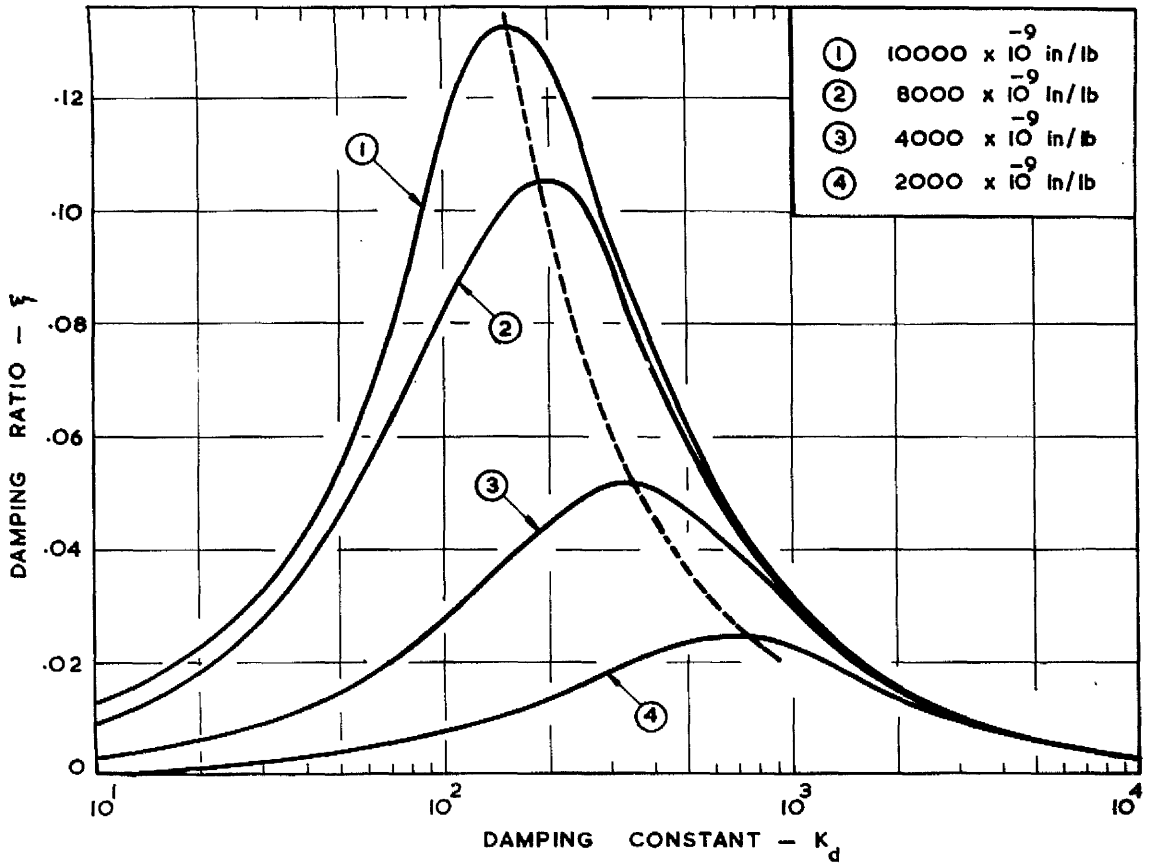

FIG.17 VARIATION OF DAMPING RATIO WITH DAMPING CONSTANT FOR VARIOUS NORMAL FLEXIBILITIES

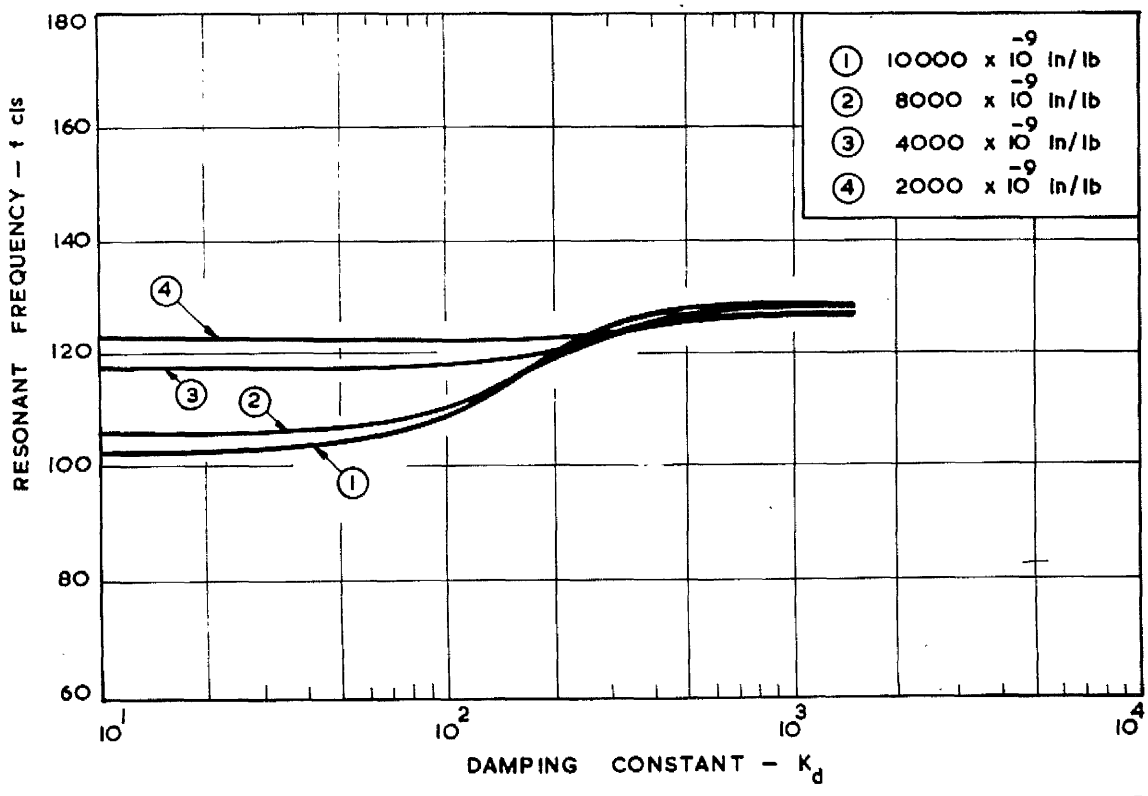

FIG.18 VARIATION OF RESONANT FREQUENCY WITH DAMPING CONSTANT

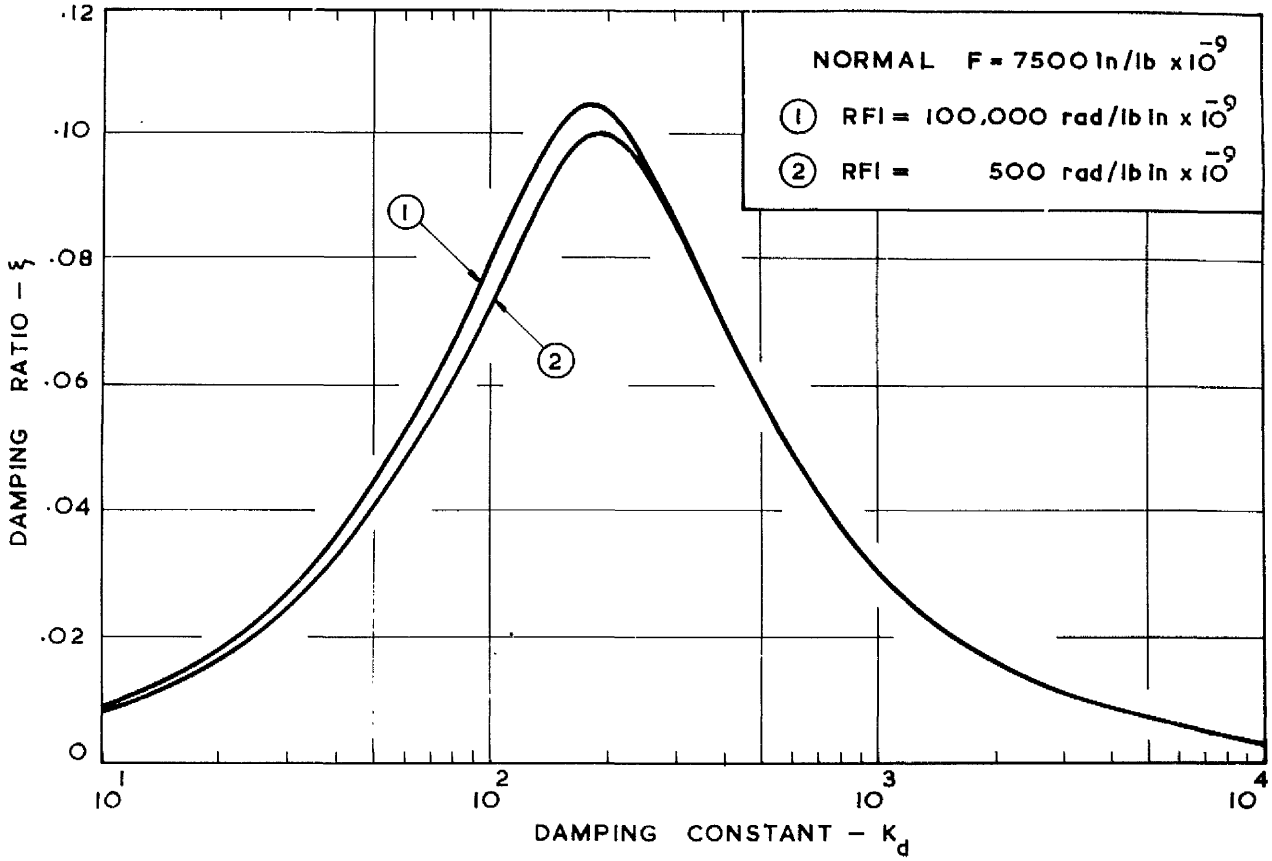

FIG.19 VARIATION OF DAMPING RATIO WITH DAMPING CONSTANT

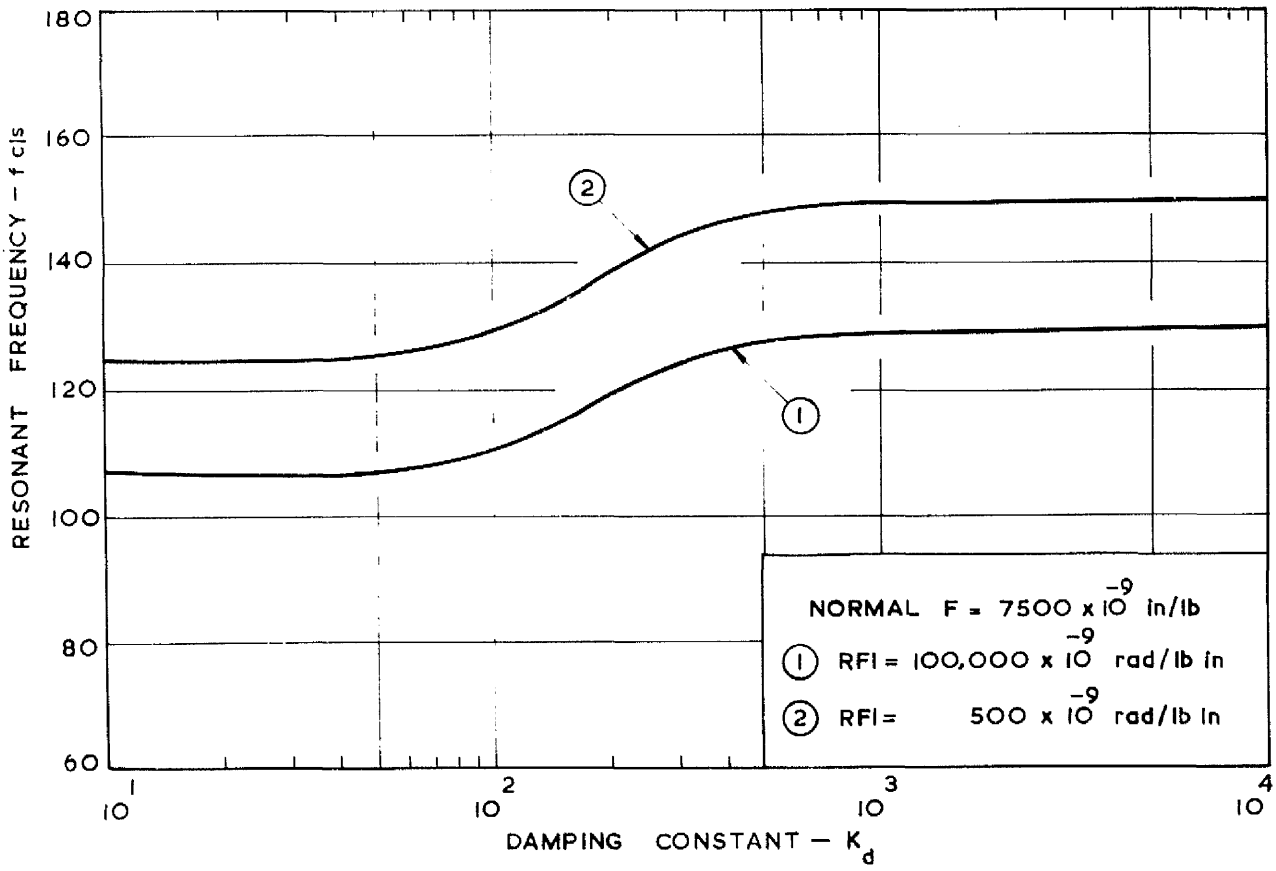

FIG. 20 VARIATION OF RESONANT FREQUENCY WITH DAMPING CONSTANT

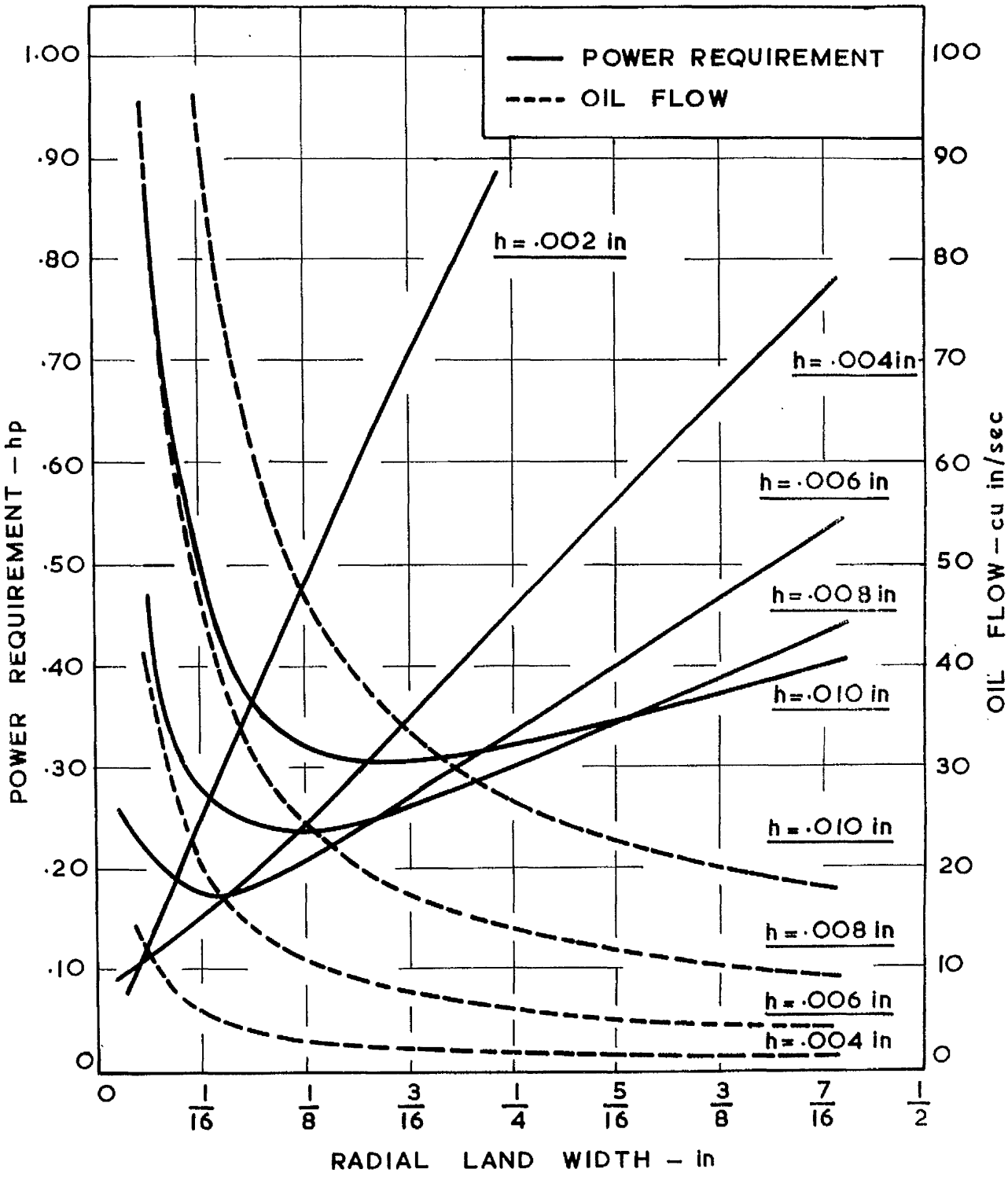

FIG. 21 VARIATION OF OIL FLOW AND POWER REQUIREMENT WITH RADIAL LAND WIDTH

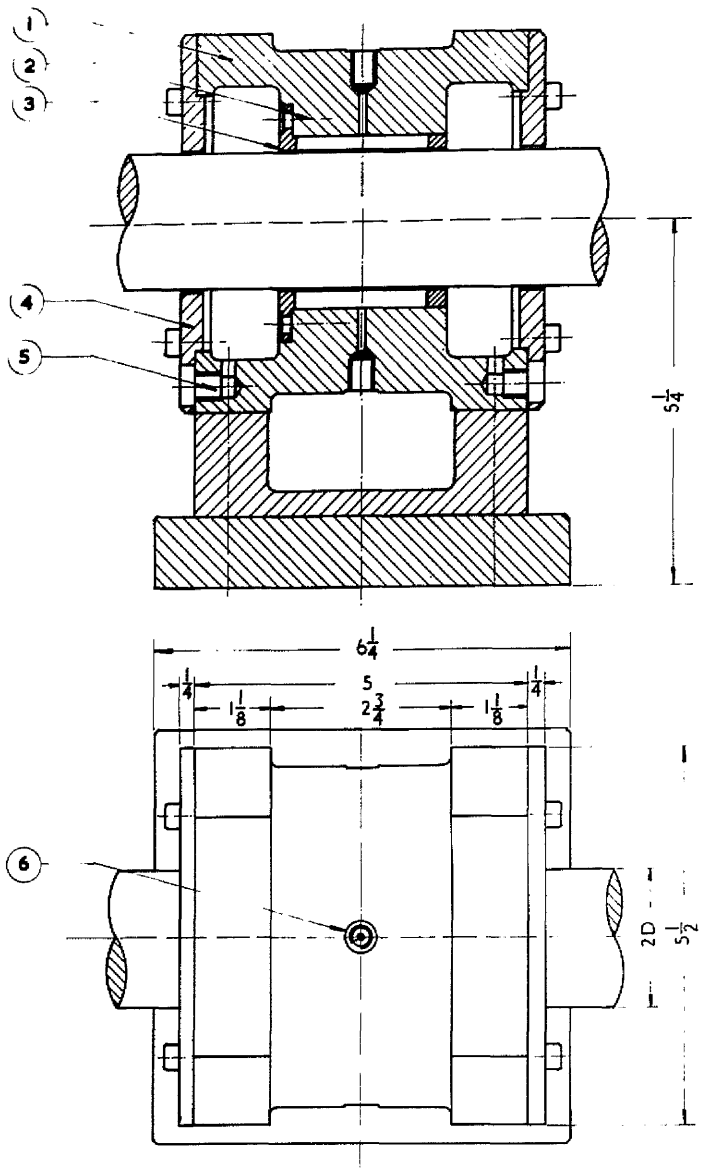

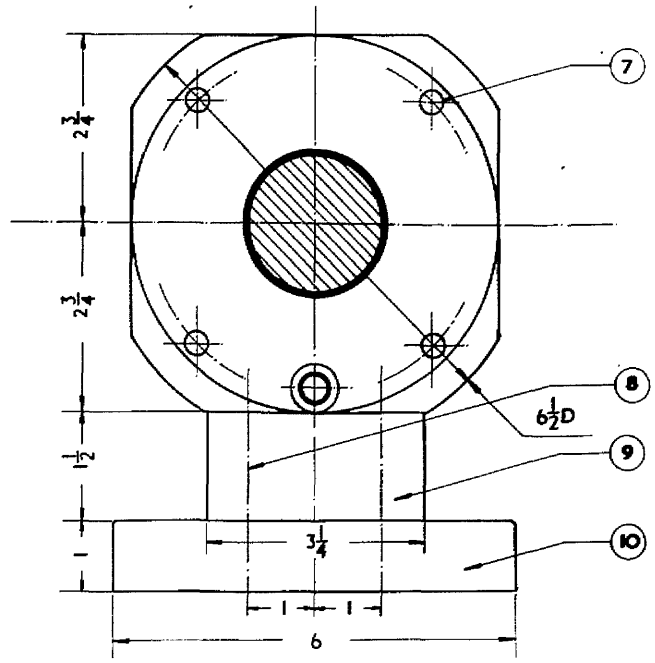

PART LIST			
NO.	NAME OF PART	NO. OF PARTS	MATERIAL
1.	MAIN BODY	1	M.S.
2.	BUSH SCREWS ¼ BSF	6	–
3.	BEARING BUSH	1	BRASS
4.	OIL COVER	2	M.S.
5.	OIL OUTLET ¼ BSP	2	–
6.	OIL INLET ⅛ BSP	8	–
7.	OIL COVER SCREWS	4	–
8.	BASE PLATE SCREWS	4	–
9.	BEARING BASE	1	M. S.
10.	BASE PLATE	1	M. S.

ALL DIMENSIONS IN INCHES

FIG.22 HYDROSTATIC OIL JOURNAL BEARING

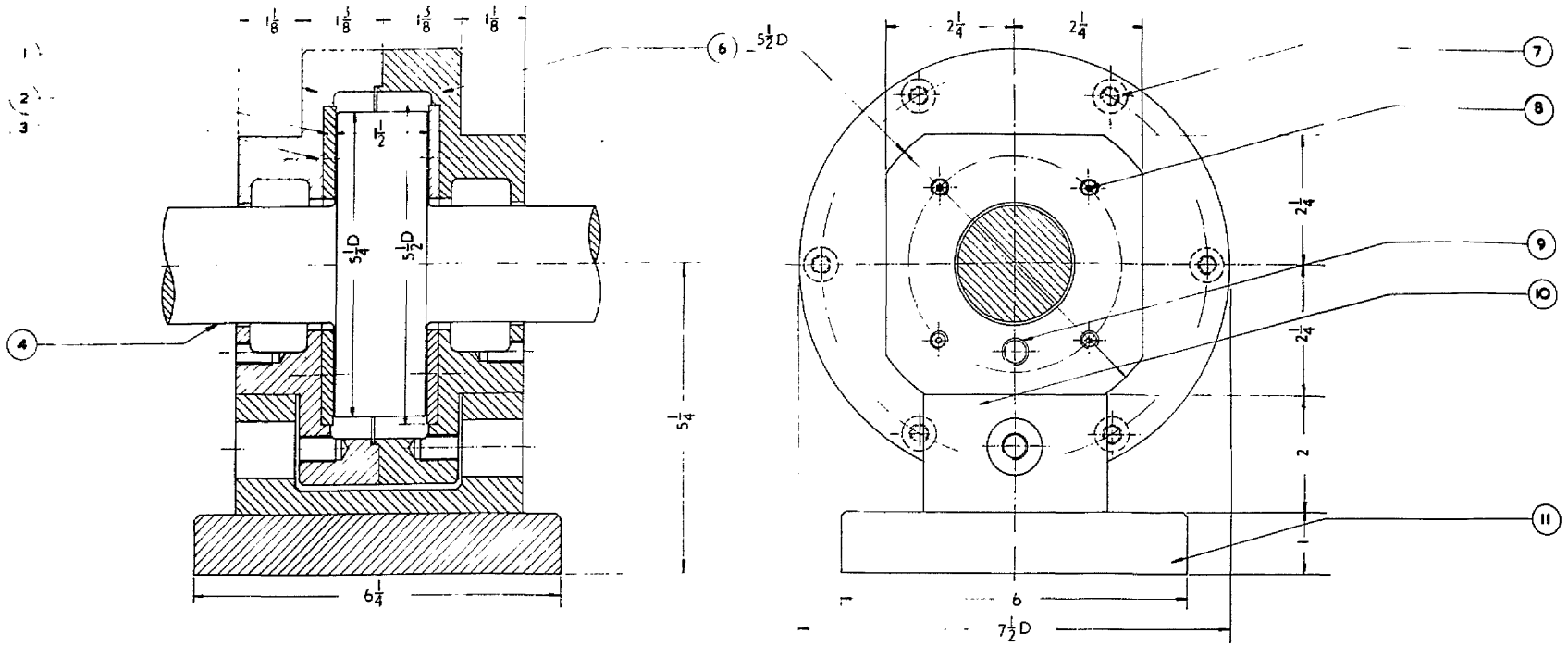

PART LIST			
NO.	NAME OF PART	NO. OF PARTS	MATERIAL
1.	LEFT COVER	1	M.S.
2.	ANNULAR PAD	2	BRASS
3.	PAD SCREWS	8	—
4.	MAIN SPINDLE	1	M.S.
5.	BASE PLATE SCREWS	6	—
6.	RIGHT COVER	1	M.S.
7	COVER SCREWS	6	—
8.	OIL INLET $\frac{1}{8}$ B.S.P.	8	—
9	OIL OUTLET $\frac{1}{4}$ B.S.P.	4	—
10.	BEARING BASE	1	M.S.
11.	BASE PLATE	1	M.S.

ALL DIMENSIONS IN INCHES

FIG.23 HYDROSTATIC OIL THRUST BEARING

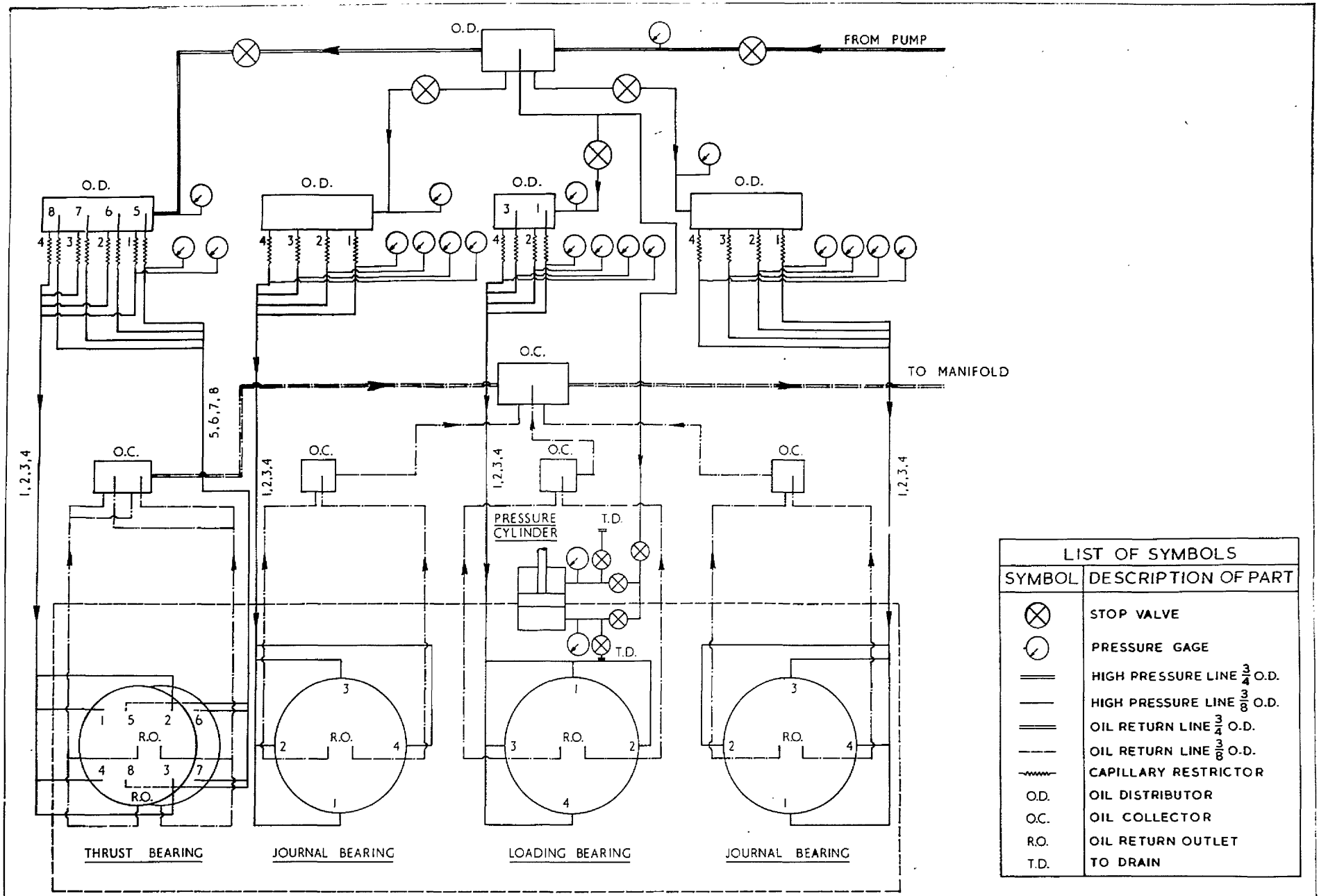

LIST OF SYMBOLS	
SYMBOL	DESCRIPTION OF PART
⊗	STOP VALVE
◴	PRESSURE GAGE
═══	HIGH PRESSURE LINE $\frac{3}{4}$ O.D.
———	HIGH PRESSURE LINE $\frac{3}{8}$ O.D.
═══	OIL RETURN LINE $\frac{3}{4}$ O.D.
- - -	OIL RETURN LINE $\frac{3}{8}$ O.D.
∿∿∿	CAPILLARY RESTRICTOR
O.D.	OIL DISTRIBUTOR
O.C.	OIL COLLECTOR
R.O.	OIL RETURN OUTLET
T.D.	TO DRAIN

FIG. 24 HYDRAULIC CIRCUIT DIAGRAM

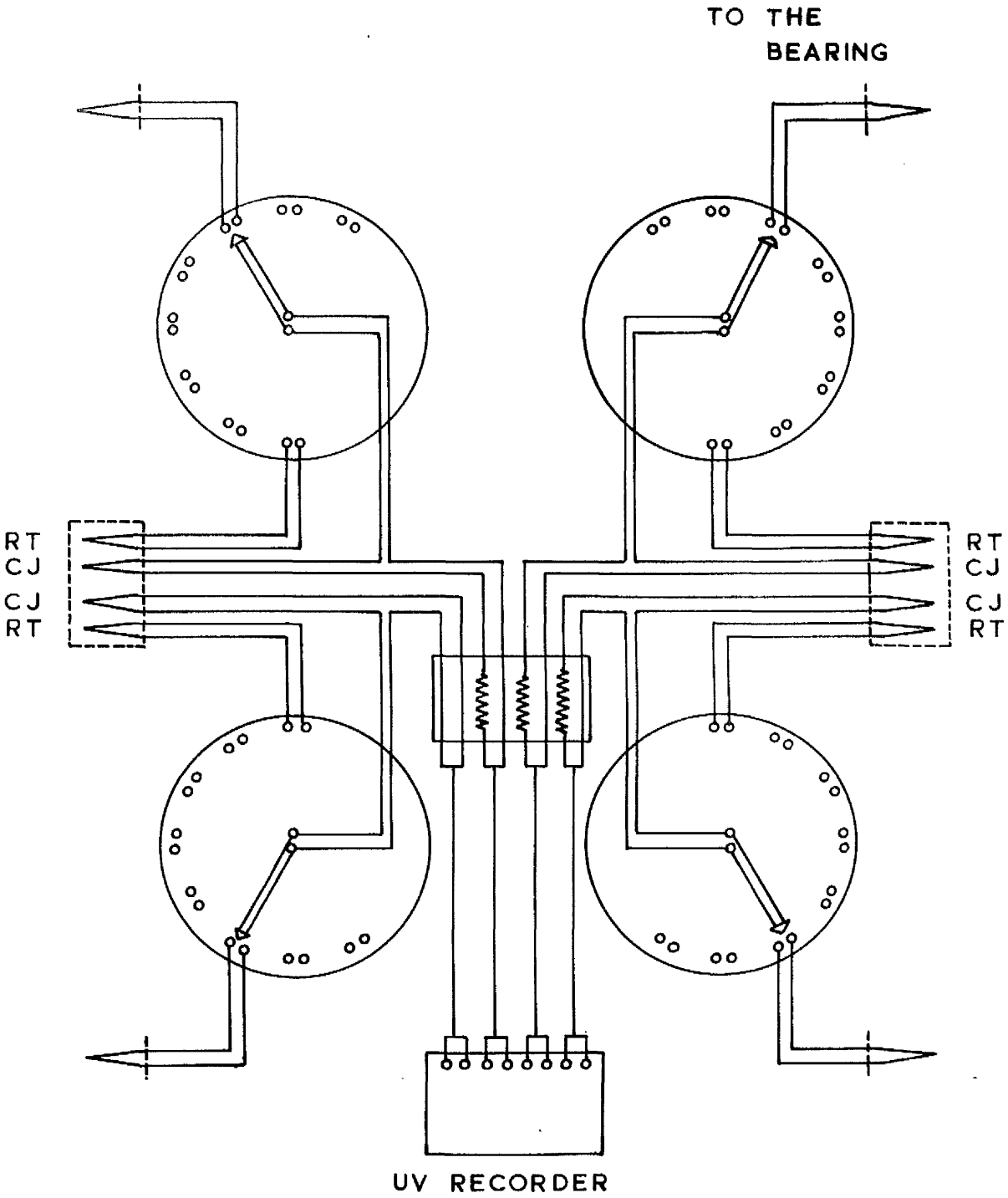

CJ COLD JUNCTION RT REFERENCE THERMOCOUPLE

FIG. 25 SCHEMATIC DIAGRAM OF THE CIRCUIT FOR TEMPERATURE MEASUREMENT IN JOURNAL BEARINGS

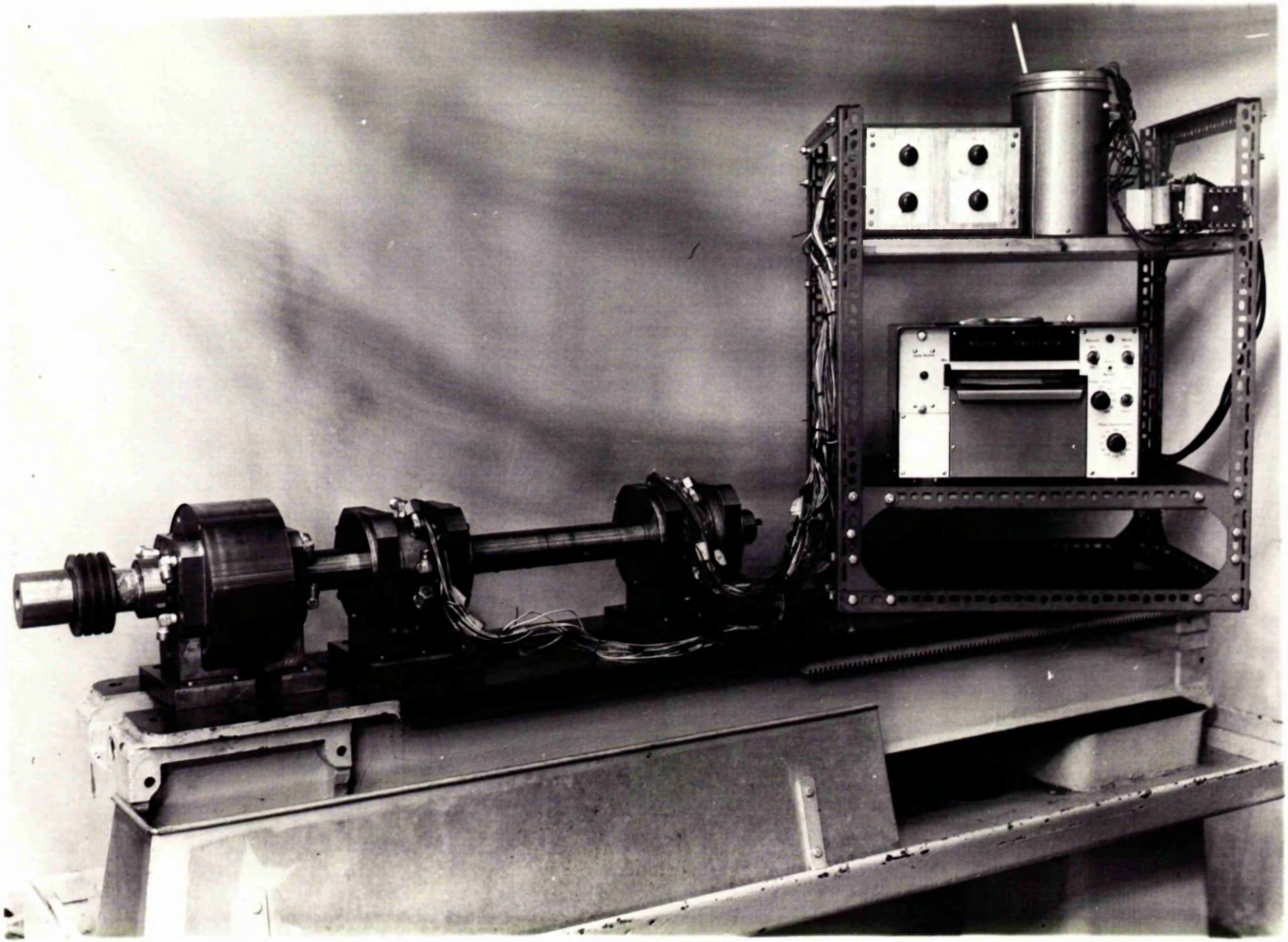

FIG. 26 TEMPERATURE MEASUREMENT IN THE BEARING SYSTEM.

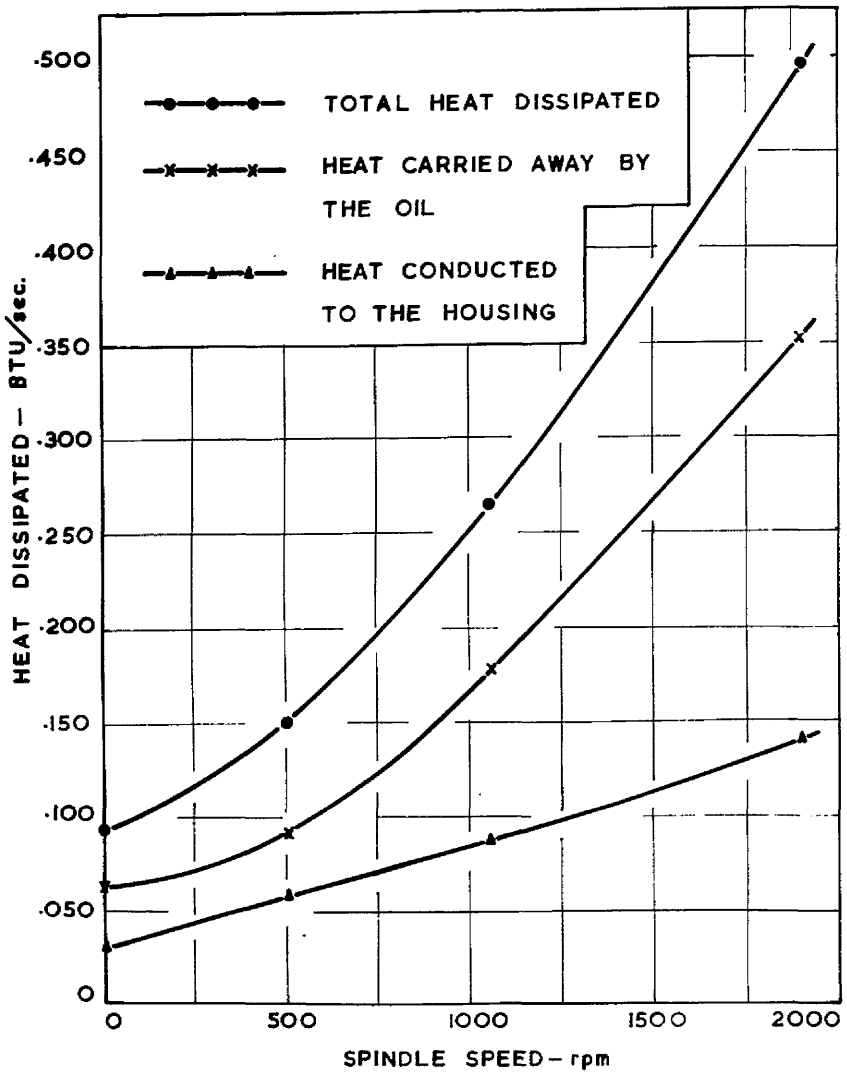

FIG.27 HEAT DISSIPATED IN THE BEARING FOR VARIOUS SPINDLE SPEEDS

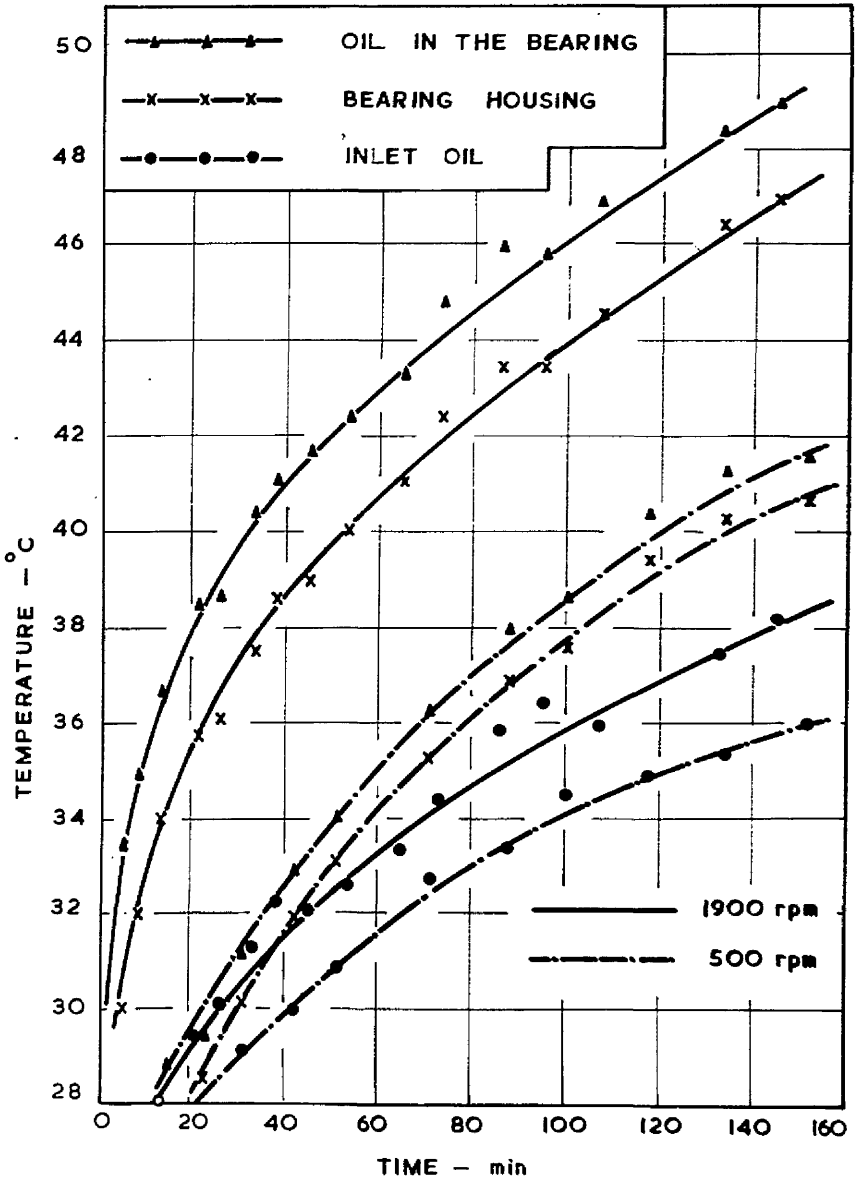

FIG. 28 TEMPERATURE RISE IN THE BEARING WITH TIME OF RUNNING

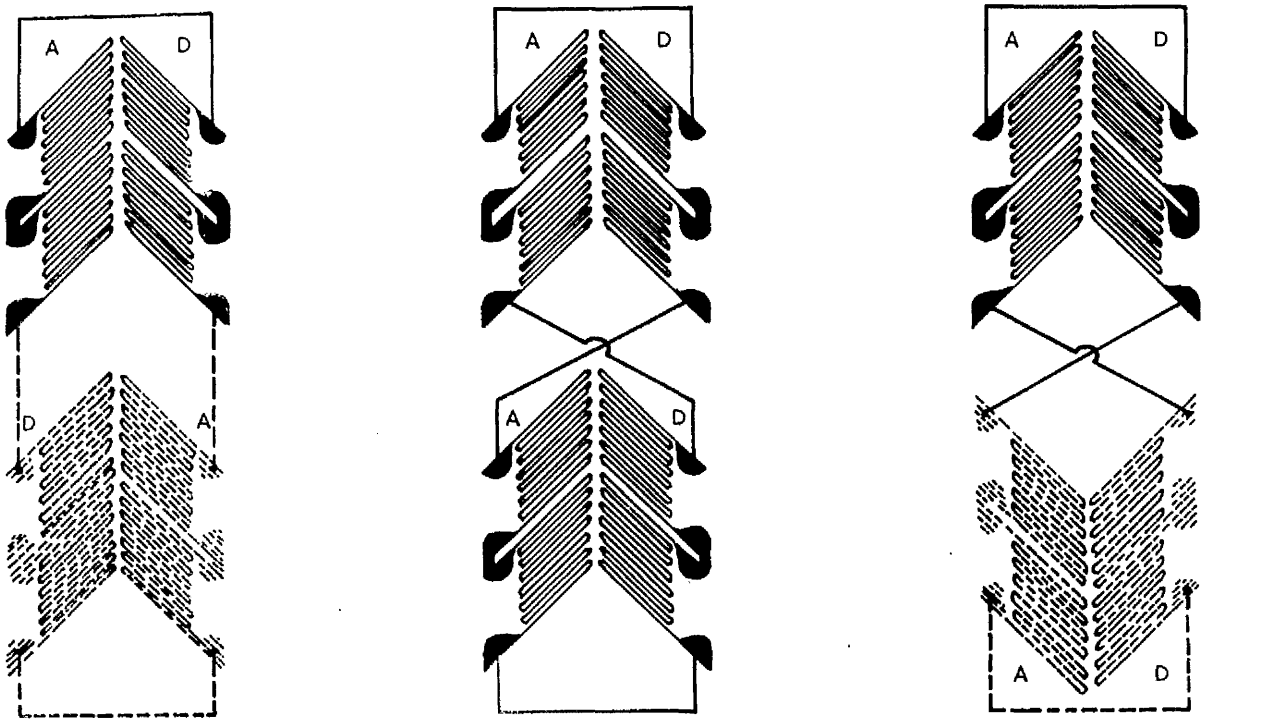

a. GAUGES MOUNTED AXIALLY, DIAMETRICALLY OPPOSITE ON THE SHAFT

b. GAUGES MOUNTED AXIALLY ON THE SAME SIDE OF THE SHAFT

c. GAUGES MOUNTED CIRCUMFERENTIALLY, DIAMETRICALLY OPPOSITE ON THE SHAFT

FIG. 29 TORQUE GAUGE WIRING DIAGRAM FOR FULL WHEATSTONE BRIDGE

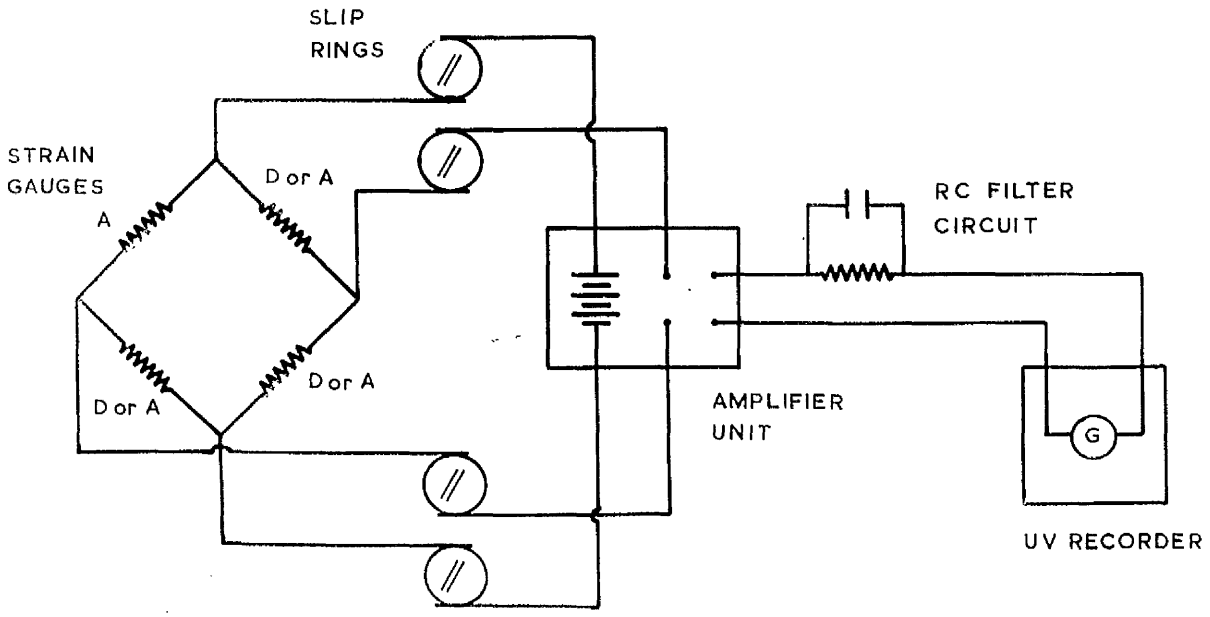

FIG. 30 WHEATSTONE BRIDGE CIRCUIT FOR TORQUE MEASUREMENT

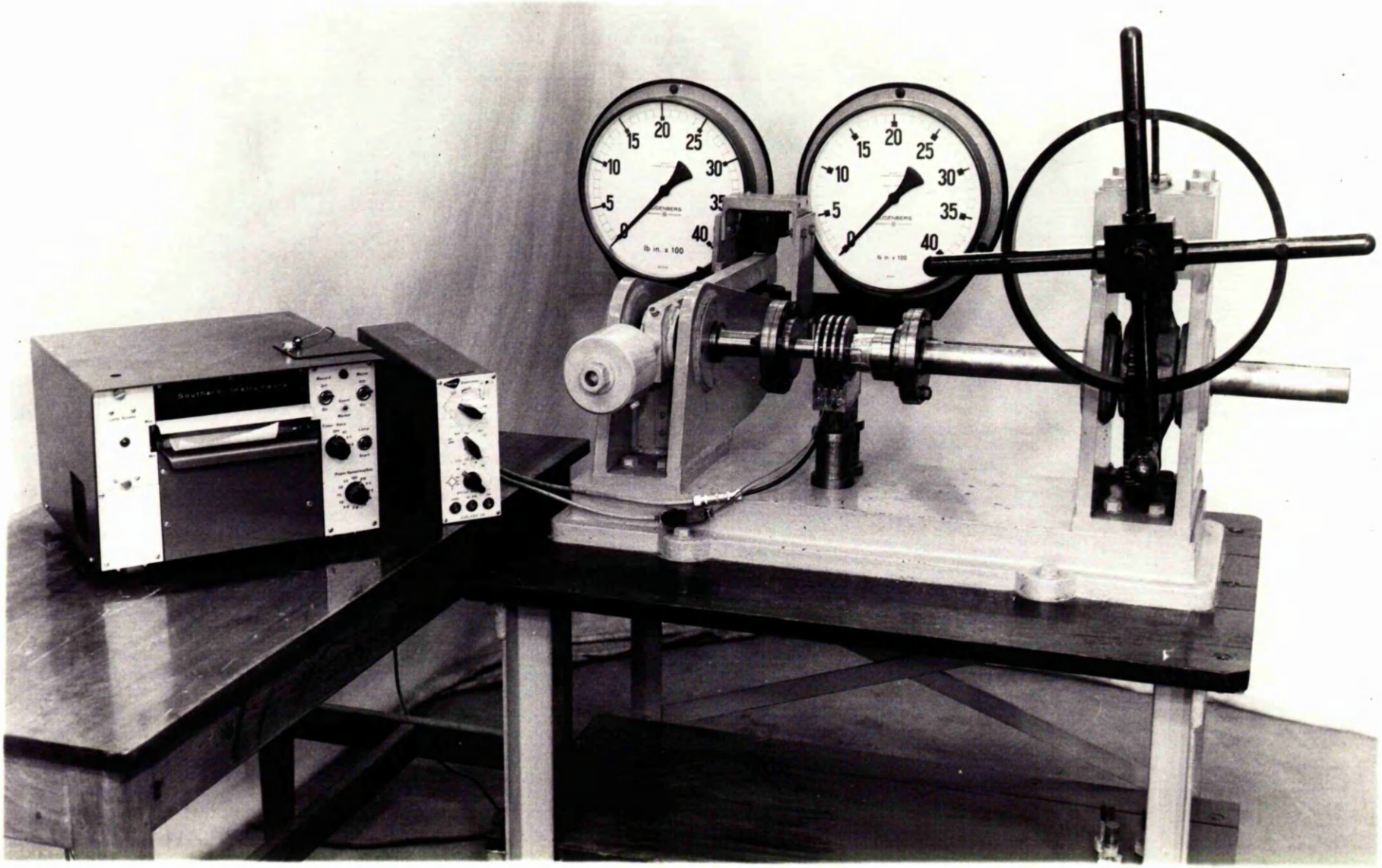

FIG. 31 TORQUE CALIBRATION OF THE STRAIN GAUGE BRIDGE CIRCUIT.

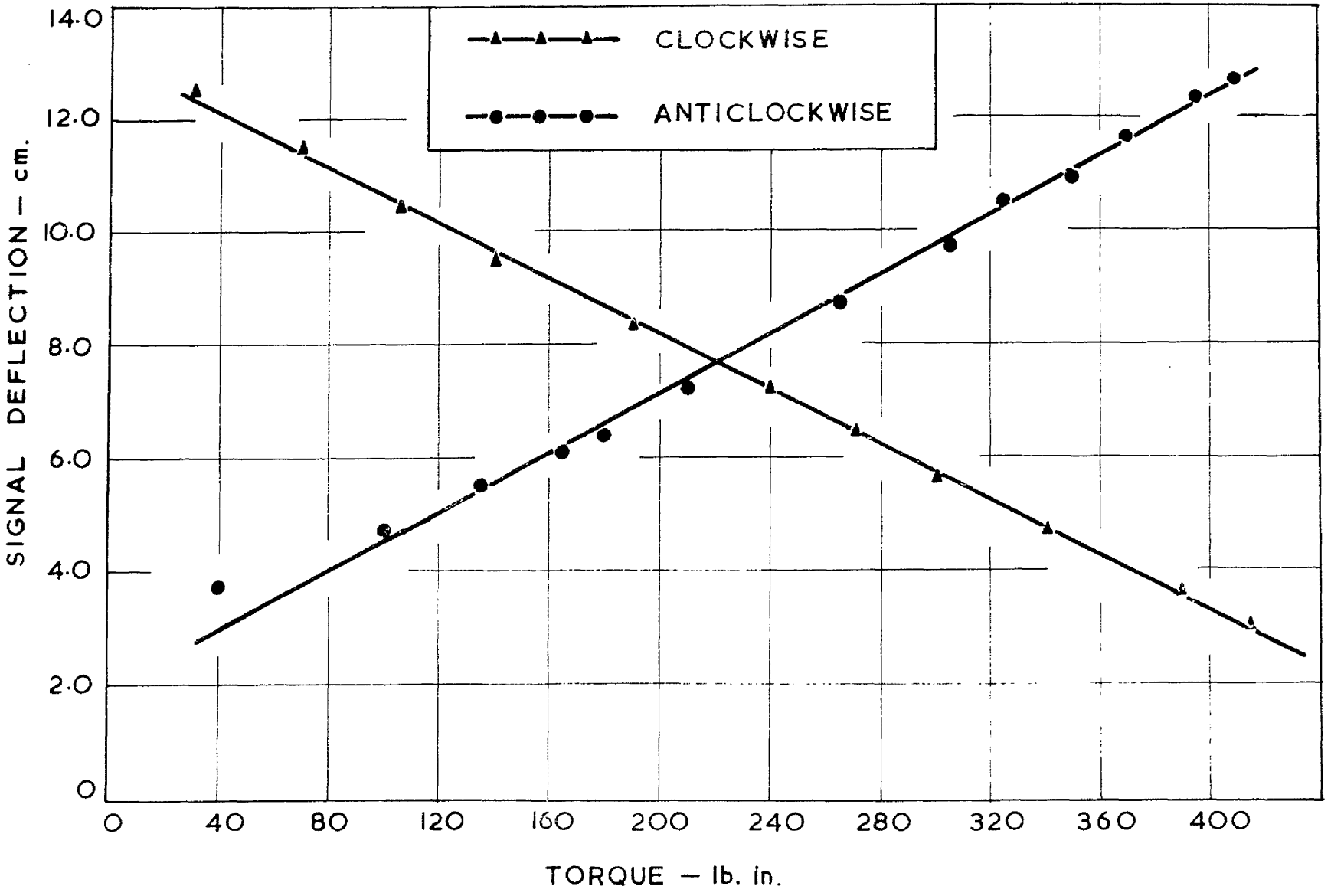

FIG.32 TORQUE CALIBRATION CURVES FOR SAUNDERS ROE TORQUE GAUGES

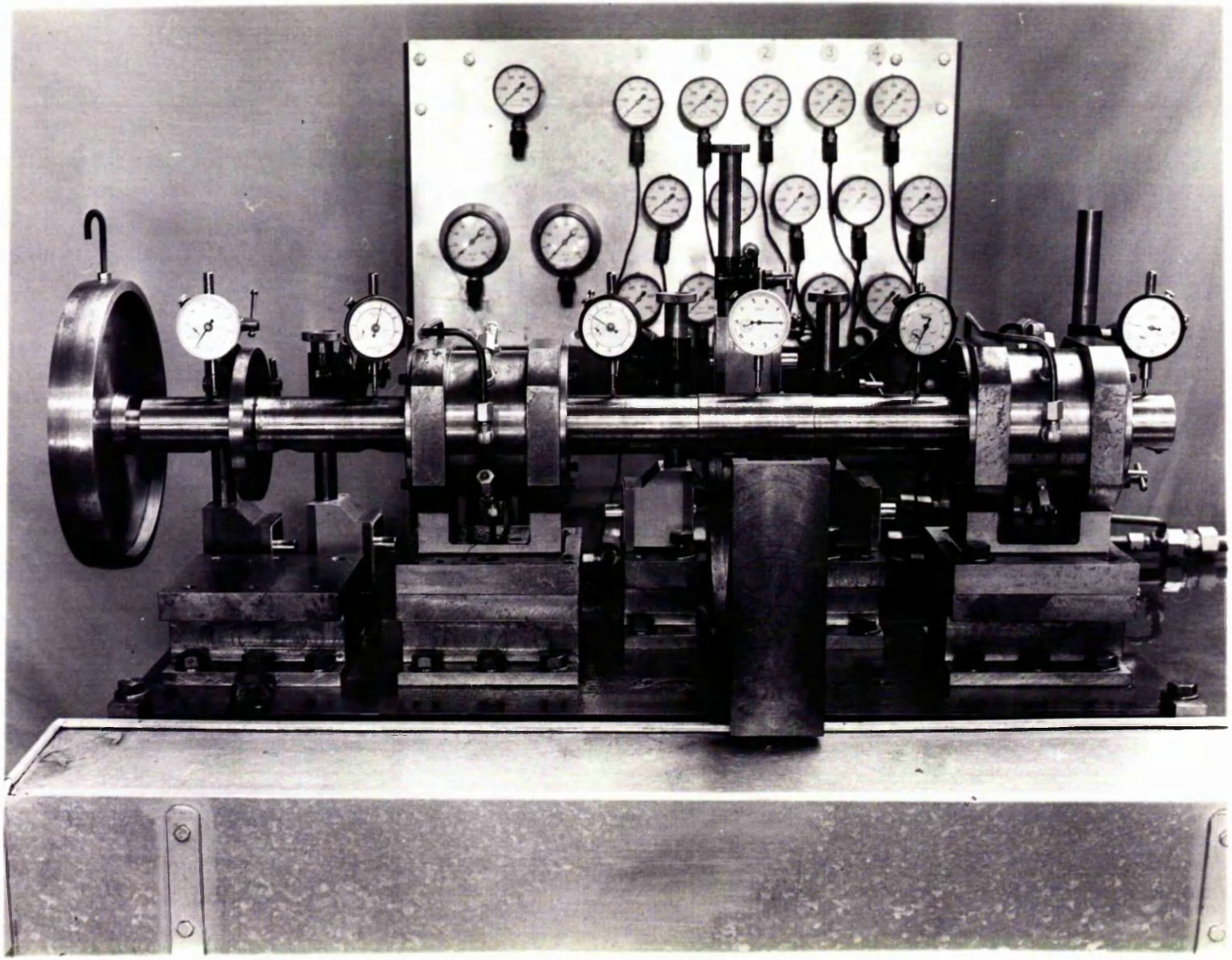

FIG. 33 STEADY LOAD DEFLECTION TESTING.

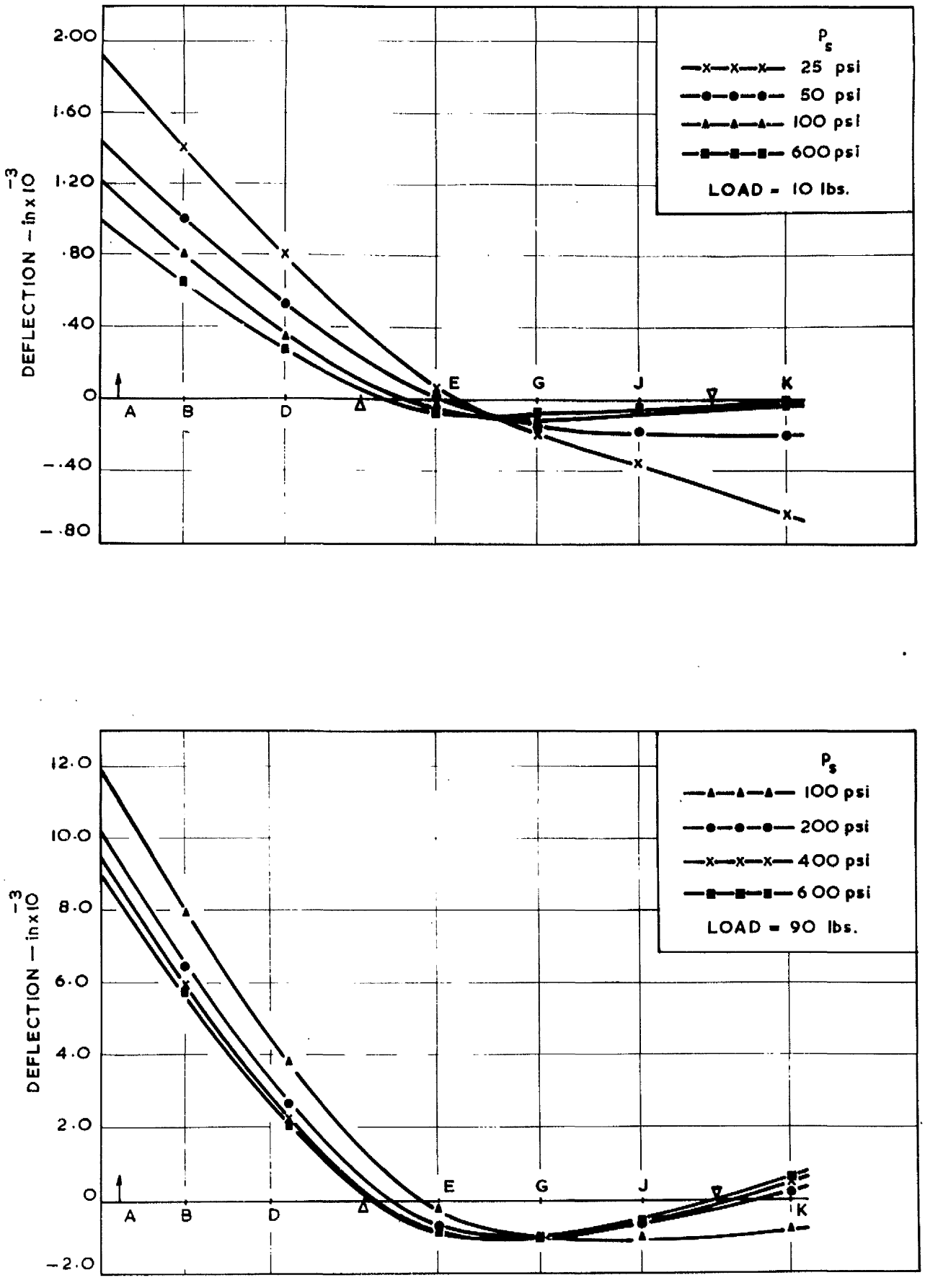

FIG.34 SPINDLE DEFLECTION CURVES FOR STEADY LOADS

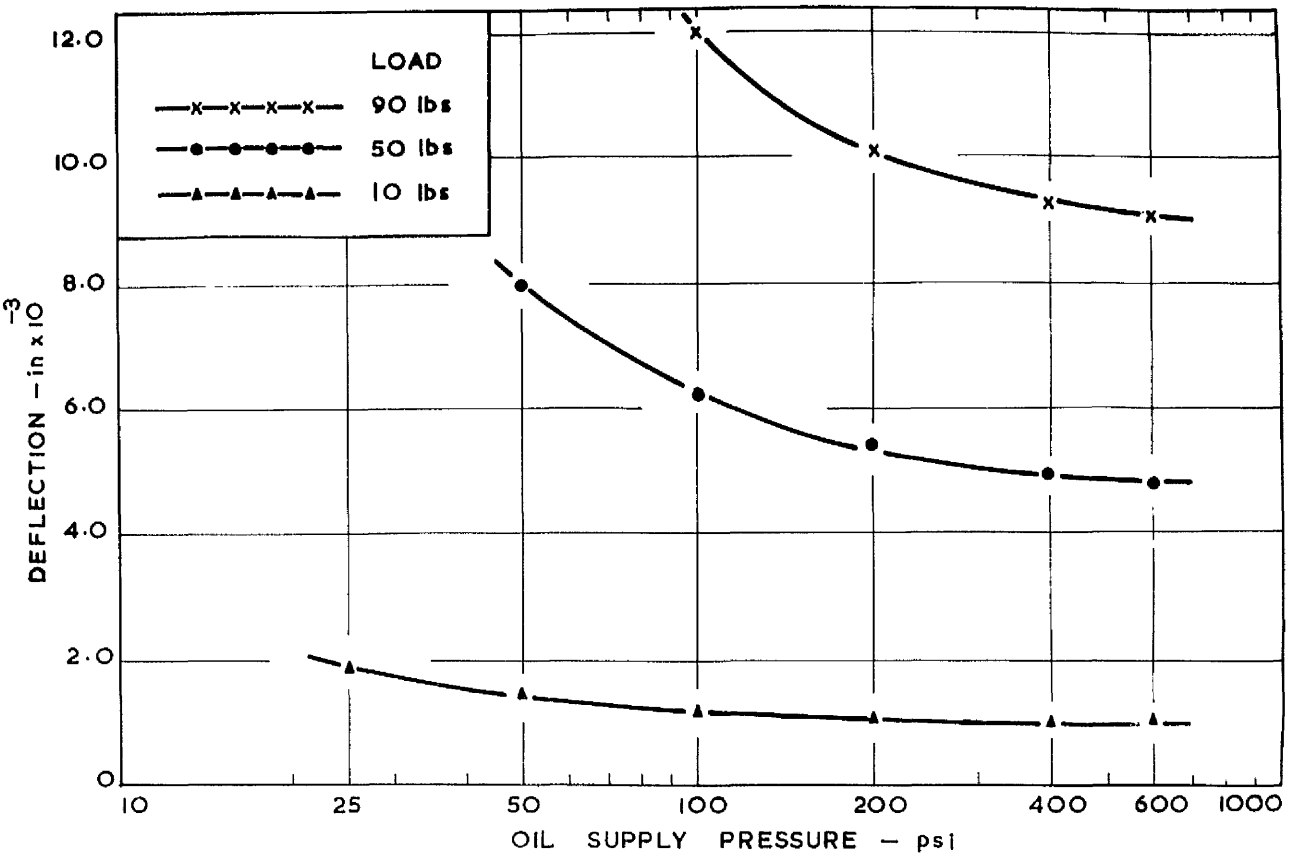

FIG. 35a SPINDLE END DEFLECTION WITH DIFFERENT SUPPLY PRESSURES

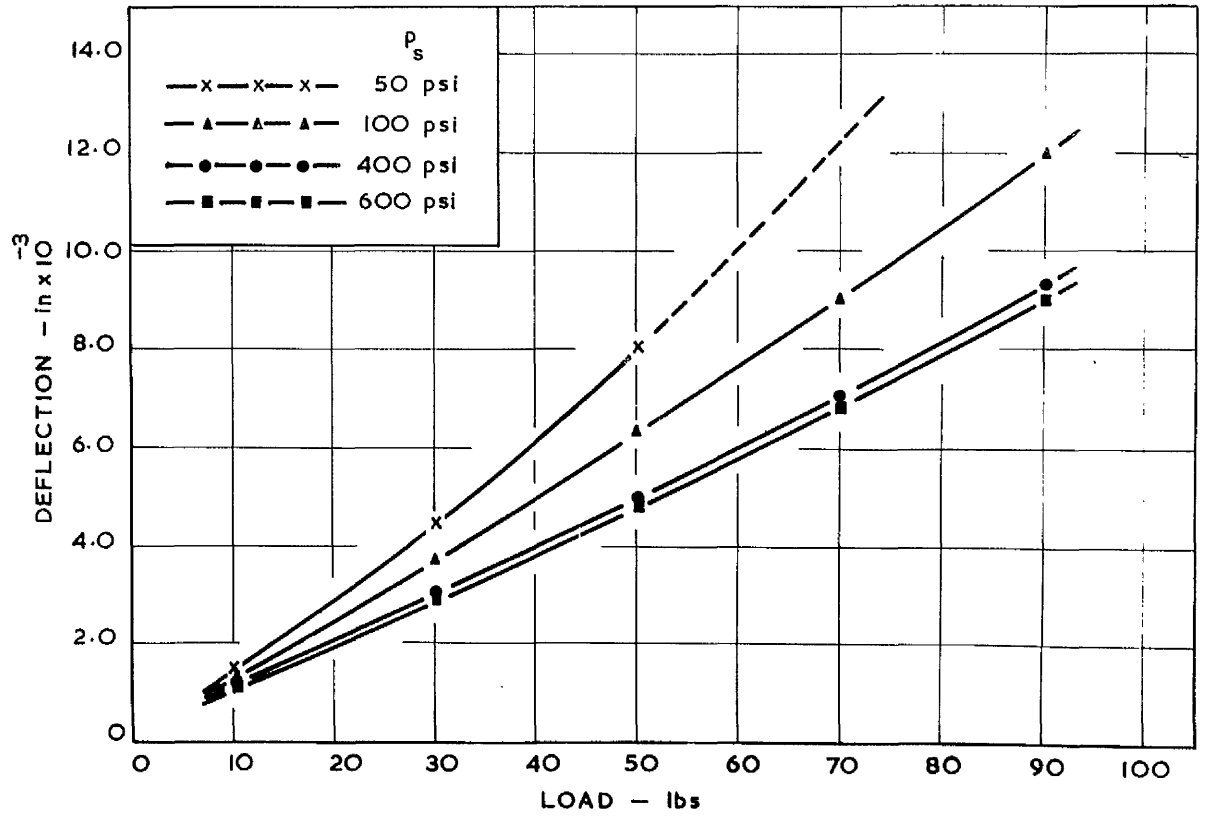

FIG. 35b VARIATION OF SPINDLE END DEFLECTION WITH END LOAD

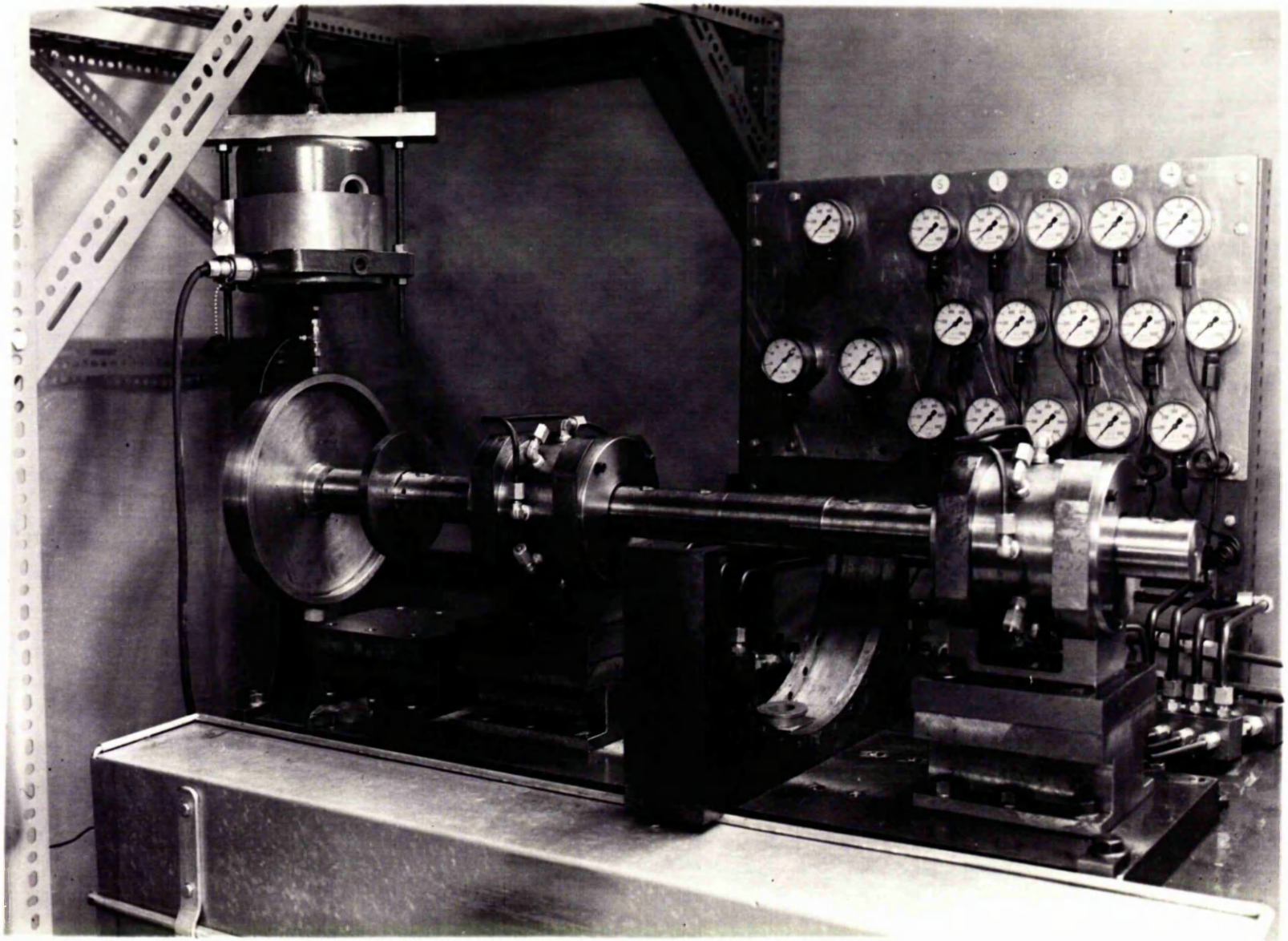

FIG. 36a DYNAMIC TESTING OF THE BEARING SYSTEM -JOURNAL BEARINGS ONLY.

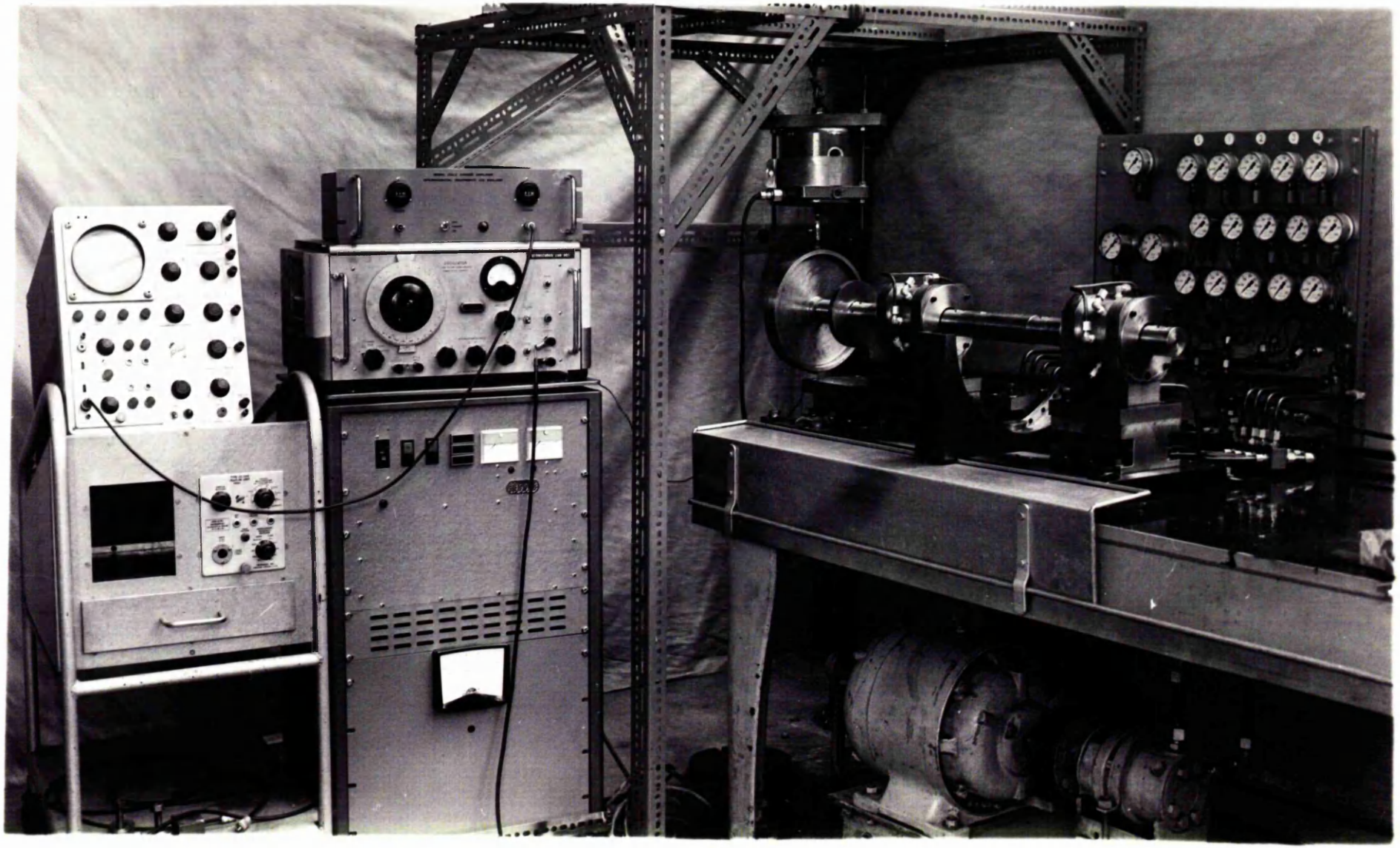

FIG. 36b DYNAMIC TESTING OF THE BEARING SYSTEM – WITH INSTRUMENTATION.

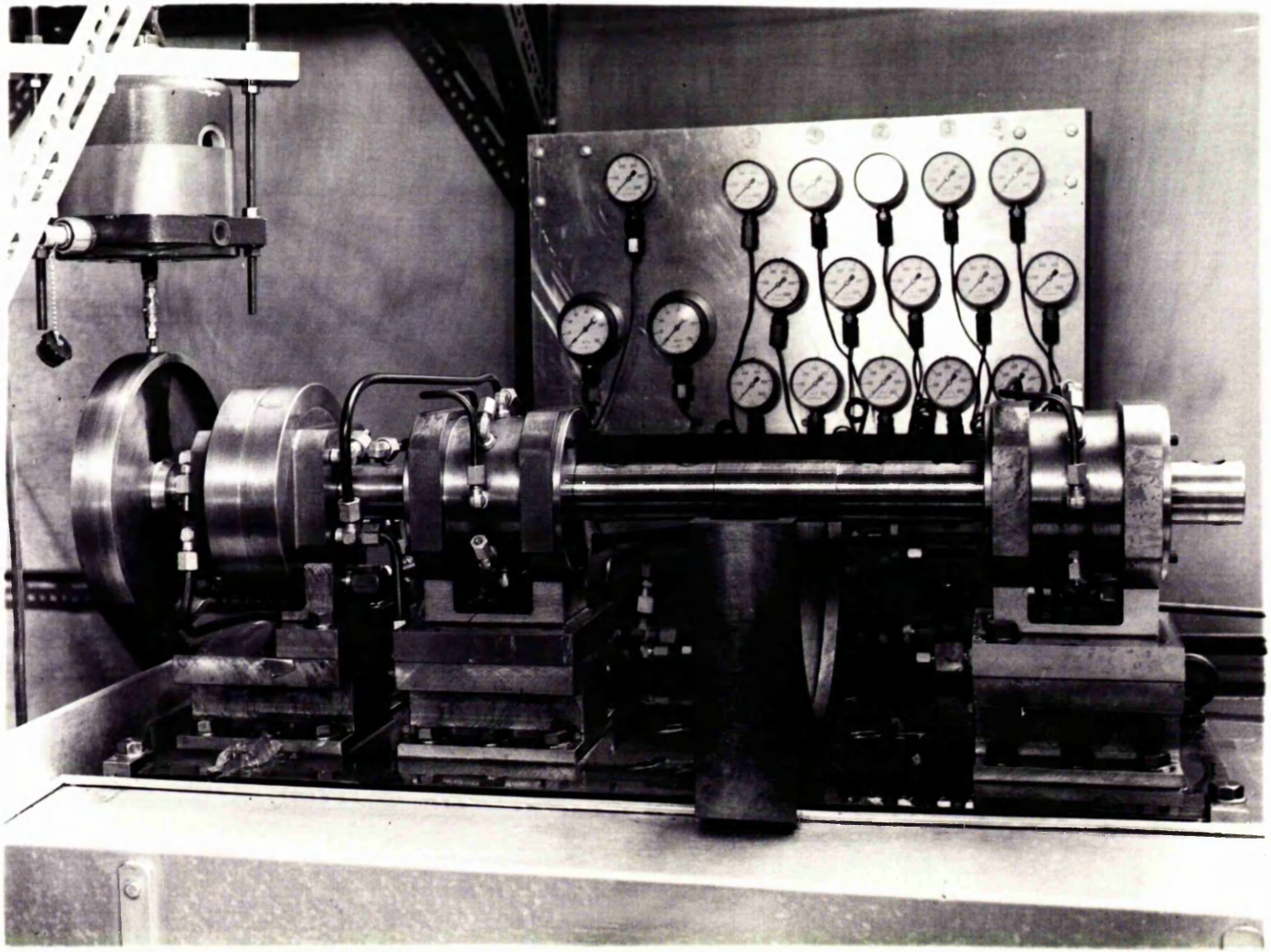

FIG. 37 DYNAMIC TESTING OF THE BEARING SYSTEM — WITH THRUST BEARING.

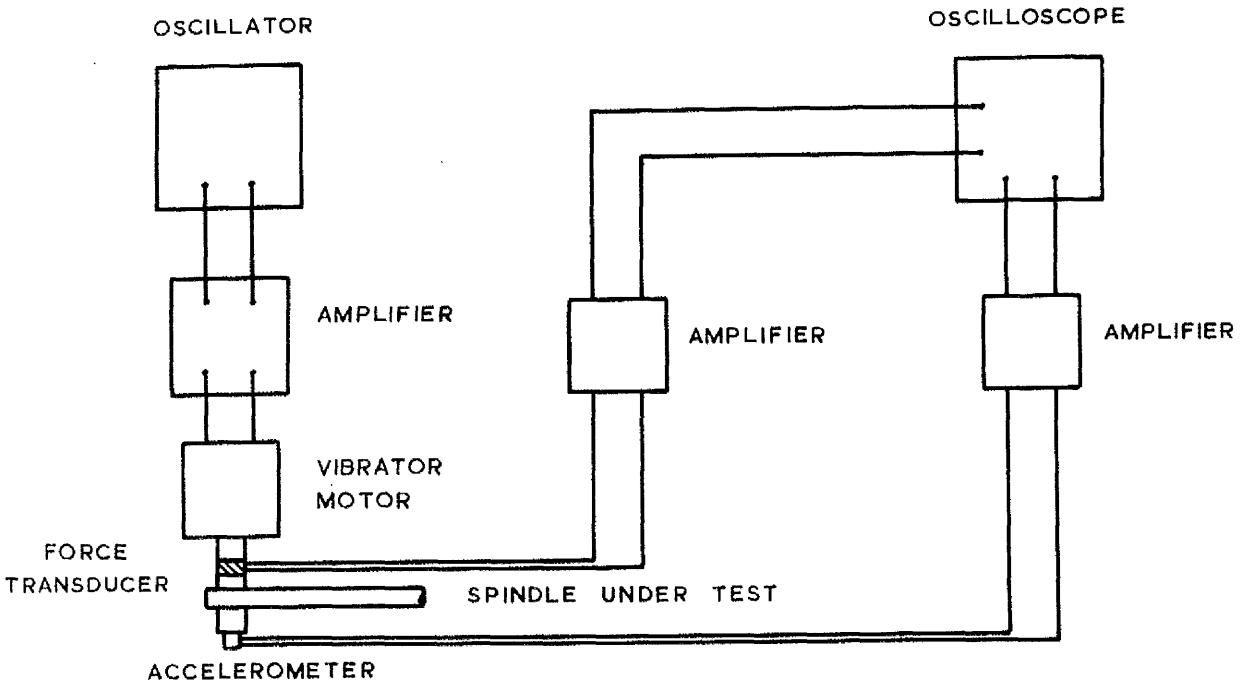

FIG. 38 CIRCUIT FOR DYNAMIC TESTING OF THE BEARING SYSTEM

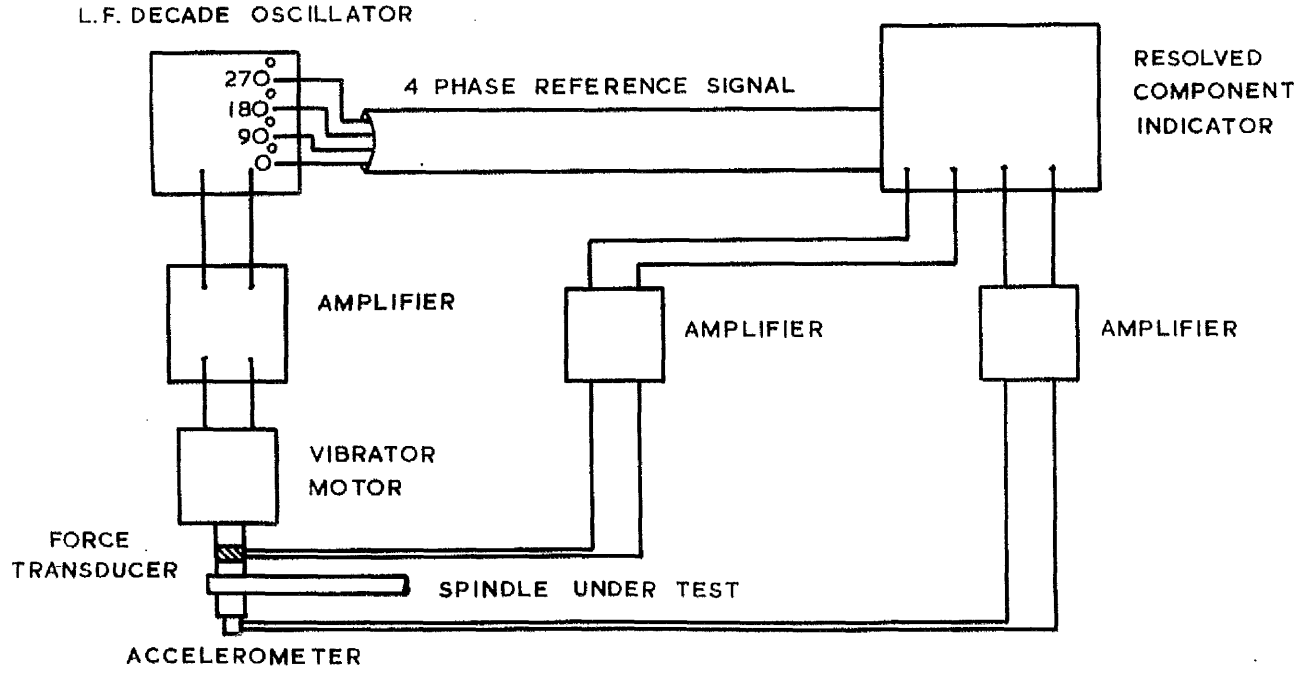

FIG. 39 CIRCUIT FOR DETERMINING THE MODAL SHAPES OF THE SPINDLE

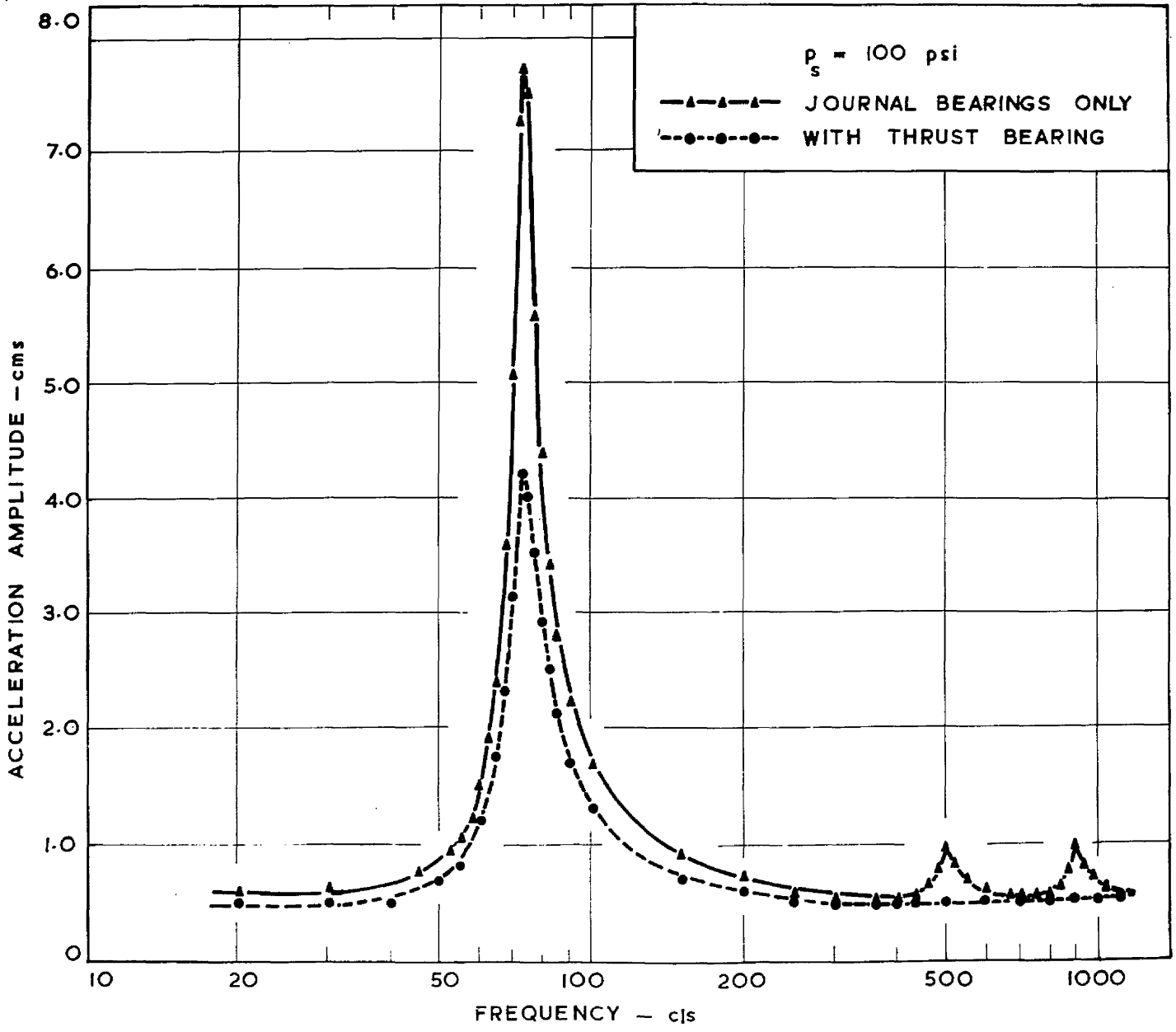

FIG.40 FREQUENCY RESPONCE CHARACTERISTICS OF THE BEARING SYSTEM

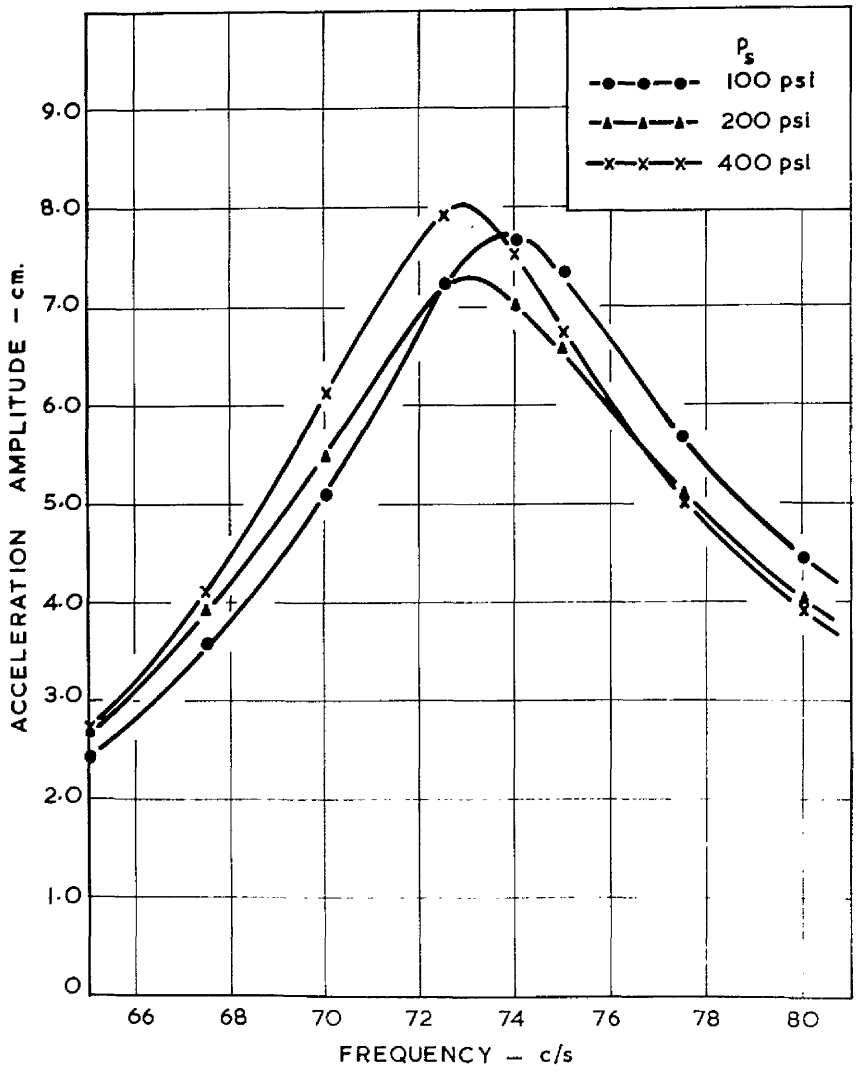

FIG.41 FREQUENCY RESPONCE CURVES FOR CALCULATION OF DAMPING RATIO

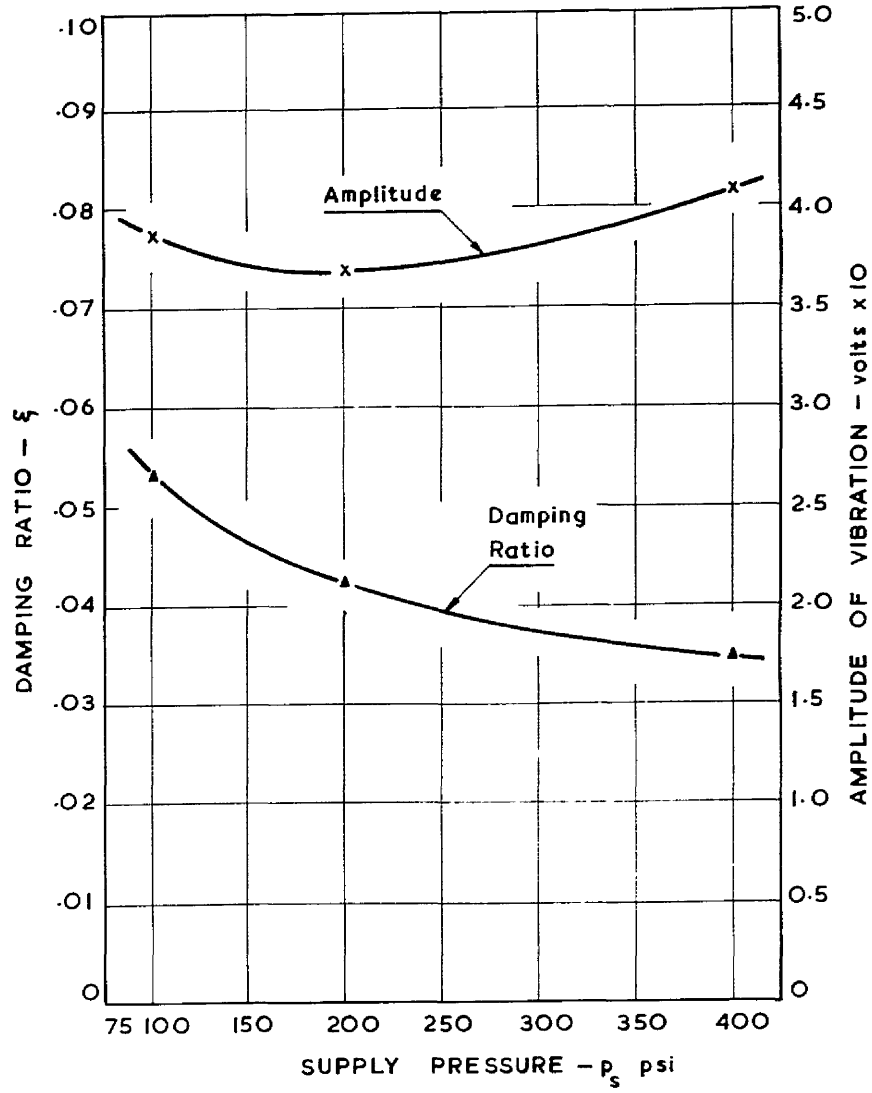

FIG. 42 VARIATION OF DAMPING RATIO AND DISPLACEMENT AMLITUDE FOR DIFFERENT BEARING SUPPLY PRESSURES

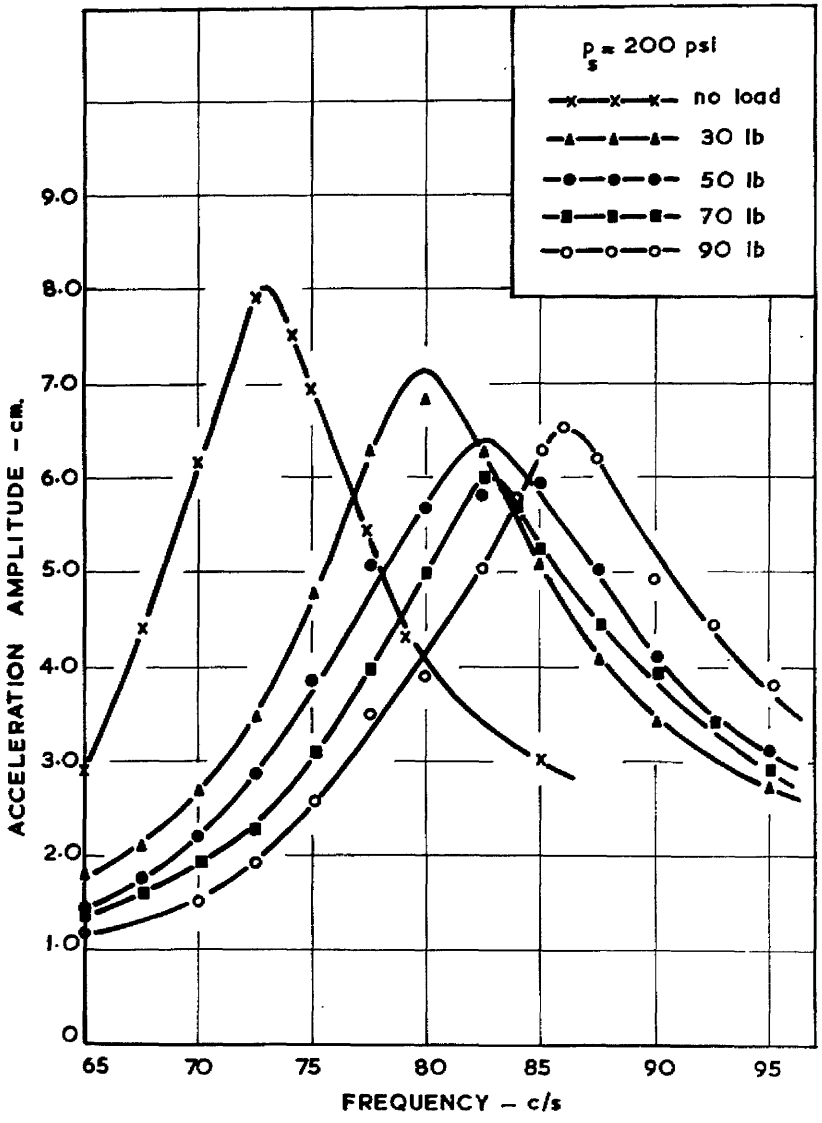

FIG.43 FREQUENCY RESPONSE CURVES WITH SPINDLE END PRELOAD

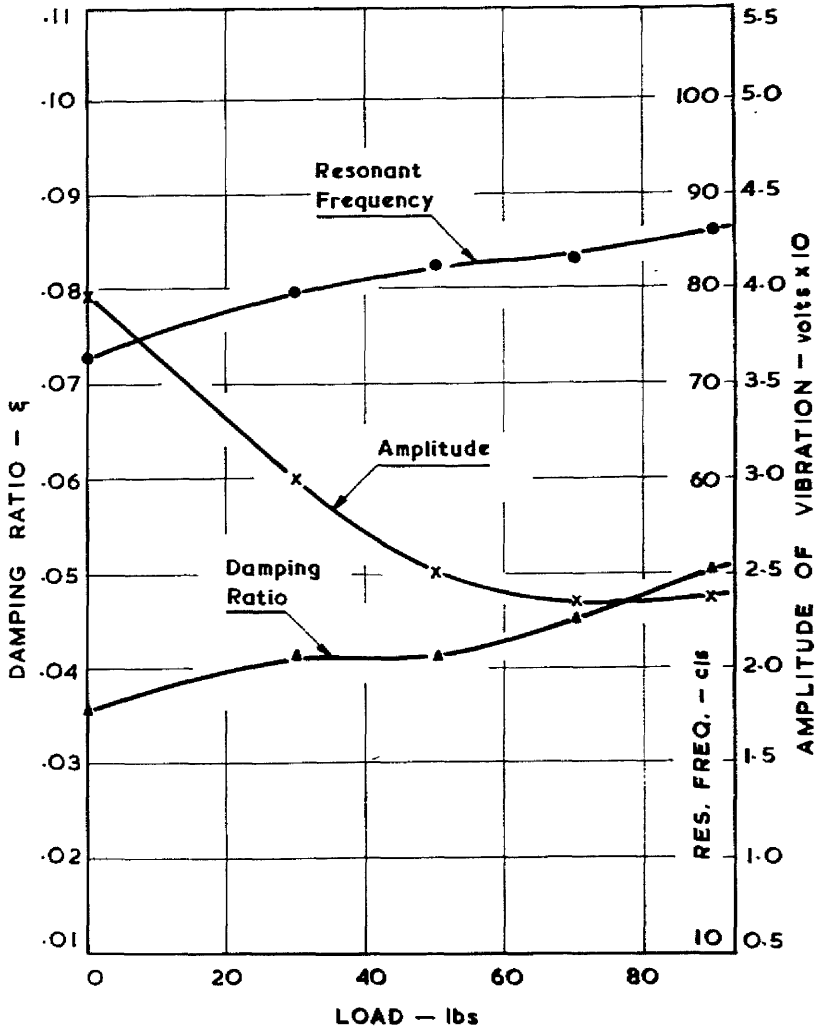

FIG. 44 VARIATION OF DAMPING RATIO, RESONANT FREQUENCY AND AMPLITUDE WITH SPINDLE END PRELOAD

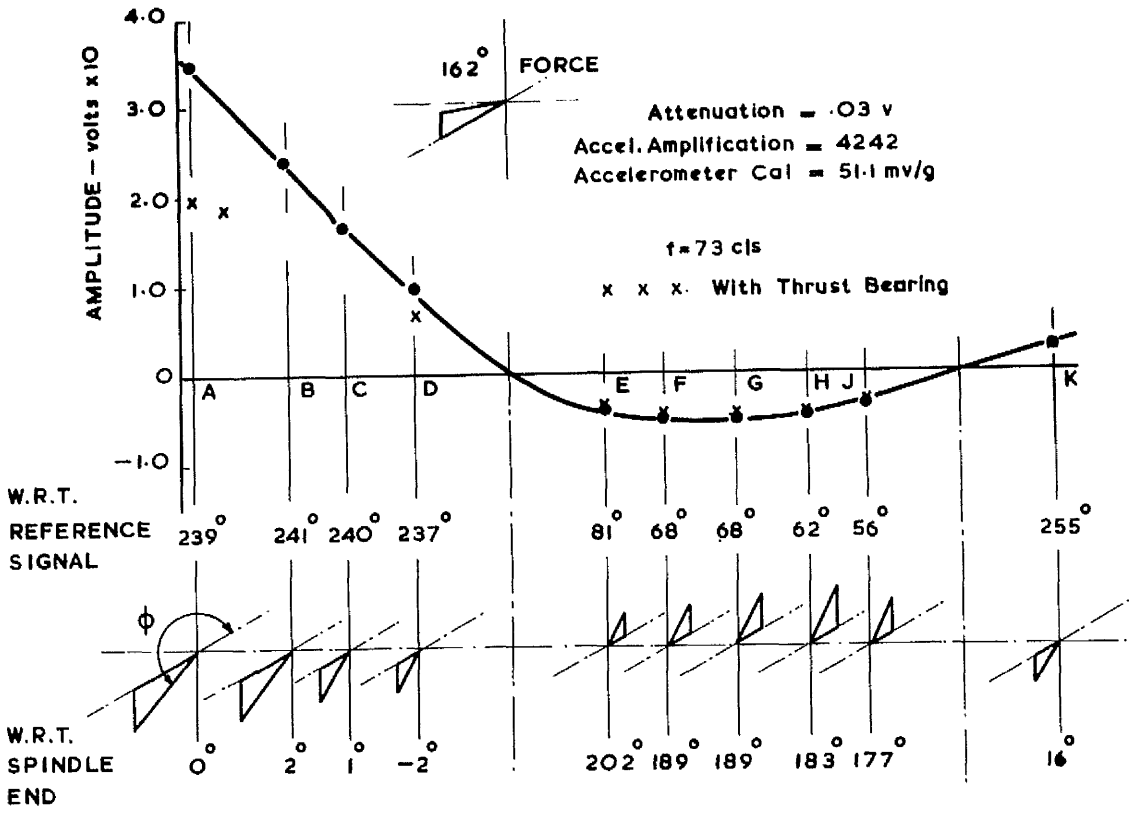

EXPERIMENTAL

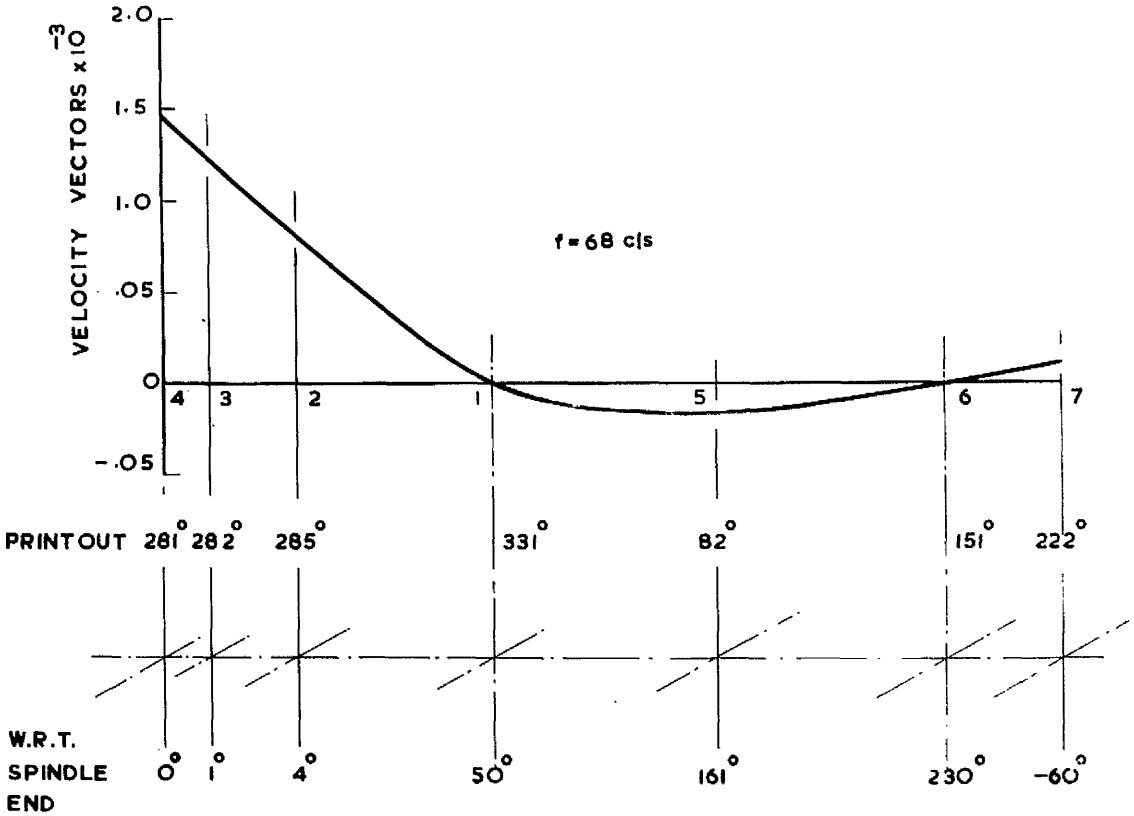

COMPUTER PROGRAM

FIG. 45 COMPARISON OF EXPERIMENTAL AND COMPUTER PROGRAM MODAL SHAPES — FIRST MODE

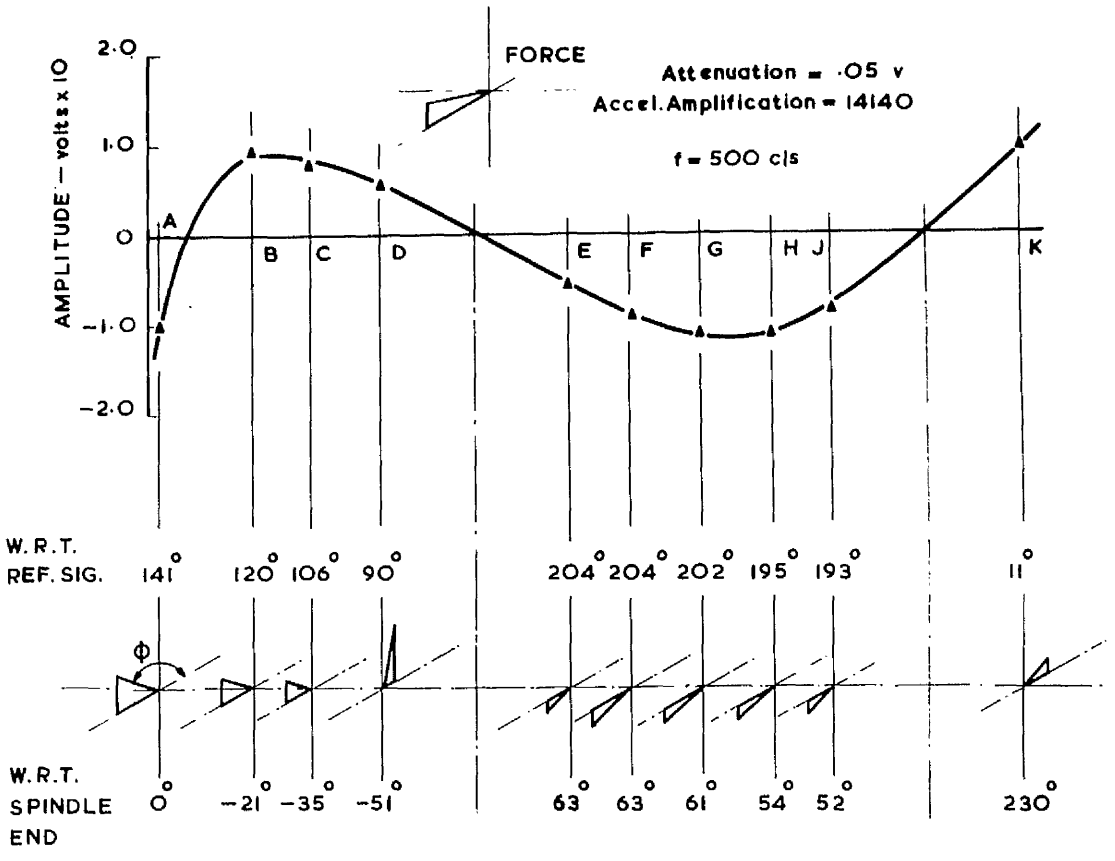

EXPERIMENTAL

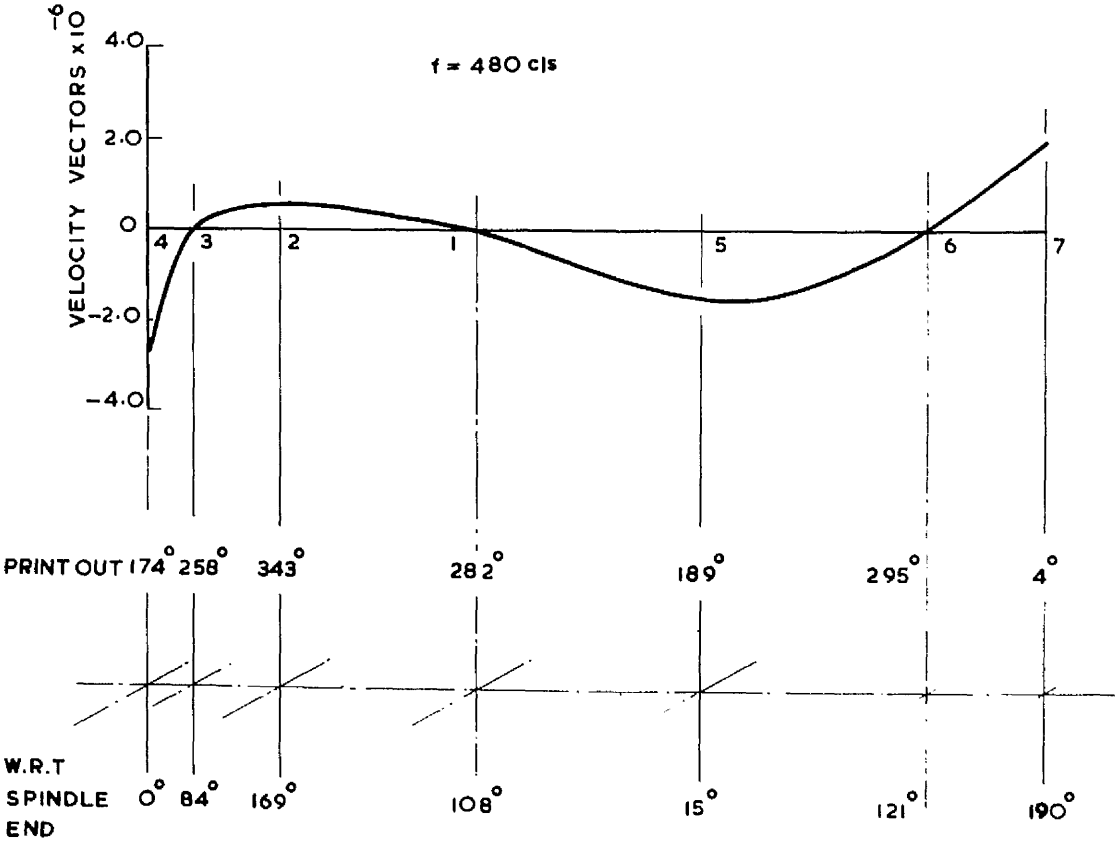

COMPUTER PROGRAM

FIG. 46 COMPARISON OF MODAL SHAPES — SECOND MODE

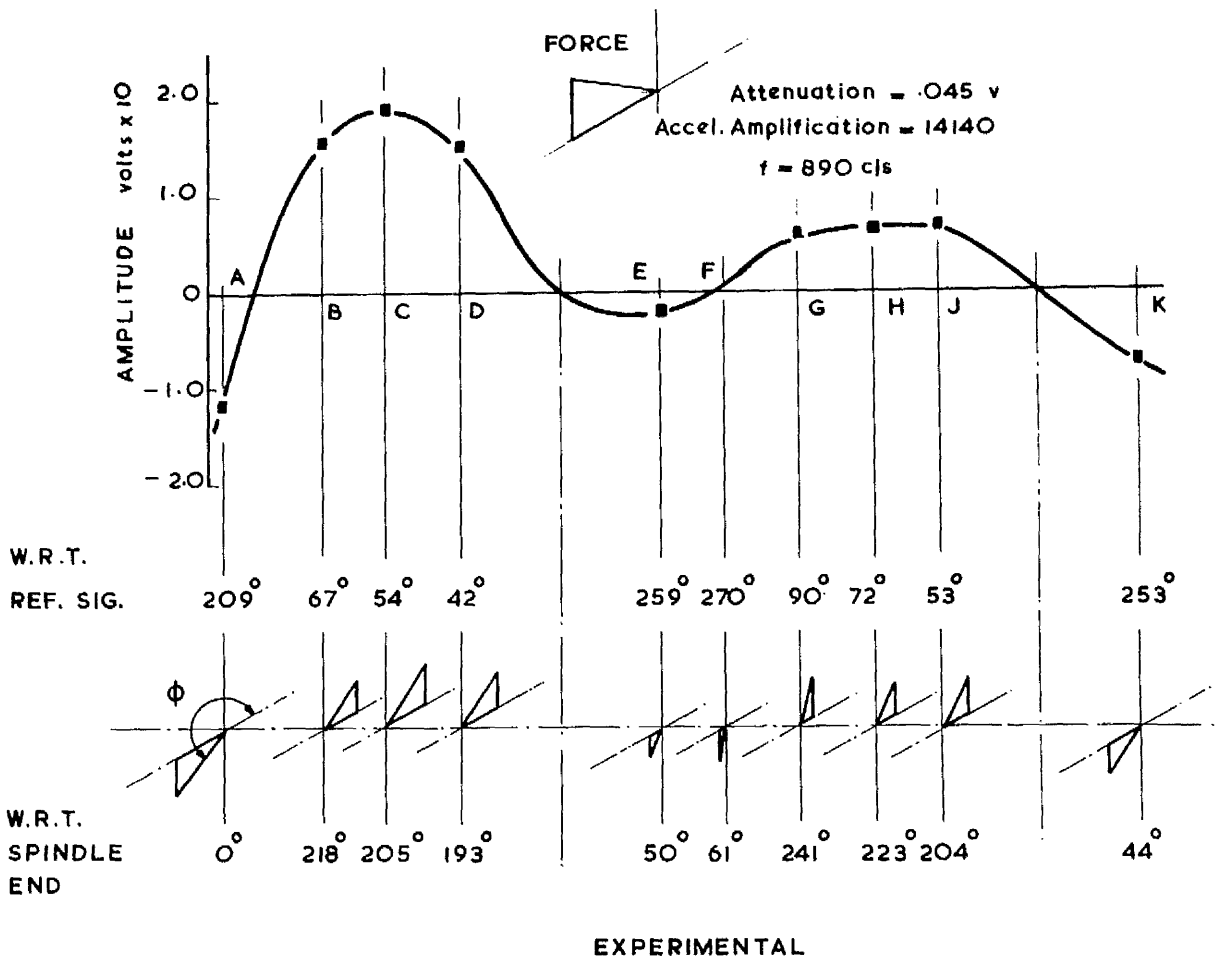

EXPERIMENTAL

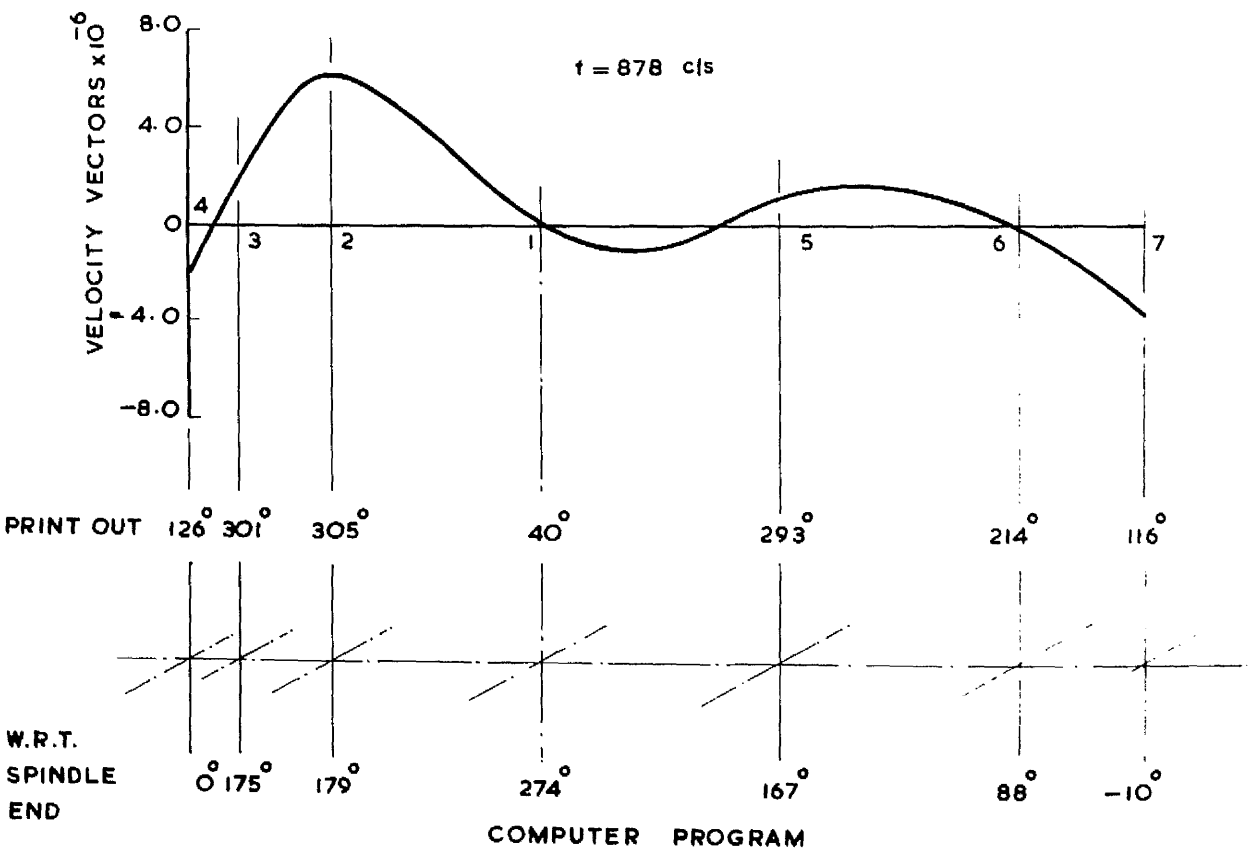

COMPUTER PROGRAM

FIG. 47 COMPARISON OF MODAL SHAPES – THIRD MODE

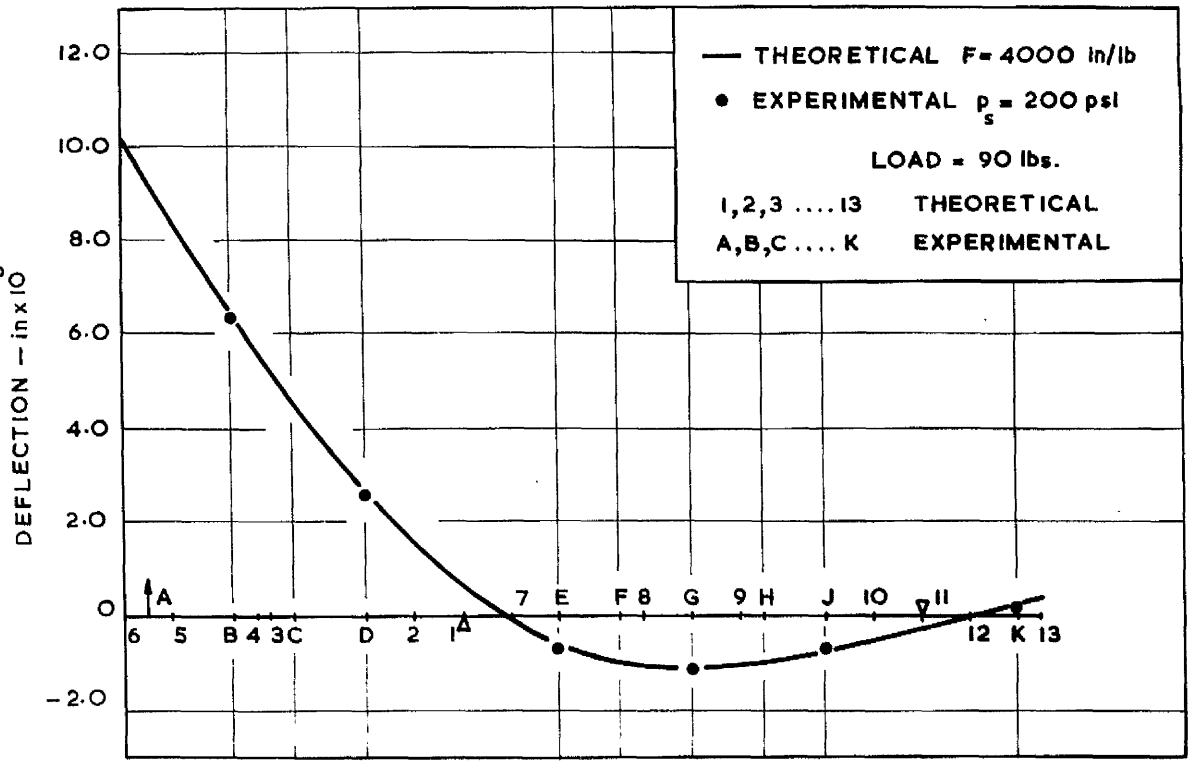

FIG.48 COMPARISON OF THEORETICAL AND EXPERIMENTAL SPINDLE DEFLECTION FOR STEADY LOAD

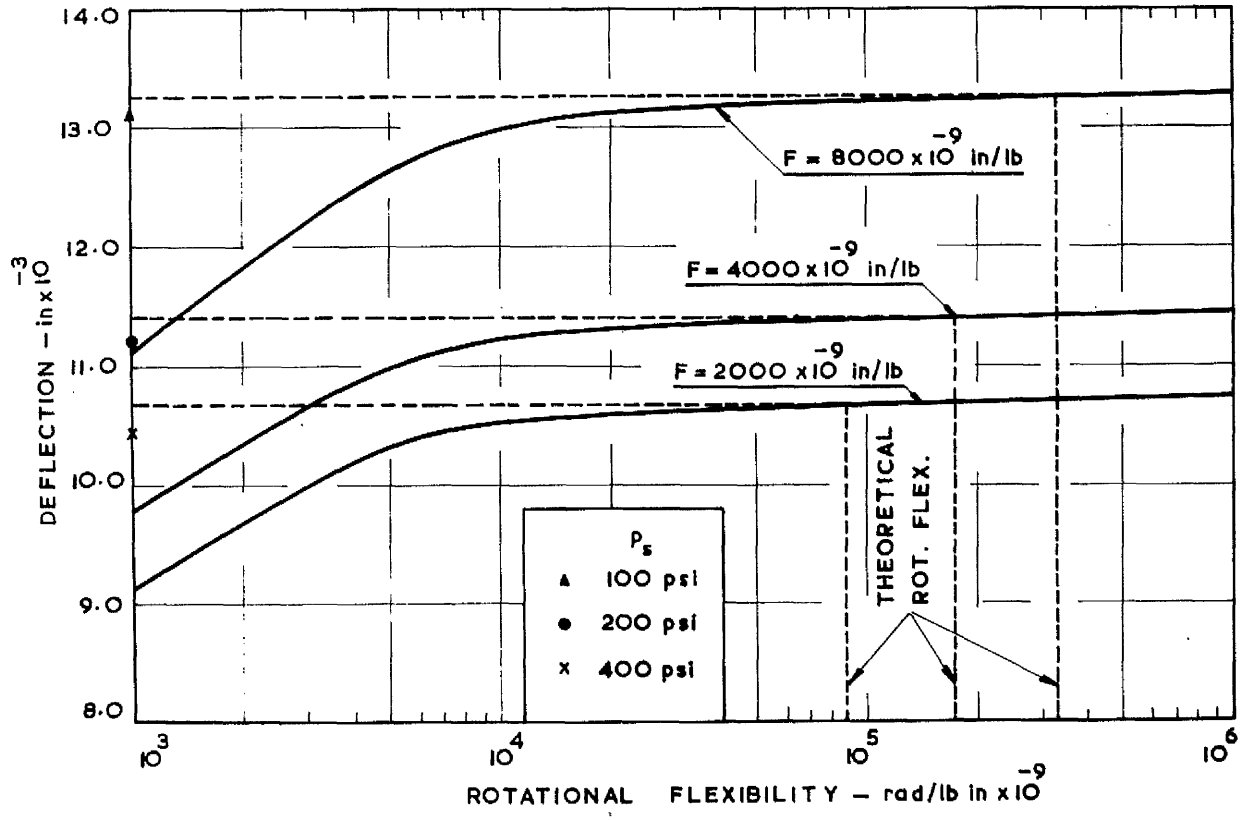

FIG.49 COMPARISON OF THEORETICAL AND EXPERIMENTAL SPINDLE END DEFLECTION

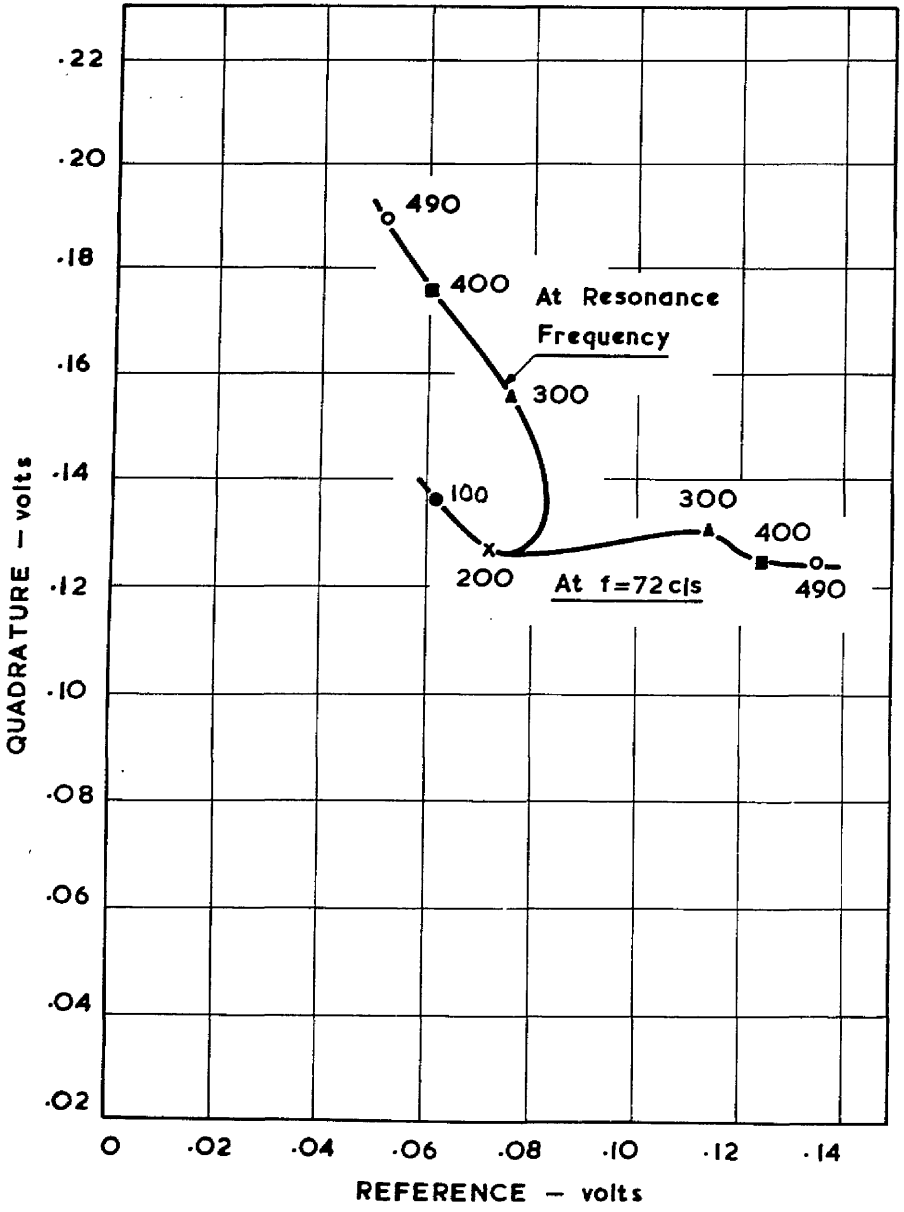

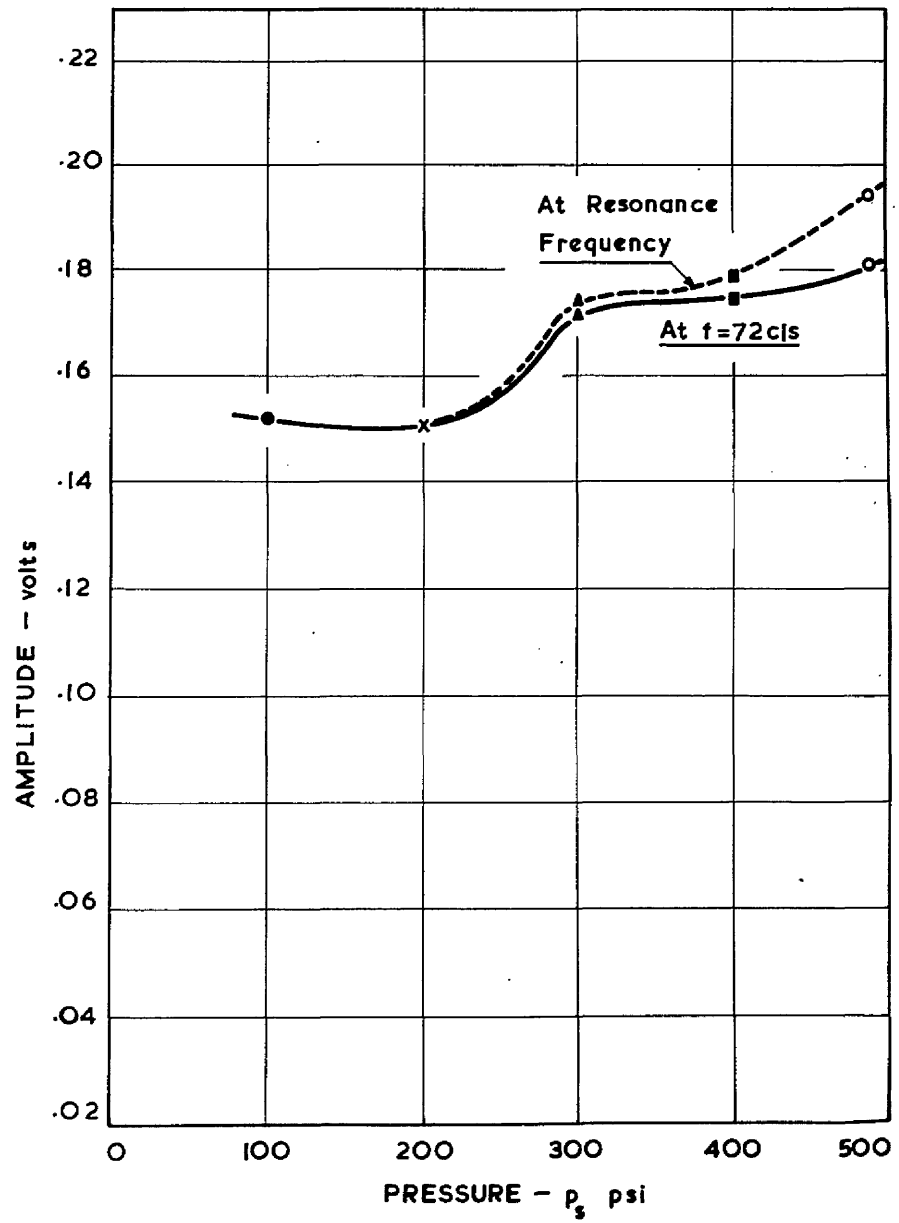

FIG. 50 VARIATION OF SPINDLE END AMPLITUDE OF VIBRATION WITH SUPPLY PRESSURE

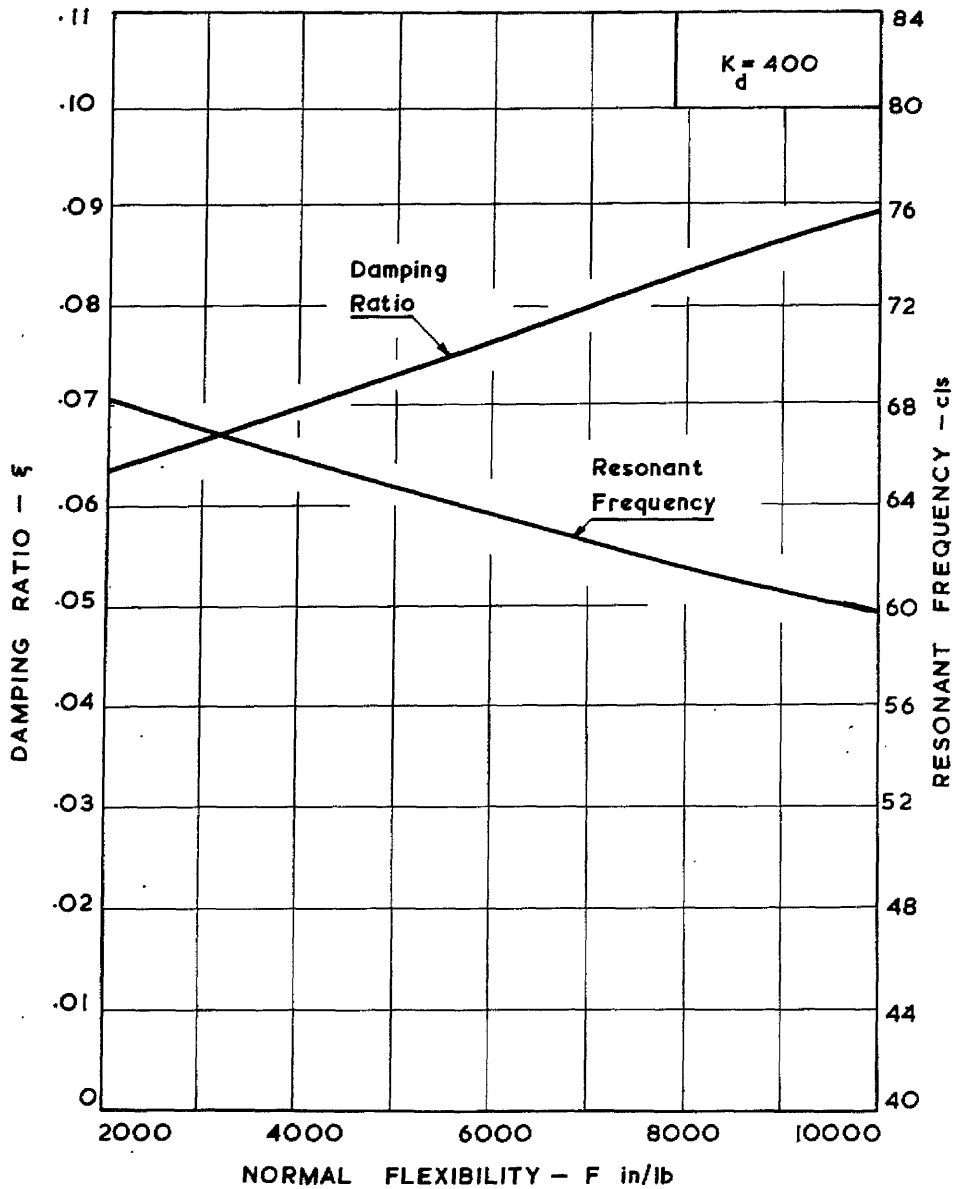

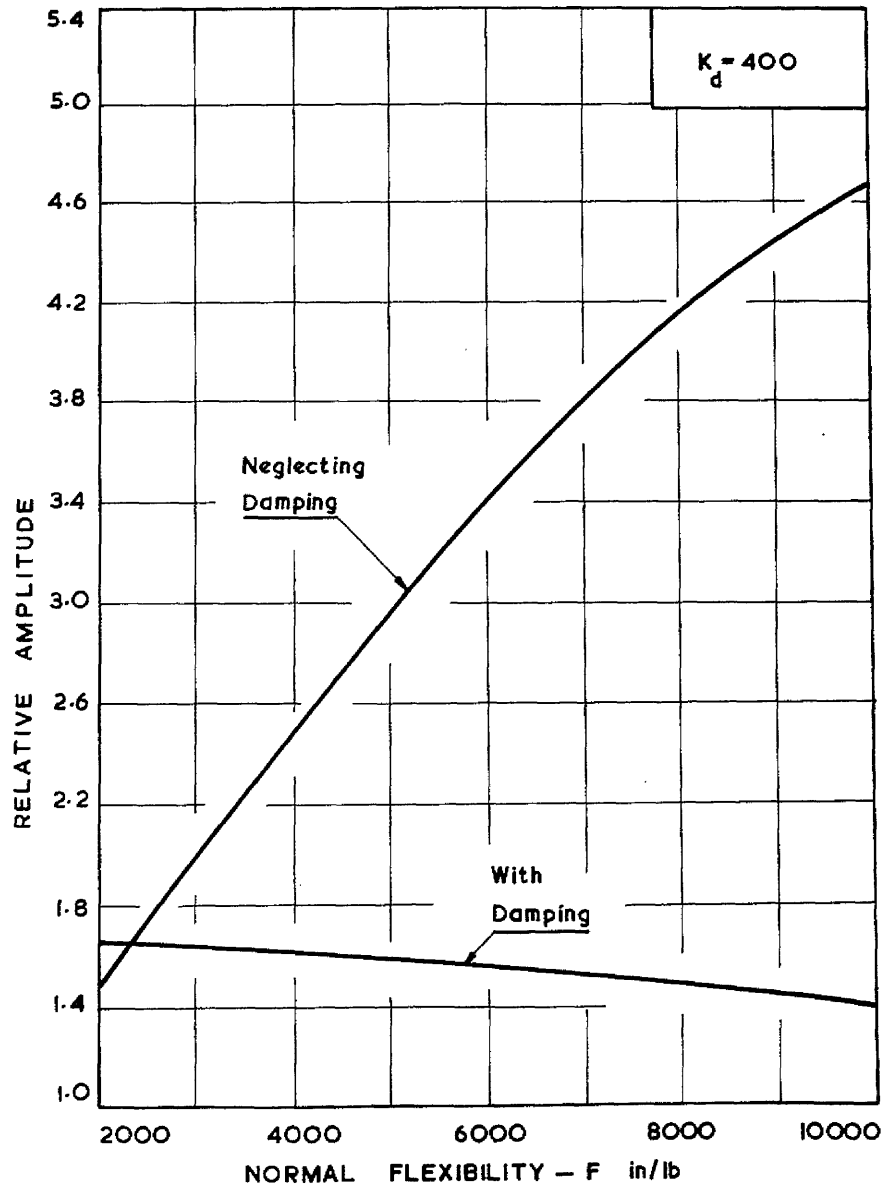

FIG. 51 VARIATION OF DAMPING RATIO, RESONANT FREQUENCY AND AMPLITUDE OF VIBRATION WITH BEARING NORMAL FLEXIBILITY

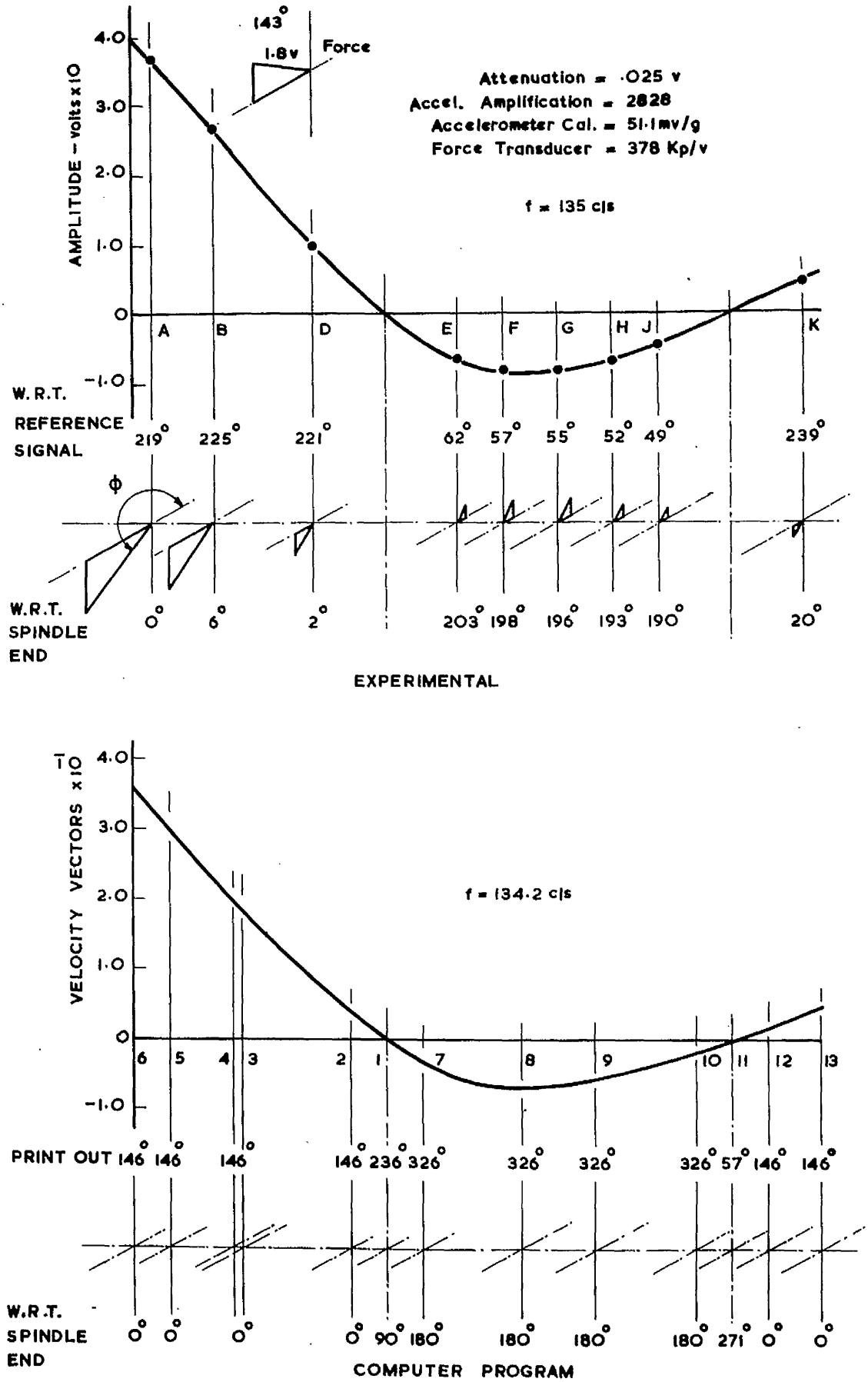

FIG.52 COMPARISON OF THE EXPERIMENTAL AND COMPUTER PROGRAM MODAL SHAPE — FIRST MODE

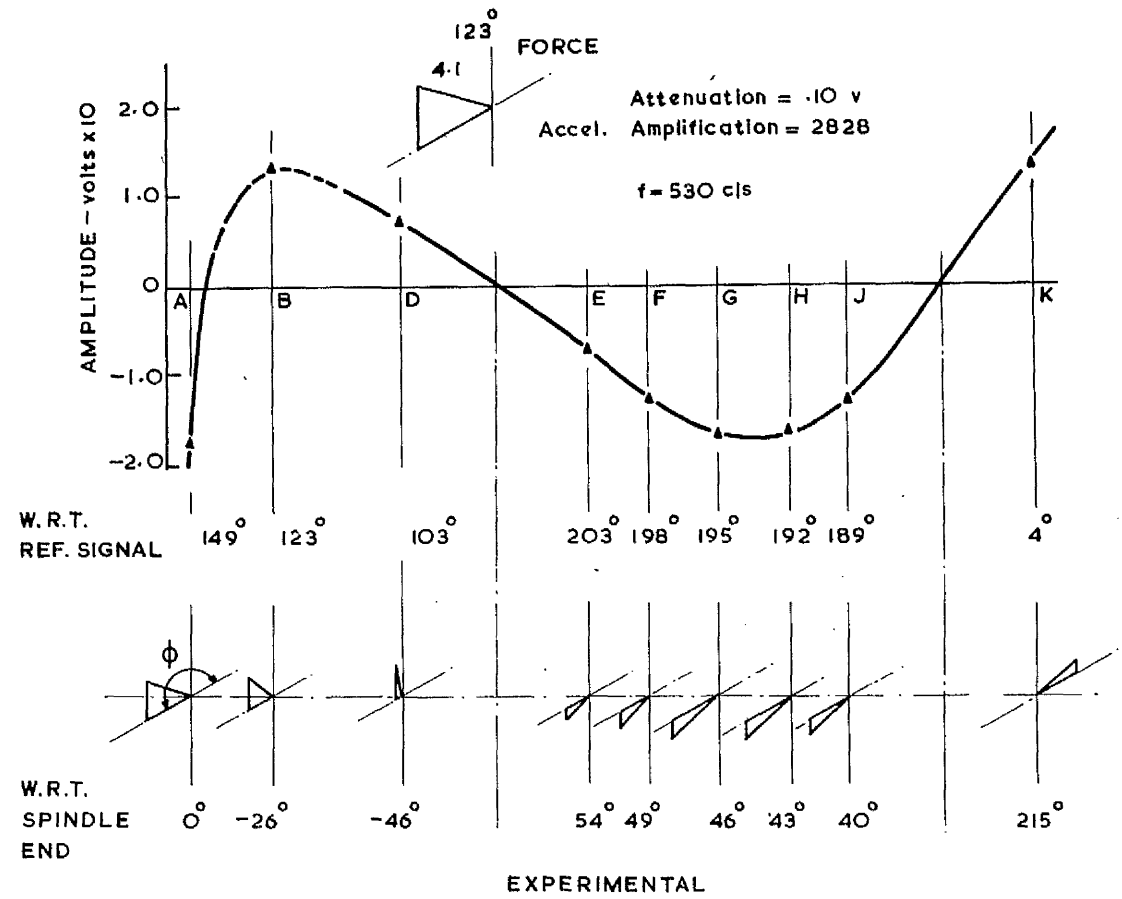

EXPERIMENTAL

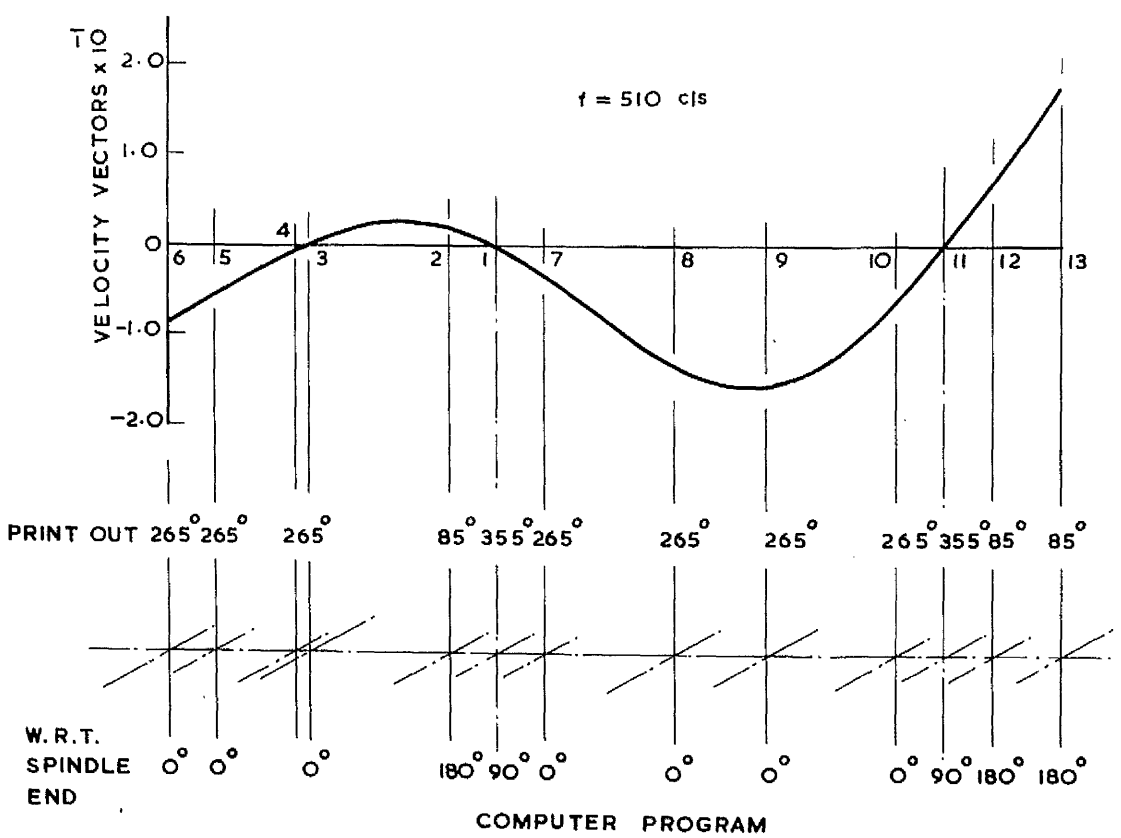

COMPUTER PROGRAM

FIG.53 COMPARISON OF MODAL SHAPES – SECOND MODE

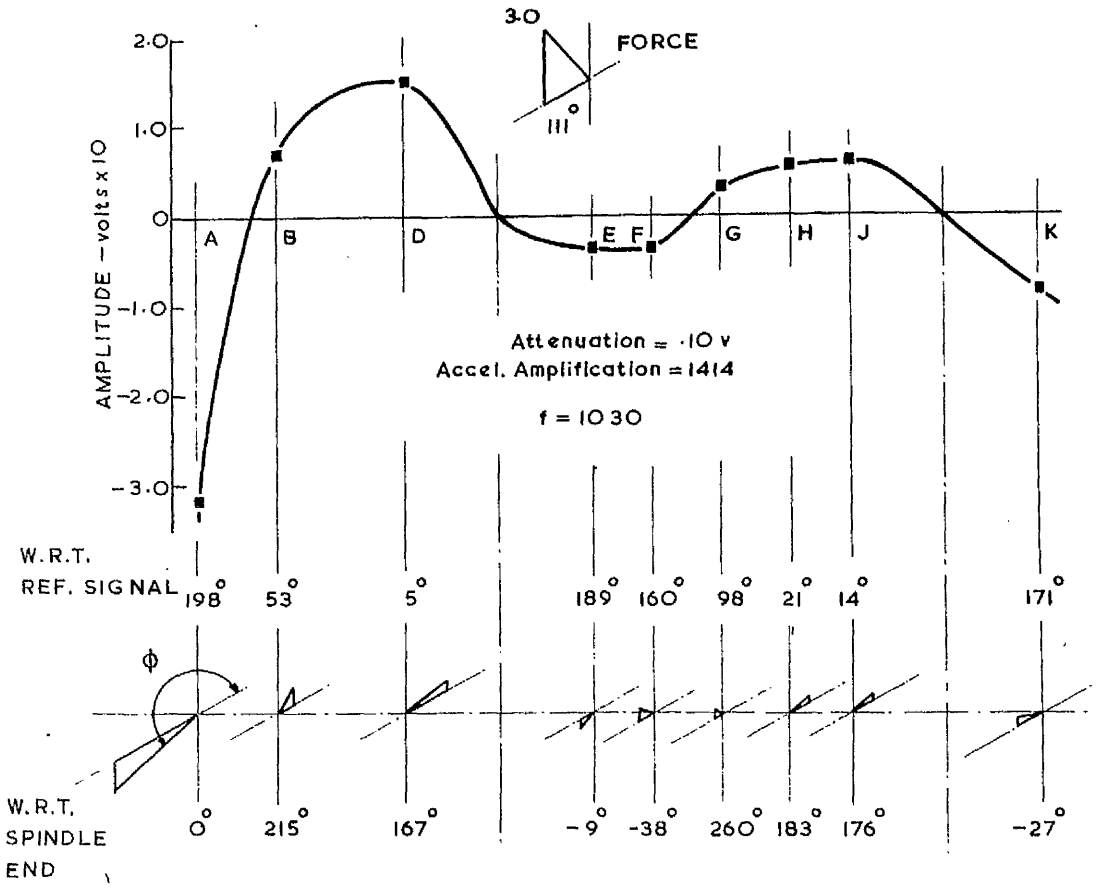

EXPERIMENTAL

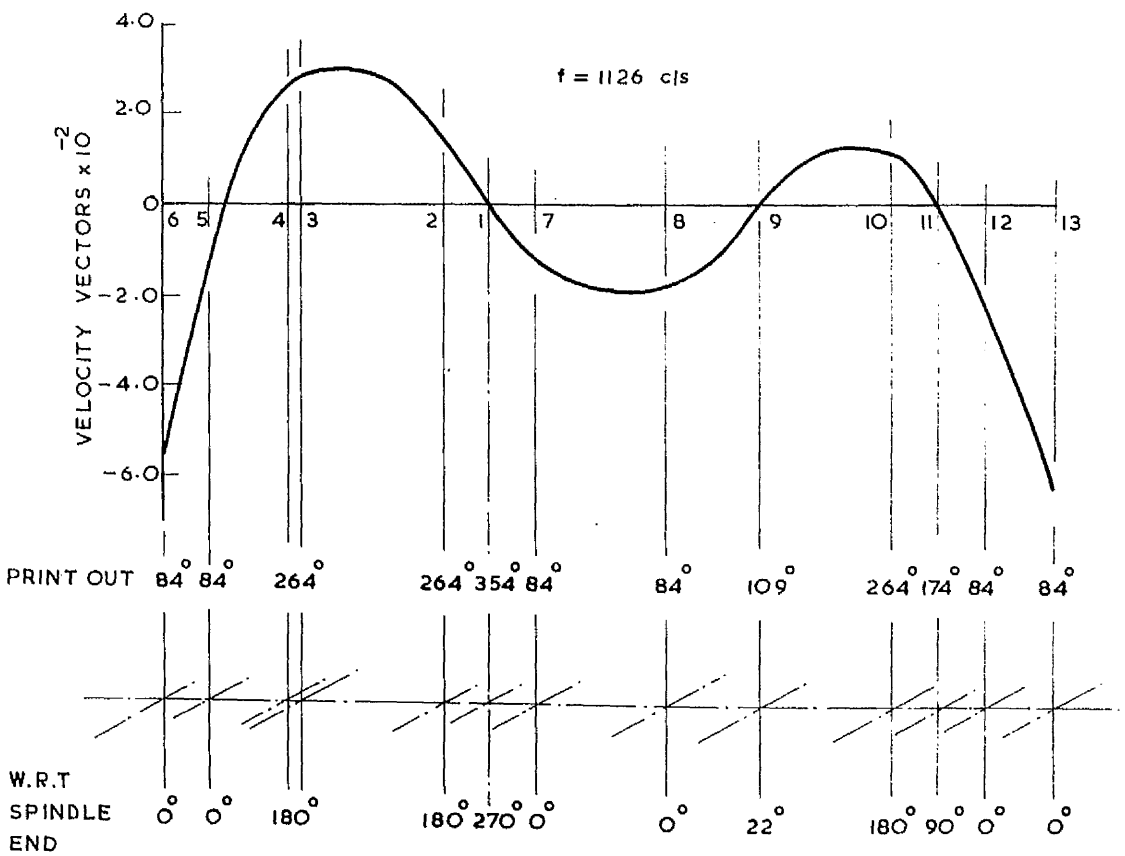

COMPUTER PROGRAM

FIG. 54 COMPARISON OF MODAL SHAPES — THIRD MODE

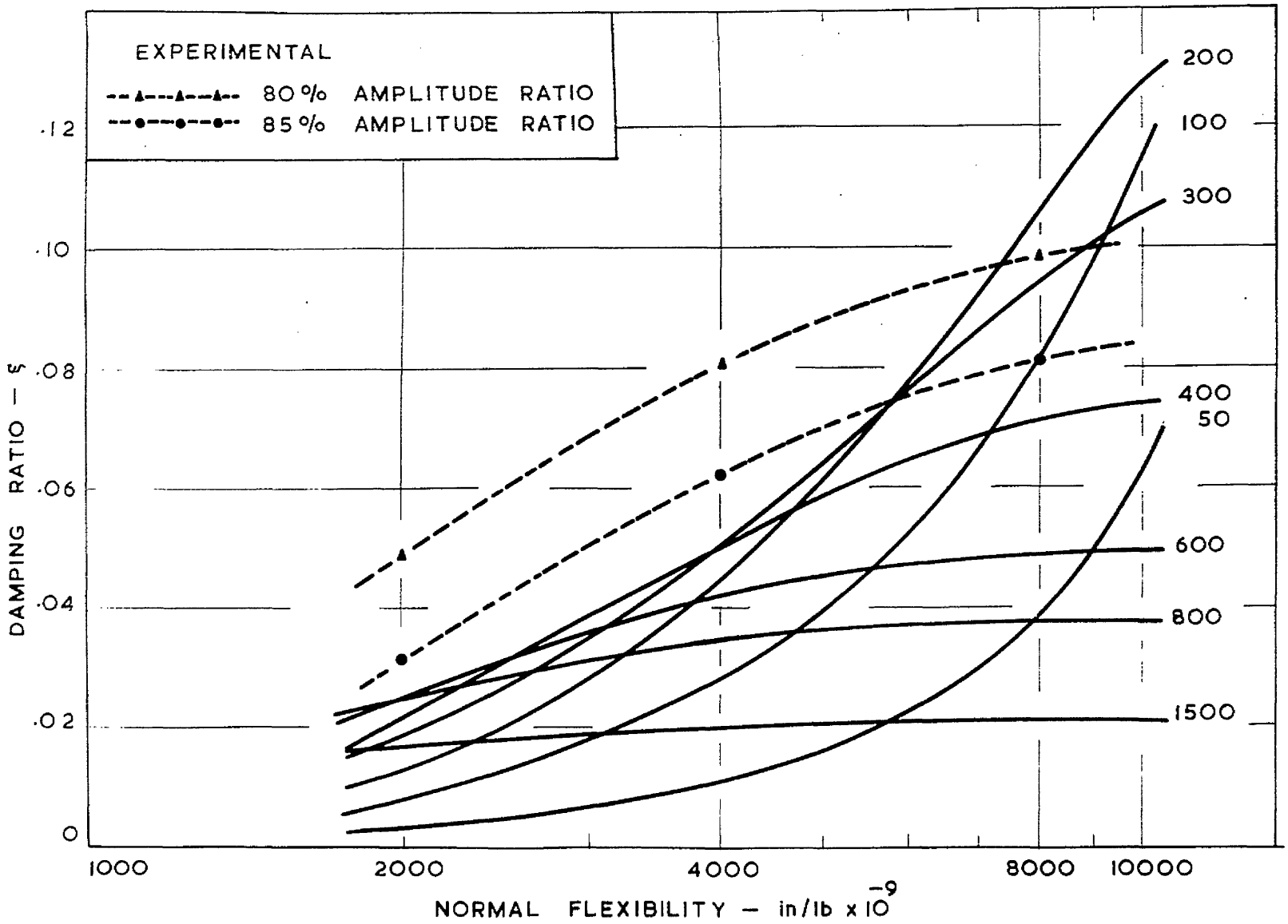

FIG. 55 VARIATION OF DAMPING RATIO WITH NORMAL FLEXIBILITY FOR DIFFERENT DAMPING CONSTANTS